Mathematisches Forschungsinstitut Oberwolfach

Report No. 15/2012

DOI: 10.4171/OWR/2012/15

Mechanics of Materials

Organised by
Reinhold Kienzler, Bremen
David L. McDowell, Atlanta
Stefan Müller, Bonn
Ewald A. Werner, München

March 18th – March 24th, 2012

Abstract. The rapid advances of modern fabrications technologies require a thorough understanding of physical and mechanical properties of materials as influenced by their atomic composition, processing history and structure at the micro- and nanometer length scales. Carbon nanotubes, nanometer sized crystals, thin films and coatings, MEMS, smart materials and bio-inspired multifunctional materials are current examples employing technologies and processes that heavily depend on material properties at very small length scales. Today's leading materials for a range of applications are hierarchical, having characteristics of structure at multiple length scales to satisfy a complex set of performance requirements and constraints. Composite materials and advanced alloy systems for transportation and infrastructure increasingly must rely on theoretical understanding at each of a range of length scales from the atomic scale upward to improve existing materials and to develop new materials to meet critical societal needs.
Modern day efforts in mechanics of materials exploit recent advances in mechanics of materials that draws upon concurrent use of solid state physics, mathematics and information technology, continuum and discrete (statistical) mechanics and materials chemistry. Advanced materials derive their outstanding properties, durability and multifunctionality from heterogeneity of their underlying microstructure. There is a richness of outstanding problem sets at the intersection of theoretical and applied mathematics and materials mechanics. This state of affairs motivates the central goals of this workshop, namely to explore new and emerging mathematical approaches to multiscale modelling of evolving microstructures and to identify new and emerging mathematical approaches to interfaces in materials.

Mathematics Subject Classification (2000): 74-XX.

Introduction by the Organisers

The workshop *Mechanics of Materials* attracted over 50 participants with broad geographic representation from Europe and the United States. This workshop was a well balanced blend of researchers with backgrounds in mathematics, mechanics and materials science. The organizers successfully recruited a significant number of younger representatives of the mentioned research communities.
The field of predictive modeling and simulation of the nonlinear behavior of microstructure-property/response relations of materials is taking on increasing global importance the desire for computer-assisted design of new and improved materials continues to build momentum. This workshop was convened to explore the status of foundational mathematical methods and approaches that support this important emerging multidiscipline. Materials are challenging to model, having both short and long range order, as well as fading memory of prior deformation and damage history. Accordingly, the mathematics of materials modeling is at the frontier of knowledge and applications.
The Oberwolfach Mechanics of Materials series has evolved to reflect cutting-edge trends in applied mechanics and mathematics of evolving microstructures and microstructure-property relations for a broad range of materials, including metals, polymers, composites, and ceramics. Based on experience gained in organizing preceding workshops on mechanics of materials, the following main topics were targeted in this workshop:

(1) New and extended variational principles for modelling multiscaled material systems with multiphysics phenomena of interest (composite and polycrystal plasticity; biological material systems).
(2) Quantitative mathematical representation of microstructures and methods for inverse analysis (i.e., localization) to simulate distributed responses of interest at the scale of microstructure.
(3) Physical interpretation and mathematical framing of boundary conditions for material interfaces such as phase and grain boundaries in field theories for line defects (dislocations), point and/or surface defects in materials, including the treatment of interfaces with constitutive equations and associated initial/boundary conditions.
(4) Mathematical methods for bridging discrete atomistic and continuum modelling methods in the vicinity of interfaces.

Topics in variational methods and associated field theories in mechanics of materials were clustered as follows:

- Variational methods (including multiscale approaches)
- Heterogeneity field mechanics
- Multiscale modeling
- Multiphysics modeling
- Atomistics and first principles modeling
- Inelasticity and evolving microstructure
- Phase transformations and moving interfaces

The basic philosophy underlying workshop presentations and discussions was to explore the frontiers of problem formulations and underlying mathematics. To enhance cross-cutting collaborative discussion, sessions addressing the above clusters were organized by participants during the opening session on Monday morning. Keynote presentations were identified along with contributed talks, and themes for discussion were outlined. This unique style of organization afforded more time for open discussion than in our prior Mechanics of Materials Workshops organized that were based on a more conventional lecture style format, and facilitated pairing of interested participants to formulate common topics flowing from workshop interactions. The closing session on Friday afternoon summarized the results of the weeklong discussions, as highlighted in the following.

Clusters 1 & 2: Variational Methods & Heterogeneity Field Mechanics

The recommendations of these two clusters were combined in view of considerable overlap. Two of the potentially most fruitful areas to focus at the intersection with mathematics include:

- Methods for passing relevant information related to dislocation fields up to a continuum scale description (e.g., back stress in continuum crystal plasticity models derived from discrete dislocation models)
- Framing descriptions at different scales within a variational framework (applications include, for example, dislocation field theory and homogenization involving generalized continua descriptions).

Several presentations evoked discussion related to Gamma-convergence:

- Application of Gamma-convergence and asymptotic homogenization for the upscaling to achieve consistent coupling of models/descriptions at different scales.
- Extension of Gamma-convergence to rate-dependent problems and dissipation.

It was concluded that interactions with experiments are necessary to formulate improved and more realistic models of interfaces, including interaction of dislocations with grain and phase boundaries in metallic systems. We are not yet in a position to lead experimental observation with theory, but can benefit by taking advantage of new characterization methods to gain more insight into the evolution of dislocation structures from complex strain path experiments. Emerging areas of considerable interest include extension of mean field dislocation theory to mesoscopic methods to facilitate enhanced overlap in the submicron regime, as well as to multiple phases (e.g., precipitates) and interfaces, and extension to multi-component material systems.

Cluster 3: Multiscale Modeling

The major theme of this cluster was the upscaling and downscaling (i.e., scale bridging) within a series of models framed with different degrees of freedom at

various length and time scales. Another stream of presentations considered transitions between two adjacent scales in continuum micromechanics.
One common point of agreement from workshop participants was that connections between atomistic and continuum models, one important type of discrete to continuous field theory scale transition, are lacking and require considerable attention in order to address the needs of materials design. In addition, several directions were identified for future work to enable mathematical foundtions for multiscale modeling:

- Development of integrated multiscale methods (as opposed to information passing between disparate models).
- Problem-specific mathematical tools based on physical insight.
- Rigorous tools for assessing invertibility of structure-property relations in very large-dimensional spaces (e.g., large degree of freedom microstructure representations).
- Fast solvers for sparse matrices to support FE^2-type methods.
- Efficient finite element formulations.
- Statistical methods to assess RVE size and convergence for dynamic processes involving microstructure evolution.
- Interconnections between complex behavior and complex microstructure topology.

Cluster 4: Multiphysics Modeling

The major theme addressed by this cluster was that of problems involving multiple physical processes and traditionally distinct governing field equations that are inherently coupled and must be considered simultaneously. It is a rich subject area in great need of efficient and robust numerical schemes, for example.
A number of issues were identified that require further clarification at the intersection of mathematics and mechanics of materials:

- Coupling transfer of energy between disparate systems based on degree of disparity and the type of approximations to be made.
- Probabilistic versus deterministic approaches.
- Experimental methods to distinguish energy dissipation versus storage during nonequilibrium deformation processes such as plastic deformation.
- Determination of heat capacity, especially considering the role of constitutive equations.
- Developing frameworks for verification and validation.
- Effects of microstructure on multiphysics phenomena such as electrochemically-induced phase transformation.
- Computing rates of chemical reactions.
- Consideration of defect clustering and its influence on coupled diffusion-inelastic deformation problems.
- Predictive modeling of fracture, fatigue, and creep phenomena.

- Multidomain integration for phenomena that are of disparate spatial and temporal order.

Cluster 5: Atomistic and First Principles Modeling

This cluster focused primarily on methods for multiple time scaling information obtained from atomistic modeling, including various methods related to transition state theory. In addition, some attention was devoted to passing information among scales in a consistent manner that minimizes additional assumptions or needs for parameter estimation.
A dominant perspective of this session was the exploitation of atomistics via continuum mechanicians as a tool to augment experiments in constructing constitutive models and estimating parameters. Potential opportunities exist in terms of providing input for higher scale models, judiciously guiding experiments, and predicting mechanisms. On the other hand, there are many challenges, including uncertainty quantification, verification and validation on more relevant problems, the complexity of the relevant configuration spaces, spatial and temporal scaling, the need for accurate yet efficient interatomic force computations, and strategies for effective use of these tools and methods.

Cluster 6: Inelasticity and Evolving Microstructure

The irreversible rearrangement of microstructure under various applied stimuli is one of the most challenging problem classes in mechanics of materials. Presentations in this cluster highlighted some of the issues with underlying mathematics of various problems.
Open Problems include:

- Definition of representative volume size in the context of numerical homogenization schemes.
- Existence of solutions for nonlinear material behavior.
- Micromechanically-based definition of state variables and derivation of corresponding balance/evolution equations, e.g. in the context of dislocation dynamics theory.

Cluster 7: Phase transformations and moving interfaces

This session explored the formation and migration of boundaries during plastic deformation. Experiments reveal these phenomena at both sub-micron and micron scales. In an analogous way to magnetic and fluid phase transformations, mathematical modeling using statistical physics was discussed starting from the crystalline level to obtain the Gibbs free energy of representative volume elements. In this way, all basic thermodynamic properties can be calculated. Equilibrium and kinetics of interfaces can be modeled within the framework of the construction of energy minimizers and based on the theory of configurational forces. A

variety of microstructures can be realized as a function of the strain state. Energy minimization is employed once again in order to study the influence of interface energies on the formation of microstructures. A mesoscopic model is presented which facilitates modeling of the competition of surface/interface energy and bulk energy associated with phase topology, giving rise to interesting scaling laws. The partial differential equations of a phase field model can be solved using the finite element method, with spatial and temporal discretization based on goal-oriented error estimates.
Three major areas of open problems were identified:

- Migration of interfaces such as phase and grain boundaries within solids. Here we see a strong connection to the field of dislocation modeling. While driving forces are to some extent understood from energetics, the resistance or rate-controlling phenomena are very difficult to assess experimentally as well as theoretically using atomistics or first principles.
- Modeling of microstructures, with specific reference to multiscale modeling. There is a strong need to derive mesosopic models from those at smaller scales in a consistent manner.
- Nucleation of microstructures. Here the different levels of heterogeneities of the material will play an important role, and interface energies will have a strong influence.

A number of areas can benefit from cooperation with mathematicians. For example, gamma-convergence and upscaling of models, local and global stability problems associated with the formation of microstructure, statistical and stochastic aspects, as well as stability, convergence and efficiency of numerical methods.

As always, the unique atmosphere of the Institute offered an extraordinary retreat from the daily pressures of communications and travel that enabled fruitful and productive collaborations to be initiated. We found the model for self-organization of sessions around major themes to be a useful construct, and intend to pursue this in future workshops with additional advance planning to further enrich the discussion and informal collaborations.

Workshop: Mechanics of Materials

Table of Contents

Abstracts

Theoretical aspects of a continuum dislocation microplasticity theory and numerical examples

Thomas Böhlke
(joint work with Stephan Wulfinghoff, Eric Bayerschen)

Modern continuum approaches for microplasticity applications try to fill the gap between size-independent, phenomenological plasticity models for macroscopic simulations and microplasticity models based on discrete objects like ab-initio methods or discrete dislocation dynamics. The formulation of phenomenological nonlocal hardening models based on plastic strain gradient measures like Nye's dislocation density tensor [4] is the most popular approach for continuum mechanical microplasticity theories and allows to reproduce many of the experimentally observed size-effects at least qualitatively. Additionally, several dislocation density-based theories have emerged that account explicitly for dislocation transport and production. The kinematical theory of Hochrainer *et al.* [1], numerically implemented by Sandfeld *et al.* [2], averages the collective motion of three-dimensional discrete, connected and curved dislocation lines.

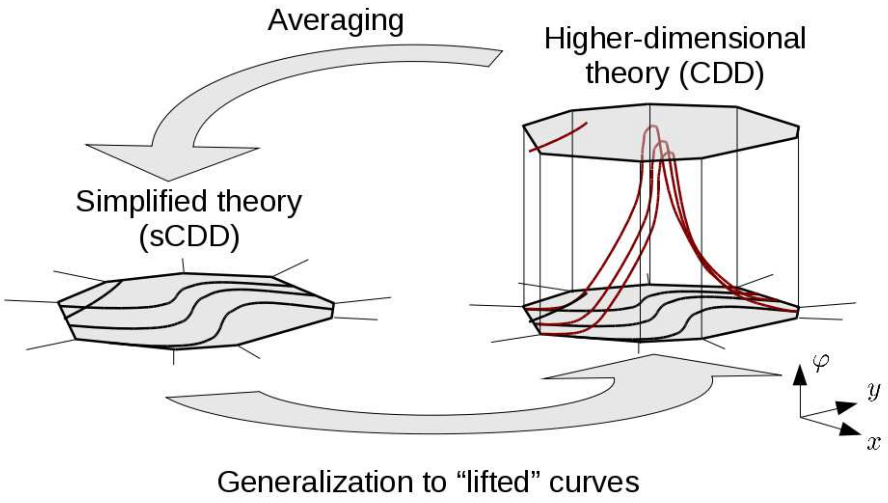

Figure 1. Higher-dimensional and simplified continuum dislocation dynamics theory

The theory can be considered as a generalization of Nye's work. Besides Geometrically Necessary Dislocations it contains detailed information on the dislocation microstructe, e.g. the total line length per unit volume and the average dislocation curvature. As the theory is numerically expensive in three-dimensional multislip applications, a simplified version (see e.g. Sandfeld *et al.* [3]) of the kinematical continuum mechanical dislocation-density framework is considered in the presentation based on two evolution equations for the dislocation density ρ_t and the average dislocation curvature $\bar{k}$ (see Figure 1). The dislocation velocity ν

couples the dislocation field problem to the elasto-visco-plastic crystal plasticity framework via Orowan's equation $\dot{\gamma} = \rho_t b \nu$, where γ is the plastic slip. The kinetic coupling based on hardening approaches like the Taylor-relation $\tau_Y \sim \sqrt{\rho_t}$ as well as boundary conditions are also discussed. Three-dimensional model problems are discussed in detail in order to highlight the advantages of the dislocation based approach.

References

[1] T. Hochrainer, M. Zaiser, P. Gumbsch, A three-dimensional continuum theory of dislocations: kinematics and mean field formulation. *Philosophical Magazine* **87** (2007), 1261–1282.
[2] S. Sandfeld, T. Hochrainer, M. Zaiser, P. Gumbsch, Numerical implementation of a 3D continuum theory of dislocation dynamics and application to micro-bending, *Philosophical Magazine* **90** (2010), 3697–3728.
[3] S. Sandfeld, T. Hochrainer, M. Zaiser, P. Gumbsch, Continuum modeling of dislocation plasticity: Theory, numerical implementation, and validation by discrete dislocation simulations. *J. Mater. Res.* **26** (2011), 623–632.
[4] J.F. Nye, Some geometrical relations in dislocated crystals. *Acta Metallurgica* **1** (1953), 153–162.

Particle shape effects on global and local behavior of particle reinforced composites

Helmut J. Böhm
(joint work with Azra Rasool)

Continuum models of the mechanical and conduction behavior of particle reinforced composites have typically assumed inhomogeneities to be spherical. The present contribution uses FE-based periodic homogenization for studying aspects of the influence of particle shape on the large-grained and small-grained, thermomechanical and thermal conduction behavior of two-phase particle reinforced composites containing convex, polyhedral, equi-axed inhomogeneities.

The modeling strategy is based on using a number of relatively small synthetic volume elements, each containing some 20 uniformly sized, randomly positioned and, where applicable, randomly oriented spherical, octahedral, cube-shaped or tetrahedral inhomogeneities. Appropriate periodic phase arrangements were generated by a modified random sequential addition algorithm. Five statistically equivalent volume elements were set up per particle shape, all results pertaining to a given shape being ensemble averages. Generic, isotropic material properties were prescribed to the constituents for evaluating the effective responses, interfaces between particles and matrix being assumed to be perfect. Six linearly independent elastic load cases, one thermoelastic load case and three linearly independent conduction cases were evaluated for obtaining the homogenized elastic, thermal expansion and thermal conduction tensors, respectively. The effective elastic tensors, which show some anisotropy after ensemble averaging, were "isotropized" by extracting the closest isotropic tensors [1]. Phase averages and standard deviations

of the microfields at the phase and particle levels were evaluated by approximate numerical integration, the volume integrals being replaced by sums of integration point data weighted by the integration point volumes.

All results on the homogenized thermoelastic and conduction behavior fulfill the pertinent two-point and, where available, three-point bounds, the standard deviations of the moduli being some two orders of magnitude smaller than the corresponding ensemble averages. Moderate, but consistent particle shape effects are predicted, with spheres giving rise to the lowest and tetrahedra to the highest effective moduli. In the linear range the phase averages show moderate particle shape effects, and the phase-level standard deviations of the local stress fields in the matrix are nearly independent of the particle shapes. However, the distributions of stresses or fluxes within the polygonal inhomogeneities are much wider than the ones pertaining to spherical particles, the effect again being most pronounced for the tetrahedra. Similarly, the intra-particle fluctuations of the stress and flux components are predicted to be markedly higher for polyhedral than for spherical inhomogeneities. Details and further results are given in [2]. A generally analogous ordering of shape effects was also obtained for the elastoplastic responses under tensile uniaxial loading [3], where particle shape effects on residual strains after unloading may be pronounced.

A number of issues can be identified that require further work. Whereas the present model geometries appear to be adequate for studying the homogenized behavior, this is not as clear for the fine-grained responses. Accordingly, approximate (physical) representative volume elements (RVEs) obtained on the basis of homogenization may differ from RVEs pertinent to local responses. Second, there appear to be practically no results in the literature on conditions for and the orders of singular behavior at the vertices and edges of polyhedral inclusions embedded in a matrix. Finally, the influence of the actual shapes of vertices and edges on the local behavior of the composites may warrant further study.

References

[1] Q.C. He, A. Curnier, *A More Fundamental Approach to Damaged Elastic Stress–Strain Relations*, Int. J. Sol. Struct. **32** (1995), 1433–1457.

[2] A. Rasool, H.J. Böhm, *Effects of Particle Shape on the Macroscopic and Microscopic Linear Behaviors of Particle Reinforced Composites*, Int. J. Engng .Sci. (2012), in print.

[3] A. Rasool, *Improved Multi-Particle Unit Cell Models for Studying Particle Reinforced Composites*, Doctoral Thesis, Vienna University of Technology, (2011).

Aspects of differential geometry and tensor calculus in anholonomic configuration space

John D. Clayton

In the context of finite deformation mechanics, a tangent mapping is anholonomic over some domain when it is not a gradient of a motion; conversely, a deformation gradient is holonomic when it is integrable to a motion field everywhere in that domain. This brief report addresses covariant differentiation for four possible choices of basis vectors in anholonomic space. As an example from continuum physics, the theory is applied towards description of divergence of the heat flux. An extensive treatment of anholonomic mathematics can be found in a recent article [1]; however, this report includes material not found in [1], and vice-versa.

As suggested by Schouten [2], consideration of differential geometry of anholonomic spaces dates back to at least 1926 [3]. Many important identities are derived in [2, 4]. Various coordinate systems and associated metric tensors in anholonomic space are considered in [5], with particular focus on convected basis and Cartesian representations. Correspondences among mathematical objects from differential geometry and their continuum physical counterparts in defect field theory of crystals are described at length in a more recent monograph [6].

The present description is limited to the time-independent case, such that spatial coordinates x^a are related to reference coordinates X^A by one-to-one and at least twice-differentiable mappings $x^a(X)$ and $X^A(x)$, with X a material particle and x its spatial representation. Let the usual holonomic deformation gradient $\boldsymbol{F}(X)$ be decomposed multiplicatively as

$$\boldsymbol{F} = \bar{\boldsymbol{F}}\tilde{\boldsymbol{F}}, \qquad F^a_{\ .A} = \bar{F}^a_{\ .\alpha}\tilde{F}^\alpha_{\ .A}; \tag{1}$$

$$\boldsymbol{F} = \partial_A x^a \boldsymbol{g}_a \otimes \boldsymbol{G}^A, \qquad \bar{\boldsymbol{F}} = \bar{F}^a_{\ .\alpha}\boldsymbol{g}_a \otimes \tilde{\boldsymbol{g}}^\alpha, \qquad \tilde{\boldsymbol{F}} = \tilde{F}^\alpha_{\ .A}\tilde{\boldsymbol{g}}_\alpha \otimes \boldsymbol{G}^A. \tag{2}$$

Denoting $\partial_A = \partial/\partial X^A$ and $\partial_a = \partial/\partial x^a$, partial differentiation proceeds as

$$\partial_\alpha(\cdot) \overset{\text{def}}{=} \bar{F}^a_{\ .\alpha}\partial_a(\cdot) = \tilde{F}^{-1A}_{\ \ .\alpha}\partial_A(\cdot), \qquad \partial_A(\cdot) = \partial_A x^a \partial_a(\cdot) = F^a_{\ .A}\partial_a(\cdot). \tag{3}$$

Attention is restricted to a simply connected domain in reference and current configurations such that $\{X^A\}$ and $\{x^a\}$ are global coordinate charts. Let indices in brackets be skew, e.g., $A_{[AB]} \overset{\text{def}}{=} \frac{1}{2}(A_{AB} - A_{BA})$. Since X^A and x^a are holonomic coordinates,

$$\partial_{[A}\partial_{B]}(\cdot) = 0, \quad \partial_{[a}\partial_{b]}(\cdot) = 0; \quad \partial_{[A}F^a_{\ .B]} = 0, \quad \partial_{[a}F^{-1A}_{\ \ .b]} = 0. \tag{4}$$

Similar identities do not always hold for $\partial_\alpha(\cdot)$ since $\bar{\boldsymbol{F}}^{-1}$ and $\tilde{\boldsymbol{F}}$ are not necessarily integrable functions of x^a or X^A. Anholonomic object $\boldsymbol{\kappa}$ obeys [1, 2]

$$\kappa^{\cdot\cdot\alpha}_{\beta\chi} \overset{\text{def}}{=} -\bar{F}^{-1\alpha}_{\ \ .a}\partial_{[\beta}\bar{F}^a_{\ .\chi]} = -\tilde{F}^\alpha_{\ .A}\partial_{[\beta}\tilde{F}^{-1A}_{\ \ .\chi]} = -\kappa^{\cdot\cdot\alpha}_{\chi\beta}; \tag{5}$$

$$\partial_{[\alpha}\partial_{\beta]}(\cdot) = -\kappa^{\cdot\cdot\chi}_{\alpha\beta}\partial_\chi(\cdot). \tag{6}$$

Holonomic charts $\{\tilde{x}^\alpha(X)\}$ [or $\{\tilde{x}^\alpha(x)\}$] exist in a one-to-one fashion with X or x if and only if $\kappa^{\cdot\cdot\alpha}_{\beta\chi} = 0$ throughout a simply connected domain.

Let $\boldsymbol{A}$ be a generic differentiable tensor field. Covariant differentiation in anholonomic space is defined as

$$(7)\quad \nabla_\nu A^{\alpha\ldots\phi}_{\gamma\ldots\mu} \overset{\text{def}}{=} \partial_\nu A^{\alpha\ldots\phi}_{\gamma\ldots\mu} + \Gamma^{\cdot\cdot\alpha}_{\nu\rho} A^{\rho\ldots\phi}_{\gamma\ldots\mu} + \cdots + \Gamma^{\cdot\cdot\phi}_{\nu\rho} A^{\alpha\ldots\rho}_{\gamma\ldots\mu} - \Gamma^{\cdot\cdot\rho}_{\nu\gamma} A^{\alpha\ldots\phi}_{\rho\ldots\mu} - \cdots - \Gamma^{\cdot\cdot\rho}_{\nu\mu} A^{\alpha\ldots\phi}_{\gamma\ldots\rho}.$$

Connection coefficients can be expressed in general form as [2]

$$(8)\qquad \Gamma^{\cdot\cdot\alpha}_{\beta\chi} = \tfrac{1}{2}\tilde{g}^{\alpha\delta}(\partial_{\{\beta}\tilde{g}_{\delta\chi\}} - 2T_{\{\beta\delta\chi\}} + 2\kappa_{\{\beta\delta\chi\}} + M_{\{\beta\delta\chi\}}),$$

where $\tilde{g}^{\alpha\chi}\tilde{g}_{\chi\beta} = \delta^\alpha_\beta$ and the following definitions apply:

$$(9)\qquad (\cdot)_{\{\alpha\beta\chi\}} \overset{\text{def}}{=} (\cdot)_{\alpha\beta\chi} - (\cdot)_{\beta\chi\alpha} + (\cdot)_{\chi\alpha\beta}, \qquad (\cdot)_{\beta\chi\delta} \overset{\text{def}}{=} (\cdot)^{\cdot\cdot\alpha}_{\beta\chi}\tilde{g}_{\delta\alpha};$$

$$(10)\qquad \tilde{g}_{\alpha\beta} \overset{\text{def}}{=} \tilde{\boldsymbol{g}}_\alpha \cdot \tilde{\boldsymbol{g}}_\beta, \quad T^{\cdot\cdot\alpha}_{\beta\chi} \overset{\text{def}}{=} \Gamma^{\cdot\cdot\alpha}_{[\beta\chi]} + \kappa^{\cdot\cdot\alpha}_{\beta\chi}, \quad M_{\alpha\beta\chi} \overset{\text{def}}{=} -\nabla_\alpha \tilde{g}_{\beta\chi}.$$

In this report attention is restricted to metric connections so that $M_{\alpha\beta\chi} = 0$ and

$$(11)\qquad \partial_\alpha \tilde{\boldsymbol{g}}_\beta = \Gamma^{\cdot\cdot\chi}_{\alpha\beta}\tilde{\boldsymbol{g}}_\chi, \qquad \partial_\alpha \tilde{\boldsymbol{g}}^\beta = -\Gamma^{\cdot\cdot\beta}_{\alpha\chi}\tilde{\boldsymbol{g}}^\chi;$$

$$(12)\qquad \partial_\alpha \ln\sqrt{\tilde{g}} = \Gamma^{\cdot\cdot\beta}_{\alpha\beta}, \qquad \nabla_\alpha \epsilon_{\beta\chi\delta} = \partial_\alpha \epsilon_{\beta\chi\delta} - \Gamma^{\cdot\cdot\phi}_{\alpha\phi}\epsilon_{\beta\chi\delta} = 0;$$

$$(13)\qquad \tilde{g} \overset{\text{def}}{=} \det(\tilde{g}_{\alpha\beta}), \qquad \epsilon_{\alpha\beta\chi} \overset{\text{def}}{=} \sqrt{\tilde{g}}e_{\alpha\beta\chi}, \qquad \epsilon^{\alpha\beta\chi} \overset{\text{def}}{=} (1/\sqrt{\tilde{g}})e^{\alpha\beta\chi}.$$

The covariant derivative of a generic differentiable vector field $\boldsymbol{V} = V^\alpha \tilde{\boldsymbol{g}}_\alpha$ is then

$$(14)\qquad \nabla \boldsymbol{V} = \partial_\beta \boldsymbol{V} \otimes \tilde{\boldsymbol{g}}^\beta = (\partial_\beta V^\alpha + \Gamma^{\cdot\cdot\alpha}_{\beta\chi}V^\chi)\tilde{\boldsymbol{g}}_\alpha \otimes \tilde{\boldsymbol{g}}^\beta.$$

Total covariant derivatives of two-point tangent mappings $\tilde{\boldsymbol{F}}$ and $\bar{\boldsymbol{F}}^{-1}$ are [1, 6]

$$(15)\qquad \tilde{F}^\alpha_{\cdot A:B} \overset{\text{def}}{=} \partial_B \tilde{F}^\alpha_{\cdot A} + \Gamma^{\cdot\cdot\alpha}_{\beta\chi}\tilde{F}^\beta_{\cdot B}\tilde{F}^\chi_{\cdot A} - \Gamma^{\cdot\cdot C}_{BA}\tilde{F}^\alpha_{\cdot C} = \tilde{F}^\alpha_{\cdot A:\beta}\tilde{F}^\beta_{\cdot B};$$

$$(16)\qquad \bar{F}^{-1\alpha}_{\quad\cdot a:b} \overset{\text{def}}{=} \partial_b \bar{F}^{-1\alpha}_{\quad\cdot a} + \Gamma^{\cdot\cdot\alpha}_{\beta\chi}\bar{F}^{-1\beta}_{\quad\cdot b}\bar{F}^{-1\chi}_{\quad\cdot a} - \Gamma^{\cdot\cdot c}_{ba}\bar{F}^{-1\alpha}_{\quad\cdot c} = \bar{F}^{-1\alpha}_{\quad\cdot a:\beta}\bar{F}^{-1\beta}_{\quad\cdot b}.$$

Metrics and Levi-Civita connections in reference and current configurations are

$$(17)\qquad G_{AB} \overset{\text{def}}{=} \boldsymbol{G}_A \cdot \boldsymbol{G}_B = \partial_A \boldsymbol{X} \cdot \partial_B \boldsymbol{X}, \qquad \Gamma^{\cdot\cdot A}_{BC} \overset{\text{def}}{=} \tfrac{1}{2}G^{AD}\partial_{\{B}G_{DC\}};$$

$$(18)\qquad g_{ab} \overset{\text{def}}{=} \boldsymbol{g}_a \cdot \boldsymbol{g}_b = \partial_a \boldsymbol{x} \cdot \partial_b \boldsymbol{x}, \qquad \Gamma^{\cdot\cdot a}_{bc} \overset{\text{def}}{=} \tfrac{1}{2}g^{ad}\partial_{\{b}g_{dc\}}.$$

Letting $g = \det(g_{ab})$ and $G = \det(G_{AB})$, Jacobian determinants are [5, 6]

$$(19)\quad J = \sqrt{g/G}\det(\partial_A x^a) = \bar{J}\tilde{J}, \quad \bar{J} = \sqrt{g/\tilde{g}}\det(\bar{F}^a_{\cdot\alpha}), \quad \tilde{J} = \sqrt{\tilde{g}/G}\det(\tilde{F}^\alpha_{\cdot A}).$$

Piola's identities for possibly anholonomic Jacobian determinants are then [1, 4, 6]

$$(20)\quad (\tilde{J}\tilde{F}^{-1A}_{\quad\cdot\alpha})_{:A} = \epsilon_{\alpha\beta\chi}\epsilon^{ABC}\tilde{F}^\beta_{\cdot A}\tilde{F}^\chi_{\cdot[B:C]}, \quad (\bar{J}^{-1}\bar{F}^a_{\cdot\alpha})_{:a} = \epsilon_{\alpha\beta\chi}\epsilon^{abc}\bar{F}^{-1\beta}_{\quad\cdot a}\bar{F}^{-1\chi}_{\quad\cdot[b:c]}.$$

Let $\bar{\boldsymbol{q}} = \bar{q}^\alpha \tilde{\boldsymbol{g}}_\alpha$ denote the heat flux vector referred to anholonomic space, let $k^{\alpha\beta}$ denote a covariant constant positive semi-definite tensor of thermal conductivity with the particular form dictated by the material symmetry group, and let θ denote temperature. Nanson's formula and energy invariance among configurations lead to relationships among $\bar{\boldsymbol{q}}$, spatial flux $\boldsymbol{q}$, and reference flux $\boldsymbol{Q}$:

$$(21)\qquad \bar{q}^\alpha = \bar{J}\bar{F}^{-1\alpha}_{\quad\cdot a}q^a = \tilde{J}^{-1}\tilde{F}^\alpha_{\cdot A}Q^A = -k^{\alpha\beta}\partial_\beta\theta.$$

Heat transfer per unit anholonomic volume is the divergence [6, 7]

$$\begin{aligned}\bar{\nabla}_\alpha \bar{q}^\alpha &\overset{\text{def}}{=} \nabla_\alpha \bar{q}^\alpha + \bar{q}^\alpha \bar{J}(\bar{J}^{-1}\bar{F}^a_{\cdot\alpha})_{:a} = \nabla_\alpha \bar{q}^\alpha + \bar{q}^\alpha \tilde{J}^{-1}(\tilde{J}\tilde{F}^{-1A}_{\quad\cdot\alpha})_{:A} \\ &= \tilde{J}^{-1}\nabla_A Q^A = \bar{J}\nabla_a q^a.\end{aligned} \tag{22}$$

Four choices of basis $\{\tilde{\boldsymbol{g}}_\alpha\}$ are considered. In the first case, the anholonomic object is assumed to vanish such that Euclidean position vector $\tilde{\boldsymbol{x}}(X)$ exists:

$$\tilde{\boldsymbol{g}}_\alpha = \partial_\alpha \tilde{\boldsymbol{x}}, \quad \Gamma^{\cdot\cdot\alpha}_{\beta\chi} = \tfrac{1}{2}\tilde{g}^{\alpha\delta}\partial_{\{\beta}\tilde{g}_{\delta\chi\}}, \quad (\tilde{J}\tilde{F}^{-1A}_{\quad\cdot\alpha})_{:A} = 0, \quad (\bar{J}^{-1}\bar{F}^a_{\cdot\alpha})_{:a} = 0; \tag{23}$$

$$\bar{\nabla}_\alpha \bar{q}^\alpha = \partial_\alpha \bar{q}^\alpha + \bar{q}^\alpha \partial_\alpha \ln\sqrt{\tilde{g}} = -k^{\alpha\beta}(\partial_\alpha\partial_\beta\theta - \Gamma^{\cdot\cdot\chi}_{\alpha\beta}\partial_\chi\theta). \tag{24}$$

In the second case, Cartesian intermediate bases $\{\boldsymbol{e}_\alpha\}$ are assigned, but tangent maps need not be integrable:

$$\tilde{\boldsymbol{g}}_\alpha \overset{\text{def}}{=} \boldsymbol{e}_\alpha, \quad \tilde{g}_{\alpha\beta} = \delta_{\alpha\beta}, \quad \Gamma^{\cdot\cdot\alpha}_{\beta\chi} = 0, \quad \nabla_\alpha(\cdot) = \partial_\alpha(\cdot); \tag{25}$$

$$\bar{\nabla}_\alpha \bar{q}^\alpha = \partial_\alpha \bar{q}^\alpha + \bar{q}^\alpha \bar{J}\partial_a(\bar{J}^{-1}\bar{F}^a_{\cdot\alpha}) = -k^{\alpha\beta}[\partial_\alpha\partial_\beta\theta + \bar{J}\partial_a(\bar{J}^{-1}\bar{F}^a_{\cdot\alpha})\partial_\beta\theta]. \tag{26}$$

In the third case, $\{\tilde{\boldsymbol{g}}_\alpha\}$ are chosen coincident with reference basis vectors $\{\boldsymbol{G}_A\}$; object $\kappa^{\cdot\cdot\alpha}_{\beta\chi}$, torsion $T^{\cdot\cdot\alpha}_{\beta\chi}$, and curvature from $\Gamma^{\cdot\cdot\alpha}_{\beta\chi}$ all may be nonzero [1]; and

$$\tilde{\boldsymbol{g}}_\alpha \overset{\text{def}}{=} \delta^A_\alpha \boldsymbol{G}_A, \quad \Gamma^{\cdot\cdot\alpha}_{\beta\chi} = \tilde{F}^{-1B}_{\quad\cdot\beta}\delta^\alpha_A\delta^C_\chi\Gamma^{\cdot\cdot A}_{BC}, \quad \nabla_\alpha V^\beta = \tilde{F}^{-1A}_{\quad\cdot\alpha}\nabla_A V^B\delta^\beta_B; \tag{27}$$

$$\bar{\nabla}_\alpha \bar{q}^\alpha = -k^{\alpha\beta}[\partial_\alpha\partial_\beta\theta - \tilde{F}^{-1A}_{\quad\cdot\alpha}\delta^B_\beta\delta^\chi_C\Gamma^{\cdot\cdot C}_{AB}\partial_\chi\theta + \tilde{J}^{-1}(\tilde{J}\tilde{F}^{-1A}_{\quad\cdot\alpha})_{:A}\partial_\beta\theta]. \tag{28}$$

In the fourth case, $\{\tilde{\boldsymbol{g}}_\alpha\}$ are chosen coincident with spatial basis vectors $\{\boldsymbol{g}_a\}$; object $\kappa^{\cdot\cdot\alpha}_{\beta\chi}$, torsion $T^{\cdot\cdot\alpha}_{\beta\chi}$, and curvature from $\Gamma^{\cdot\cdot\alpha}_{\beta\chi}$ all may be nonzero [1]; and

$$\tilde{\boldsymbol{g}}_\alpha \overset{\text{def}}{=} \delta^a_\alpha \boldsymbol{g}_a, \quad \Gamma^{\cdot\cdot\alpha}_{\beta\chi} = \bar{F}^b_{\cdot\beta}\delta^\alpha_a\delta^c_\chi\Gamma^{\cdot\cdot a}_{bc}, \quad \nabla_\alpha V^\beta = \bar{F}^a_{\cdot\alpha}\nabla_a V^b\delta^\beta_b; \tag{29}$$

$$\bar{\nabla}_\alpha \bar{q}^\alpha = -k^{\alpha\beta}[\partial_\alpha\partial_\beta\theta - \bar{F}^a_{\cdot\alpha}\delta^b_\beta\delta^\chi_c\Gamma^{\cdot\cdot c}_{ab}\partial_\chi\theta + \bar{J}(\bar{J}^{-1}\bar{F}^a_{\cdot\alpha})_{:a}\partial_\beta\theta]. \tag{30}$$

The second case (Cartesian) is most common and presumably most practical for materials of arbitrary anisotropy; the third or fourth cases may prove useful for structures with curved shapes and hexagonal or isotropic symmetry.

References

[1] J.D. Clayton, *On anholonomic deformation, geometry, and differentiation*, Mathematics and Mechanics of Solids (2012), in press, DOI:10.1177/1081286511429887.

[2] J.A. Schouten, *Ricci Calculus*, Springer-Verlag, Berlin (1954).

[3] G. Vranceanu, *Sur les espaces non holonomes*, C R Academie Sciences **183** (1926), 852–854.

[4] W. Noll, *Materially uniform simple bodies with inhomogeneities*, Archive for Rational Mechanics and Analysis **27** (1967), 1–32.

[5] J.D. Clayton, D.J. Bammann, D.L. McDowell, *Anholonomic configuration spaces and metric tensors in finite strain elastoplasticity*, International Journal of Non-Linear Mechanics **39** (2004), 1039–1049.

[6] J.D. Clayton, *Nonlinear Mechanics of Crystals*, Springer, Dordrecht (2011).

[7] J.D. Clayton, *A continuum description of nonlinear elasticity, slip and twinning, with application to sapphire*, Proceedings of the Royal Society of London A **465** (2009), 307–334.

Simplified Methods for rate dependent processes based on a thermodynamic variational principle

Alan C. F. Cocks

A wide range of rate dependent processes can be analysed using the variational functional

$$\Pi = \Psi + \dot{G}\,, \tag{1}$$

where Ψ is a global rate potential and $\dot{G}$ is the rate of change of Gibbs free energy. Each of these quantities can be expressed in terms of suitable rate degrees of freedom that describe the evolution of the state of a body. The appropriate combination of these rates is that which minimises the functional. This condition follows directly from the requirement that is convex. This framework can be used to develop detailed numerical models in terms of many degrees of freedom. It can also provide a framework for the development of simpler models in terms of a small number of degrees of freedom. This latter approach is ideally suited to the development of multiscale models. It allows simplification to be made at one scale which are thermodynamically and kinetically consistent and which naturally filter information to provide that which is most important for the development of models at a higher scale. This methodology has been applied to an extensive range of problems in which a wide range of different kinetic processes contribute to the material and/or component response, including surface/interface/boundary/bulk diffusion, interface reactions, attachment/detachment and evaporation/condensation processes, and linear and non-linear viscous processes. These are all captured through suitable functional forms for the rate potential. Similarly, the approach can accommodate thermodynamic driving forces arising from mechanical, electrical or chemical effects, through identification of the major contributions to $\dot{G}$.

Models of the sintering of particulate systems and of sintering and mud-cracking in thermal barrier coatings have been developed by assuming simple geometric profiles of necks between contacting particles and asperities. Similarly, models for the growth of cavities and cracks in creeping solids and the growth of quantum dots have been developed by assuming simple shapes of the voids, cracks or dots, which have either been guided by detailed numerical simulations or experimental observations. The choice of simple representative profiles allows the state to be represented by a limited number of internal variables. Use of the variational principle then provides constitutive relationships for the material behaviour and evolution laws for the internal state variables, which can be represented in terms of convex potentials.

The variational principle has also allowed detailed and simplified models of dislocation climb to be developed. At elevated temperatures edge dislocations can move normal to their slip plane by either emitting or absorbing vacancies. When combined with a continuity equation which relates the diffusive flux into the core to the rate of climb, the variational functional provides: the chemical potential for vacancy diffusion, in terms of the local vacancy concentration and stress state;

the Peach-Kohler and drag forces for dislocation climb; the governing diffusion equation, which is a function of local state; and boundary conditions. These equations can be solved using conventional finite element techniques, but fine meshes are required adjacent to the dislocation cores to fully capture the details of the local diffusion process. This severely limits the scale of problem that can be analysed. Detailed simulations of small groups of dislocations reveal that limited climb (less than the length of the Burgers vector) occurs as the vacancy concentration field moves towards a steady state. This observation allows terms which relate to changes of the local concentration of vacancies to be simply removed from the variational functional. The variational functional can be simplified further by assuming a uniform effective diffusivity throughout the body, with the magnitude of this diffusivity and the effective size of the dislocation cores determined by calibration against a wide range of simulations using the set of equations generated from the full variational principle. These observations and simplifications allow the diffusional interaction of the dislocations to be modelled as a classical multi-source potential problem. This potential problem can be cast within the framework of the variational principle, where now the only degrees of freedom are the climb velocities of the dislocations. This reduced model, when combined with conventional models of dislocation climb, allows large arrays of dislocations to be analysed and avoids the need to solve a computationally expensive background field problem for the diffusional interaction of the dislocations.

Generalized continuum crystal plasticity

Samuel Forest

The micromorphic medium, as invented by Eringen and Mindlin, represents one of the most general continuum theories. The links between the micromorphic continuum and the plasticity of crystalline materials has been recognized very early by Eringen himself. Lattice directions in a single crystal can be regarded as directors that rotate and deform as they do in a micromorphic continuum. The fact that lattice directions can be rotated and stretched in a different way than material lines connecting individual atoms, especially in the presence of static or moving dislocations, illustrates the independence between directors and material lines in a micromorphic continuum, even though their deformations can be related at the constitutive level.

The identification of a micromorphic continuum from the discrete atomic single crystal model is possible based on proper averaging relations. Analytical solutions have been provided that give the generalized stress fields around individual screw or edge dislocations embedded in an elastic generalized continuum medium, like the micromorphic medium. The physical meaning of such a calculation is the account of non–local elasticity at the core of dislocations that may suppress or limit the singularity of the stress fields. For instance, non singular force and couple stress were determined for a screw dislocation embedded in a gradient micropolar medium that combines the first strain gradient with independent rotational degrees

of freedom. The unphysical singularities at the core of straight screw and edge dislocations are also removed when the second gradient of strain is introduced in the theory, while the first strain gradient is not sufficient.

The next step is to consider the collective behaviour of dislocations in a single crystal by means of the continuum theory of dislocations. The material volume element is now assumed to contain a large enough number of dislocations for the continuum theory of dislocation to be applicable. Non–homogeneous plastic deformations induce material and lattice incompatibilities that are resolved by a suitable distribution of the dislocation density tensor field which is a second rank statistical mean for a population of arbitrary dislocations inside a material volume element [10]. Nye's fundamental relation linearly connects the dislocation density tensor to the lattice curvature field of the crystal. This fact has prompted many authors to treat a continuously dislocated crystal as a Cosserat continuum. The Cosserat approach records only the lattice curvature of the crystal but neglects the effect of the rotational part of the elastic strain tensor, which is a part of the total dislocation density tensor [5]. Full account of plastic incompatibilities is taken in strain gradient plasticity theories, starting from the original work by Aifantis up to recent progress in [9]. Formulation of crystal plasticity within the micromorphic framework is more recent and was suggested in [3] for a large spectrum of crystal defects, including point defects and disclinations. Limiting the discussion to dislocation density tensor effects, also called geometrically necessary dislocation (GND) effects, it was shown in [5], within a small deformation setting, how the micromorphic model can be used to predict grain and precipitate size effects in laminate crystalline materials. In particular, the micromorphic model is shown to deliver more general scaling laws than conventional strain gradient plasticity. These models represent extensions of the conventional crystal plasticity theory that accounts for single crystal hardening and lattice rotation but does not incorporate the effect of the dislocation density tensor.

The objective of the present work is, first, to formulate a finite deformation micromorphic extension of conventional crystal plasticity to account for GND effects in single crystals, and, second, to show that the micromorphic approach can also be used to predict grain size effects in polycrystals. The first part represents an extension to finite deformation of the model proposed in [1, 5]. It also provides new analytical predictions of size effects on the yield stength and kinematic hardening of laminate microstructures made of an elastic layer and an elastic–plastic single crystal layer undergoing single slip [7, 8]. The theory is called the *microcurl* model because the evaluation of the curl of the microdeformation, instead of its full gradient, is sufficient to account for the effect of the dislocation density tensor. The second part is dedicated to finite element simulations showing the continuum description of pile–up formation around hard particles in metal single crystal matrix [2] and on the effect of grain size on the overall mechanical response and the development of intragranular plastic strain fields of polycrystals [4].

The models proposed in this work for single crystals fall in the class of anisotropic elastoviscoplastic micromorphic media for which constitutive frameworks at finite deformations have been proposed [6].

References

[1] O. Aslan, N. M. Cordero, A. Gaubert, S. Forest, *Micromorphic approach to single crystal plasticity and damage*, International Journal of Engineering Science **49** (2011), 1311–1325.

[2] H. J. Chang, A. Gaubert, M. Fivel, S. Berbenni, O. Bouaziz, S. Forest, *Analysis of particle induced dislocation structures using three-dimensional dislocation dynamics and strain gradient plasticity*, Computational Materials Science **52** (2012), 33–39.

[3] J. D. Clayton, D. J. Bamman, D. L. McDowell, *A geometric framework for the kinematics of crystals with defects*, Philosophical Magazine **85** (2005), 3983–4010.

[4] N. M. Cordero, S. Forest, E. P. Busso, S. Berbenni, M. Cherkaoui, *Grain size effects on plastic strain and dislocation density tensor fields in metal polycrystals*, Computational Materials Science **52** (2012), 7–13.

[5] N.M. Cordero, A. Gaubert, S. Forest, E. Busso, F. Gallerneau, S. Kruch, *Size effects in generalised continuum crystal plasticity for two–phase laminates*, Journal of the Mechanics and Physics of Solids **58** (2010), 1963–1994.

[6] S. Forest, *The micromorphic approach for gradient elasticity, viscoplasticity and damage*, ASCE Journal of Engineering Mechanics **135** (2009), 117–131.

[7] S. Forest, *Some links between cosserat, strain gradient crystal plasticity and the statistical theory of dislocations*, Philosophical Magazine **88** (2008), 3549–3563.

[8] S. Forest, R. Sedláček, *Plastic slip distribution in two–phase laminate microstructures: Dislocation–based vs. generalized–continuum approaches*, Philosophical Magazine A **83** (2003), 245–276.

[9] M. Gurtin, *A gradient theory of single–crystal viscoplasticity that accounts for geometrically necessary dislocations*, Journal of the Mechanics and Physics of Solids **50** (2002), 5–32.

[10] B. Svendsen, *Continuum thermodynamic models for crystal plasticity including the effects of geometrically-necessary dislocations*, J. Mech. Phys. Solids **50**, 1297–1329.

The missing flow rule?

Gilles A. Francfort

(joint work with Alessandro Giacomini)

In this very short talk we revisit our Oberwolfach talk of December 2011 during the Workshop entitled: "Variational Methods for Evolution ".

We assume perfect small strain elasto-plastic evolution in the absence of inertia and body loads (for simplicity sake). Thus the only driving mechanism is a boundary displacement $w(x,t)$ on the Dirichlet part of the boundary.

Then, the restriction that the deviatoric part of the Cauchy stress $\sigma_D(t)$ should remain within the set of admissible stresses K, together with the balance equation $\operatorname{div} \sigma(t) = 0$, immediately implies that the tangential part of the surface traction $\sigma(t)\nu$ – where ν is the outer normal to a point at the Dirichlet boundary of the domain – must satisfy

$$(\sigma(t)\nu)_\tau = (\sigma_D(t)\nu)_\tau \in (K\nu)_\tau,$$

with obvious notation.

But, since at such a point, the plastic strain is given by $[w(t)-u(t)]\odot\nu$ ($u(x,t)$ being the displacement field), it is natural, if adopting the Clausius-Duhem view of the positivity of the mechanical dissipation, to expect a boundary flow rule, namely

$$[\dot{w}(t)-\dot{u}(t)]\in N_{(K\nu)_\tau}((\sigma_D\nu)_\tau).$$

Above, $N_{(K\nu)_\tau}(\xi)$ is the normal cone (a cone of vectors) to the set $(K\nu)_\tau$ (a set of vectors orthogonal to ν) at ξ.

That flow rule is not implied by the bulk flow rule and must be added to the traditional set of equations governing the evolution if Hill's maximum plastic work principle is expected.

Similarly, in the case of a multiphase material, then, at the interface between phases i anf j (with associated sets of admissible stresses K_i and K_j), one has

$$(\sigma_D\nu)_\tau\in(K_i\nu)_\tau\cap(K_j\nu)_\tau.$$

So one should also obey the following flow rule:

$$\dot{u}_i-\dot{u}_j\in N_{(K_i\nu)_\tau\cap(K_j\nu)_\tau}((\sigma_D\nu)_\tau).$$

Absent such a rule, the problem will be undetermined because of the possible presence of plastic slips along such interfaces. That flow rule seems to be absent from the mechanics literature.

Also, this is the only flow rule that will abide by Hill's maximum plastic work principle, so that there is no possibility of constitutively "modeling" interfacial behavior. That behavior is set by that inside the phases.

References

[1] G.A. Francfort, A. Giacomini, *Small Strain Heterogeneous Elastoplasticity Revisited*, Comm. Pure Applied Math., to appear.

Equilibrium and kinetics of interface boundaries and chemical reactions fronts in elastic solids

Alexander B. Freidin

(joint work with Mikhail Antimonov, Andrej Cherkaev, E.N. Vilchevskaya, I.K. Korolev, D.O. Volkova)

Considering solids undergoing stress-induced and stress-assisted phase or chemical transformations we focus on the following problems.

• *Phase transitions limit surfaces and exact energy lower bounds construction.*

We construct direct and reverse transformations surfaces in strain space based on two approaches. The first one is based on local thermodynamic equilibrium considerations and uses a semi-inverse method. The shape of the new phase nucleus is prescribed (layer, cylinder, ellipsoid) and external strains are found at which the boundary of such a nucleus can satisfy the local equilibrium conditions (including the Maxwell relation). Then geometric parameters of the nucleus shape

and orientation can be found in dependence of the external strains (see, e.g., [1, 2] and references therein). We construct the surfaces of the appearance of new phase equilibrium seeds of various shape in strain space and after discussion of the the new phase domains stability we consider an envelope of such surfaces as a kind of transformation surface.

The second approach is based on construction of an exact energy lower bound for a composite with a fixed volume fraction of the new phase. We construct such a bound using translation estimates (see, e.g., the monographs [3, 4] and references therein), and compute the corresponding fields in an optimal microstructure. We show that, depending on a strain state, the bound is attained if the microstructure is a first, second or third order laminate. For arbitrary isotropic phases and arbitrary average strains we find the microstructure parameters in dependence of the average strains. We note that two types of second order laminate are needed to cover the whole strain space: with normals which coincide with the eigenvectors of the average strain tensor and with normals which do not lie in the eigenplane of the strain tensor – so called declined second order laminates (cf. with [5]). As a result we find all optimal microstructures for a 3D elastic two-phase composite.

Then, given an average strain, we find the equilibrium new phase volume fraction minimizing the energy lower bound with respect to the volume fraction. Those strains at which the equilibrium volume fraction tends to zero form the transformation limit surface in strain space. Finally we compare the transformation surfaces and microstructures for the direct and reverse transformations obtained by two approaches.

• *Kinetics of interphase boundaries in elastic solids.*

We consider a moving interphase boundary within the frameworks of configuration (driving) forces concept. We write down the kinetic relationship as an equation that relates the interface velocity, the strains on one side of the interface and the normal to the interface [1]. Strains at which this equation can be satisfied form a so called "modified" phase transition zone (PTZ) in a strain space.

The PTZs for the case of the equilibrium interface were constructed earlier (see, e.g., [2] and references therein). Here we focus on the modified PTZ-boundaries and demonstrate that the modified PTZ-boundaries construction in a case of stationary moving interface gives the answer to the following two questions:

– Given interface velocity, what are the strains which can exist at the interface?

– How does strain state affect the interface orientation with respect to the strain tensor axis?

Giving examples of the PTZ construction we examine how material parameters and strains affect the interface velocity and local orientation.

• *Kinetics of chemical reactions fronts propagation in deformable solids.*

Finally we consider a propagating stress-assisted chemical reaction front propagation implying a reaction such as silicon oxidation.

After deriving an expression of the entropy production due to the reaction front propagation we construct the chemical affinity tensor as a combination of Eshelby stress tensors of the solid constituents and a chemical potential of a gaseous constituent [7]. We determine a transformation strain tensor produced by the chemical reaction in dependence of the reaction parameters. We demonstrate that the transformation strain produces internal stresses which in turn affect the chemical reaction front kinetics. We discuss how external and internal stresses can accelerate or decelerate the reaction front propagation.

Acknowledgement: This work was supported by the Russian Foundation for Basic Research (10-01-00670-a), National Science Foundation (DMS-0707974), Sandia National Laboratories and the Program for Fundamental Research of RAS.

References

[1] A.B. Freidin, *On new phase inclusions in elastic solids*, Z. Angew. Math. Mech. **87** (2007), 102–116.
[2] A.B. Freidin, L.L. Sharipova, *On a model of heterogeneous deformation of elastic bodies by the mechanism of multiple appearances of new phase layers*, Meccanica, **41** (2006), 321–339.
[3] A.V. Cherkaev, *Variational Methods for Structural Optimization*. Springer-Verlag, Berlin, Heidelberg, London, 2000.
[4] G.W. Milton, *The theory of composites*, Cambgidge University Press, 2004.
[5] I.V. Chenchiah, K. Bhattacharya, *The relaxation of two-well energies with possibility unequal moduli*, Arch. Rat. Mech. Anal. **187** (2008), 409–479.
[6] R. Abeyaratne, J.K. Knowles, *Evolution of phase transitions. A continuum theory*, Cambridge University Press, Cambridge, New York, Melbourne, 2006.
[7] A.B.Freidin, *On chemical reaction fronts in nonlinear elastic solids*, Proceedings of XXXVI International Summer School-Conference APM2009, St.Petersburg. Institute for problems in mechanical Engineering. (2009), 231–237.

Comparison of spherical and cubical representative volume elements with respect to convergence, anisotropy and localization behavior

Rainer Glüge
(joint work with Martin Weber, Albrecht Bertram)

The representative volume element (RVE) technique is commonly used for the estimation of the effective properties of a micro-structured material. Mostly, cubical RVEs with periodic boundary conditions are employed, which result in a better convergence, compared to the uniform boundary conditions. In this work, the possibility of using spherical RVEs is discussed, since their use promises a reduction of the influence of the boundary, and thus a more efficient estimation of the effective material properties. We assess the convergence of spherical and cubical RVEs to the effective material behavior for the uniform and periodic boundary conditions, which are given by

$$\boldsymbol{u} = \bar{\boldsymbol{H}}\boldsymbol{x}_0, \qquad \text{linear displacement BC} \tag{1}$$

$$\boldsymbol{t} = \bar{\boldsymbol{T}}\boldsymbol{n}_0, \qquad \text{homogeneous traction BC} \tag{2}$$

$$\boldsymbol{u}^+ - \boldsymbol{u}^- = \bar{\boldsymbol{H}}(\boldsymbol{x}_0^+ - \boldsymbol{x}_0^-), \quad \boldsymbol{t}^+ = -\boldsymbol{t}^-, \quad \boldsymbol{n}_0^+ = -\boldsymbol{n}_0^- \qquad \text{coupled BC}\,. \tag{3}$$

The displacement, position in the reference placement and surface normal in the reference placement are denoted by $\boldsymbol{u}$, $\boldsymbol{x}_0$ and $\boldsymbol{n}_0$. The imposed average displacement gradient and the imposed average first Piola-Kirchhoff-stresses are written as $\bar{\boldsymbol{H}}$ and $\bar{\boldsymbol{T}}$. The coupled BC require to form pairs of surface points with opposing surface normals. In case of spherical RVE, this assignment is unique, in case of cubical RVE the surface points are usually paired such that the RVE boundary allows for a periodic arrangement, thus the common denomination as periodic BC. All these BC satisfy the Hill-Mandel-condition. However, the coupled BC are mostly preferred over the uniform BC since the latter correspond to extremal assumptions (suppress either strain or stress fluctuations on the boundary).

We assessed the RVE quality by examining different aspects of the homogenized properties of an elastic-plastic, macroscopically isotropic matrix-inclusion material. We generated a large material sample, from which we cutted out spherical and cubical RVE of different sizes. For each size, we examined 100 realizations with the different BC. The RVE has been subjected to a uniaxial tension test in the $\boldsymbol{e}_1$ direction, and Young's modulus and the Cauchy stress component σ_{11} at 10% of nominal strain have been extracted.

Anisotropy. The elastic as well as the plastic properties of the macroscale material show a cubic anisotropy for small cubical RVE, independently on the BC. This anisotropy is strongest for the periodic BC. However, this effect vanishes as the RVE size is increased.

Convergence. Considering the linear displacement boundary conditions, the spherical RVE converge faster to the effective material behavior as the RVE size is increased. Results of similar quality require cubical RVE with a volume of roughly four times the volume of the corresponding spherical RVE. For the coupled BC, the results are quite close, but the spherical RVE perform slightly better. For the homogeneous traction BC, convergence has been considered only for Young's modulus, since the RVE tend to localize extremely soon for this BC. No notable difference has been found in this case.

Localization. For this issue we considered a softening, isotropic, von Mises-plastic material. It has been assigned homogeneously on RVE with a perturbation near the center. Only the coupled BC have been employed, since the linear displacement BC do not allow for an RVE-wide localization, and the homogeneous traction BC allow for arbitrary localizations. The coupled BC are used by many researchers who address macroscale material failure by microscale mechanisms, in order to determine macroscale traction-separation laws or stability maps, for example. We subjected the RVE to a simple shear deformation, where the shear direction has been varied. It is found that the localization behavior differs markedly between cubical and spherical RVE. The spherical RVE form a single shear zone of 50% of volume fraction, and the stress-strain curves are practically independent on the shear direction. The cubical RVE display a shifting between differently

oriented shear bands, leading to non-monotonic stress-strain curves. This is due to the fact that shear banding parallel to the imposed shear direction is due to the cubic periodicity pattern not always possible. Thus, the imposed effective shearing is approximated by successive shearing in different directions. For shearing in 0° and 45° the response is softest, since shear bands can align nicely with the periodicity frame. This effect is independent on the RVE size. However, none of the RVE recovered the softening stress strain law correctly, although the RVE could be considered as practically homogeneous. Only for linear displacement BC, the microscale material law has been conducted to the macroscale. This indicates that for softening materials one should employ the linear displacement BC.

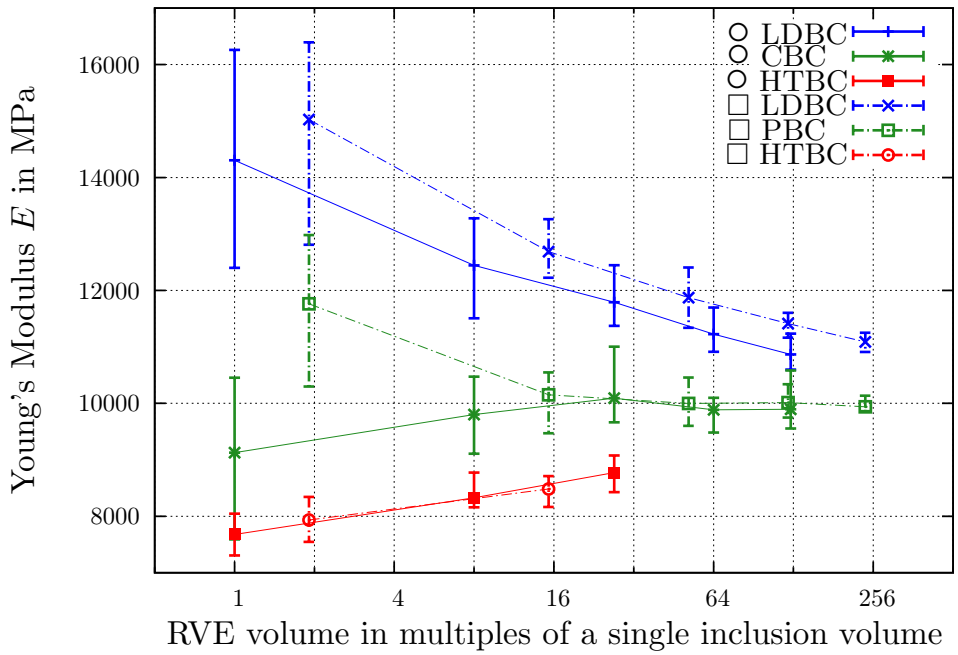

Competition of energies, interface effects and scaling laws for martensitic microstructures

Klaus Hackl
(joint work with Mehdi Goodarzi)

Martensitic materials exhibit different patterns at the micro-level consisting of laminates of twin-compatible variants. These microstructures show a variety of interesting boundary-layer phenomena like branching or needling at interphases to other variants or at grain boundaries. The patterns observed posses prominent self-similarity properties valid over a large range of scales, [4, 5].

In [1, 2, 3] we develop a model explaining these phenomena via a competition of three contributions to the energy stored in the material,

$$\min_{\mathbf{u},\mathbf{a},\mathbf{b},\lambda,h} \{\mathcal{E} : \text{for given boundary conditions}\}\,. \tag{1}$$

Here **u** denotes the macroscopic displacement vector of the material, **a** the displacement-amplitude vector of the laminate microstructure, **b** the normal vector on the twin-interface, λ the volume fraction of twin-variants, and h the lath-width of the laminate, see [1]. The total stored energy

$$\mathcal{E} = \int_\Omega \left(\psi^{\mathrm{el}} + \psi^{\mathrm{in}}\right)\ \mathrm{d}V + \int_\Gamma \psi^\Gamma\ \mathrm{d}A \tag{2}$$

is comprised of elastic strain energy ψ^{el}, interfacial energy between martensitic variants ψ^{in}, and surface energy at boundaries external to the martensitic microstructure ψ^Γ. We employ a three-field approach with volume-fraction λ of the two martensitic variants involved, lath-width h, and displacement-amplitude **u** as independent fields. Energy minimization then yields a system of partial differential equations for those variables, which in general has to be solved numerically.

The model correctly predicts the different scaling propertied observed in experiments, namely

$$\mathcal{E} \propto \gamma^{2/3}, \quad h \propto x^{2/3}, \quad h \propto L^{2/3}, \tag{3}$$

where γ is the specific twin-interface energy, x denotes the distance from an external boundary, and L is the size of a meso-scale twin block-structure, see [1, 2] for a detailed explanation.

We are able to demonstrate, that interfacial energy contributes significantly to the total stored energy in martensitic microstructures. Finally the model is able to distinguish whether a laminate terminates via branching, determined by $h \to 0$, or needling, determined by $\lambda \to 0$ or $\lambda \to 1$, at an outer boundary, both phenomena being seen in experiments. Interestingly the predicted behavior does not only depend on local material properties like specific energies, but also on the global geometry, comprising shape and size, and boundary conditions of the material body under investigation.

References

[1] M. Goodarzi, K. Hackl, *Surface energies in microstructure of martensite*, Proc. Appl. Math. Mech. **11** (2011), 369–370.

[2] M. Goodarzi, K. Hackl, *Numerical simulation of interface effects in martensitic phase transformation*, Proc. Appl. Math. Mech. **11** (2011), 371–372.

[3] K. Hackl, M. Schmidt-Baldassari, W. Zhang, G. Eggeler, *Surface energies and size-effects in shape-memory-alloys*, Mater. Sci. Engng. A **378** (2004), 499–502.

[4] R. V. Kohn, F. Otto, *Small surface energy, coarse-graining, and selection of microstructure*, Phys. D **107** (1997), 272–289.

[5] R. V. Kohn, S. Müller, *Surface energy and microstructure in coherent phase transitions*, Comm. Pure Appl. Math. **47** (1994), 405–435.

Multiscale modeling – extending the design space

Craig S. Hartley

The design of engineering structures has historically treated the materials employed as "black boxes" of immutable properties, whose values are the result of extensive testing and analysis. Generally no consideration is given to the fact that materials properties are often functions of the microstructure of the material, which follows from the processing employed to produce the material. Consequently these material properties are constraints on the design of components and as such, not considered a part of the "design space" within which modifications are possible as part of the design process.

Since the mid-1980s there has been considerable progress towards changing this paradigm by employing models of materials containing structural variables that can be manipulated as part of the design process, thus extending the design space to include the processing of materials to produce desired properties in finished components. In addition, models are increasingly being developed and employed to reduce the amount of testing and experimentation required to produce design databases of properties suitable for inclusion in engineering design software. The development and use of physics-based models of materials that link macro-scale properties, such as those employed in engineering design, to the microstructure of materials at various length and time scales broadly constitutes the field of multiscale modeling. The emerging discipline of Integrated Computational Materials Engineering (ICME) is an example of the application of the principles of multiscale modeling within the engineering community.

The following brief example illustrates one approach to developing a method of extracting a continuum field variable from the results of an advanced computational technique, discrete dislocation dynamics (DDD), that uses physics-based models of dislocation motion to calculate the development of dislocation structures in single crystals as a function of deformation. The intent of this connection is to extract information such as constitutive laws relating the local stress field, temperature and dislocation structure to the behavior of dislocations that cause permanent deformation. This information can then be cast in a form for input to models of crystal plasticity, which relate the deformation of crystalline materials to the behavior of groups of dislocations. The DDD thus provides the means to conduct virtual experiments on simulated crystals under controlled conditions to produce information for use at the next higher length scale.

Consider a crystal deforming by the motion of dislocations on several slip planes. For each slip system, we define a coordinate system based on the slip direction η, normal to the slip plane ν, and Taylor axis ξ, where the triad $(\eta\,\nu\,\xi)$ forms a right-hand set. Represent the distribution of dislocations in each slip system by three coplanar vectors formed from the projections of the dislocation lines along the slip direction (screw components) and Taylor axis (edge components). Define the Direct Dislocation Density Vector ρ^{G} as the vector sum of the projected lengths of positive and negative screw and edge segments of dislocations in the population. If the total projected lengths of screw and edge components of opposite sign occur in

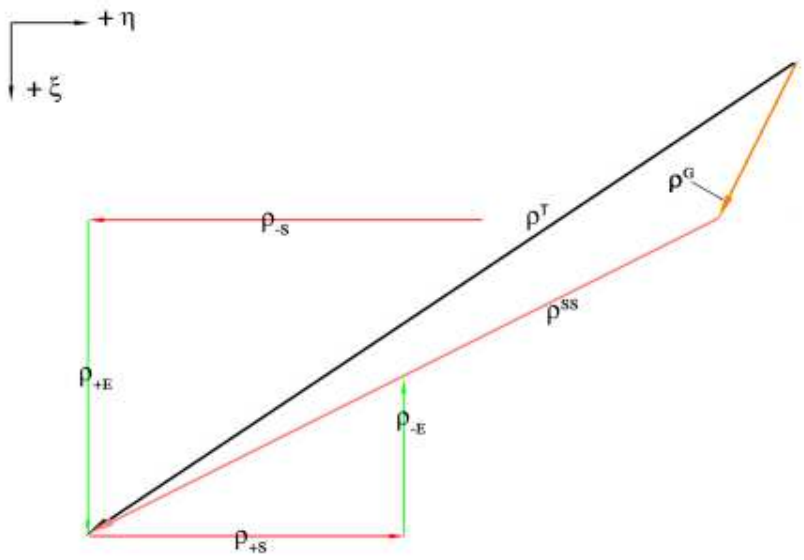

FIGURE 1. Direct and derived dislocation density vectors

equal pairs for the dislocation population, the Burgers vector flux across a section plane intersecting the slip planes is null and this vector is undefined. The Total Dislocation Density Vector ρ^{T} has screw and edge components that are equal to the L1 norms of the associated signed components. When the DDDV is not zero, the direction of the TDDV is chosen so that the vectors make an acute angle, otherwise the direction of the TDDV is undefined. The Statistically Stored DDV ρ^{SS} is the vector difference between the TDDV and the DDDV. The relationships are illustrated schematically in Figure 1.

Following the evolution of these vector components as deformed structures develop in DDD simulations or direct observations of deformed structures in transmission electron microscopy provides a means of quantifying the growth of the dislocation content and separating the contributions of the components of the TDDV, while simultaneously giving information about the screw-edge character of the dislocation distribution.

Applications in thermal and thermo-mechanically coupled problems

STEFAN HARTMANN
(joint work with K. J. Quint, S. Rothe)

In Engineering Sciences there exist a number of applications where thermal processes at large temperatures below the melting limit are of interest. For example, in metal forming the heat is applied by electrical induction in a local region in order to obtain, after the forming and the subsequent cooling process, particular material properties, see [6]. Another application are field-assisted sintering processes, where a powder material is heated, compressed and cooled down. This

process, goes very fast and the heating phase exceeds 600 Kelvin/minute. In the metal forming application large spatial temperature gradients but also large temperature rates occur, whereas in the powder compaction process very fast heating and cooling processes are applied. Moreover, all material properties describing the temperature evolution are functions of the temperature itself, for both the tools and the material itself, and the mechanical balance equations depends on the temperature-dependent material properties.

In order to understand the coupled problems mentioned above, the fully coupled and highly non-linear equations have to be investigated. In the given lecture a rigorous application of the method of vertical lines is performed, where the spatial discretization is carried out using finite elements. This yields differential-algebraic (DAE-system), ordinary differential (ODE) or systems of (non-)linear equations, see [1, 2, 3]. Which kind of mathematical structure results depends essentially on the underlying initial boundary-value problem and the constitutive model describing the material. In the case of an existing system of DAEs or ODEs higher-order diagonally implicit Runge-Kutta methods (DIRK) are applied in combination with the Multilevel-Newton algorithm, see [4, 7]. The latter is applied in order to keep the size of resulting system of non-linear equations as small as possible, because the material properties are formulated as systems of ordinary-differential equations which are point-wise independent. It turns out that the application of DIRK-methods is a promising tool because high-order methods are applicable and current implicit finite element programs remain nearly unchanged when they are extended (at least order two is obtained depending on the underlying equations). Additionally, temporal step-size control for restricting the local integration errors are applied. The time-adaptive procedure stabilizes the entire computational procedure as well. Moreover, beside the DIRK-methods, which lead coupled systems of non-linear equations, very efficient iteration-free methods are applicable, namely, Rosenbrock-type methods, [2, 5] which seems to be a promising procedure in coupled finite element analyses.

References

[1] P. Ellsiepen, S. Hartmann, *Remarks on the interpretation of current non-linear finite-element-analyses as differential-algebraic equations*, International Journal for Numerical Methods in Engineering **51** (2001), 679–707.

[2] A.-W. Hamkar, S. Hartmann, *Theoretical and numerical aspects in weak-compressible finite strain thermo-elasticity*, Journal of Theoretical and Applied Mechanics **50**(1) (2012), 3–22.

[3] S. Hartmann, *Computation in finite strain viscoelasticity: finite elements based on the interpretation as differential-algebraic equations*, Computer Methods in Applied Mechanics and Engineering **191**(13-14) (2002), 1439–1470.

[4] S. Hartmann, *A remark on the application of the Newton-Raphson method in non-linear finite element analysis*, Computational Mechanics **36**(2) (2005), 100–116.

[5] S. Hartmann, A.-W. Hamkar, *Rosenbrock-type methods applied to finite element computations within finite strain viscoelasticity*, Computer Methods in Applied Mechanics and Engineering **199**(23-24) (2010), 1455–1470.

[6] K. J. Quint, S. Hartmann, S. Rothe, N. Saba, K. Steinhoff, *Experimental validation of high-order time integration for non-linear heat transfer problems*, Computational Mechanics **48**(1) (2011), 81–96.

[7] N. Rabbat, A. Sangiovanni-Vincentelli, H. Hsieh, *A multilevel Newton algorithm with macromodeling and latency for the analysis of large-scale nonlinear circuits in the time domain*, IEEE Transactions on Circuits and Systems **26** (1979), 733–740.

Higher order alignment tensors in continuum dislocation dynamics

Thomas Hochrainer

Single crystal plasticity is mediated by the motion of dislocations. Dislocations are line like crystal defects which carry a characteristic unit of shear, the Burgers vector $\mathbf{b}$, and may move when subject to stresses. A moving dislocation crossing a crystal volume shifts the two parts of the crystal separated through the surface swept by the dislocation relative to each other by its Burgers vector. At low temperatures dislocations typically only move within planes containing the line direction and the Burgers vector. Dislocation density theories for single crystals therefore typically work on a glide system basis and dislocations are treated as planar curves within their glide plane.

There are two traditional macroscopic dislocation density measures, which are the scalar total dislocation density ρ_{t} and the dislocation density tensor α. While the statistical definition behind the scalar density is rather obvious as a line length per unit volume, the statistical nature of the dislocation density tensor is somewhat obscured by its common definition, $\alpha = \mathrm{curl}\beta^{\mathrm{p}}$, as the curl of the plastic distortion tensor β^{p}, which allows for its definition even in fully phenomenological theories which do not mention dislocations otherwise. Statistical theories of dislocations were first developed for straight parallel edge dislocations and later generalized to systems of curved dislocations [1]. The theory for curved dislocations is a mesoscopic theory in the sense that it contains variables defined on a manifold appended to each point of the crystal. These mesoscopic variables are the orientation distribution function $\rho(x,\varphi)$ and the curvature density $q(x,\varphi)$, which are both defined on the unit circle within the glide plane and which together define the dislocation density tensor of second order. To simplify the presentation we fix a glide system and choose a coordinate system, such that the Burgers vector $\mathbf{b}$ points in 1-direction and the glide plane normal $\mathbf{n}$ in 3-direction. The unit circle in the glide plane is parameterized by the angle φ to the direction of the Burgers vector in mathematically positive direction. The evolution of this tensor can be given in terms of the evolution of the density function ρ and the curvature density q as

$$\begin{aligned} \partial_t \rho &= -\mathrm{Div}\,(\rho \mathbf{V}) + vq \\ \partial_t q &= -\mathrm{Div}\,(q\mathbf{V} - \rho\vartheta\mathbf{L})\ , \end{aligned} \tag{1}$$

where Div denotes the divergence operator on the configuration space, $\mathbf{L} = (\cos\varphi, \sin\varphi, 0, \rho/q)$ is the generalized tangent vector and $\mathbf{V} = (v\sin\varphi, -v\cos\varphi, 0, \vartheta)$ is the generalized velocity with the rotational velocity $\vartheta = -\nabla_{\mathbf{L}} v$. We propose to expand the angular dependent density function ρ in irreducible fully symmetric

tensors which we call alignment tensors such that

$$\rho(l) = \frac{1}{2\pi}\left(\rho_t + \sum_{k=1}^{\infty} \frac{(2k+1)!!}{k!}\rho_{i_1\cdots i_k} l^{i_1}\cdots l^{i_k}\right), \tag{2}$$

with $l = l(\varphi) = (\cos\varphi, \sin\varphi, 0)$. The coefficients $\rho_{i_1\cdots i_k}$ are the coefficients of symmetric traceless alignment tensors obtained by integration through

$$\rho_{i_1\cdots i_k} = \int_{S^1} \rho(l)\ \underbrace{l^{i_1}\cdots l^{i_k}}_{\text{sym.traceless}}\ dS\,. \tag{3}$$

Evolution equations for these tensors can be derived from Eq. (1) , which yields a hierarchy of evolution equations which needs to be closed at low order in order to be useful. The lowest order truncation yielding a closed system of equations on slip system level is proposed for the case of an isotropic dislocation velocity v. In that case it suffices to keep the first two tensors of the tensor expansion of the density, that is the total dislocation density ρ_{t} and the dislocation density vector κ which corresponds to the geometrically necessary dislocations. Additionally one needs the zeroth order of a similar expansion for the curvature density q, which we call q_{t}. As the dislocation density vector is contained in the slip plane, $\kappa = (\kappa_1, \kappa_2, 0)$, we introduce the vector tilted clockwise by 90 degrees as $\kappa^{\perp} = (\kappa_2, -\kappa_1, 0)$. With this we find the evolution equations after a simple closure approximation as

$$\begin{aligned}
&\partial_t \rho_{\mathrm{t}} = -\mathrm{div}\left(v\kappa^{\perp}\right) + v q_{\mathrm{t}}\\
&\partial_t \kappa = -\mathrm{curl}\left(v\rho_{\mathrm{t}}\mathbf{n}\right)\\
&\partial_t q = -\mathrm{div}\left(v\tfrac{q_{\mathrm{t}}}{\rho_{\mathrm{t}}} + \tfrac{1}{2|\kappa|}\left[\left(\rho_{\mathrm{t}} + |\kappa|\right)\kappa\otimes\kappa + \left(\rho_{\mathrm{t}} - |\kappa|\right)\kappa^{\perp}\otimes\kappa^{\perp}\right]\right).
\end{aligned} \tag{4}$$

As a simple numerical example we showed that these equations are capable of predicting the line length increase and flux of dislocations, enabling for example the simulation of mechanical annealing as observed in micro-pillar experiments [2]. We view such kinematically closed system of equations on the slip system level as a prerequisite to the development of dislocation based plasticity models. Obviously there remains a lot of room for the inclusion of physics, which mainly displays in the constitutive equation for the dislocation velocity v. A multiple slip extension will moreover have to address latent hardening through the consideration of interactions between slip systems.

References

[1] T. Hochrainer, M. Zaiser, P.Gumbsch, *A three-dimensional continuum theory of dislocations: kinematics and mean field formulation*, Philos. Mag. **87** (2007), 1261–1282.

[2] Z. W. Shan et al., *Mechanical annealing and source-limited deformation in submicrometre-diameter Ni crystals*, Nature Materials **7** (2007), 115–119.

Formulation and calibration of higher-order elastic Localization relationships using the MKS approach

Surya R. Kalidindi
(joint work with Tony Fast)

Localization (opposite of homogenization) describes the spatial distribution of the response field of interest at the microscale for an imposed loading condition at the macroscale. A novel approach called Materials Knowledge Systems (MKS) has been formulated recently to build accurate, bi-directional, microstructure-property-processing linkages in hierarchical material systems to facilitate computationally efficient multi-scale modeling and simulation. This approach is built on the statistical continuum theories developed by Kröner that express the localization of the response field at the microscale using a series of highly complex convolution integrals, which have historically been evaluated analytically. The MKS approach dramatically improves the accuracy of these expressions by calibrating the convolution kernels in these expressions to results from previously validated physics-based models. All of the prior work in the MKS framework has thus far focused on calibration and validation of the first-order terms in the localization relationships. In this paper, we explore for the first time, the calibration and validation of the higher-order terms in the localization relationships. In particular, it is demonstrated that the higher-order terms in the localization relationships play an increasingly important role in the spatial distribution of elastic stress or strain fields at the microscale in composite systems with relatively high contrast.

FE^2 method for electro-mechanical boundary value problems: consistent linearization of macroscopic field equations

Marc-André Keip
(joint work with J. Schröder)

The contribution addresses the computation of the consistent macroscopic tangent within the FE^2 method for electro-mechanically coupled solids. The FE^2 method is a two-scale computational homogenization procedure based on the finite element computation of a macro-scale boundary value problem in consideration of the constitutive response of a micro-scale representative volume element (RVE) attached to each macroscopic material point. The constitutive response of the microscopic RVE is the result of the solution of a microscopic boundary value problem that is driven by energetically consistent boundary conditions. In incremental form, the constitutive relations on the macroscopic scale are given by

$$\Delta\overline{\boldsymbol{\sigma}} = \quad \overline{\mathbb{C}} : \Delta\overline{\boldsymbol{\varepsilon}} - \overline{\boldsymbol{e}}^{T}\Delta\overline{\boldsymbol{E}} \quad \text{and} \quad -\Delta\overline{\boldsymbol{D}} = -\overline{\boldsymbol{e}} : \Delta\overline{\boldsymbol{\varepsilon}} - \overline{\boldsymbol{\epsilon}}\,\Delta\overline{\boldsymbol{E}}, \tag{1}$$

where $\overline{\boldsymbol{\varepsilon}}$ and $\overline{\boldsymbol{E}}$ are the macroscopic strains and the macroscopic electric field, respectively. The macroscopic stresses and electric displacements are denoted as

$\overline{\boldsymbol{\sigma}}$ and $\overline{\boldsymbol{D}}$ and can be determined by averaging over the microscopic counterparts $\boldsymbol{\sigma}$ and $\boldsymbol{D}$ on the RVE following

$$\overline{\boldsymbol{\sigma}} := \frac{1}{V} \int\limits_{\mathrm{RVE}} \boldsymbol{\sigma} \, dv \quad \text{and} \quad \overline{\boldsymbol{D}} := \frac{1}{V} \int\limits_{\mathrm{RVE}} \boldsymbol{D} \, dv. \tag{2}$$

The macroscopic mechanical moduli $\overline{\mathbb{C}}$, piezoelectric moduli $\overline{\boldsymbol{e}}$, and dielectric moduli $\overline{\boldsymbol{\epsilon}}$ appearing in (1) are defined as the partial derivatives $\overline{\mathbb{C}} = \partial_{\overline{\boldsymbol{\varepsilon}}} \overline{\boldsymbol{\sigma}}$, $\overline{\boldsymbol{e}} = \partial_{\overline{\boldsymbol{\varepsilon}}} \overline{\boldsymbol{D}} = -\{\partial_{\overline{\boldsymbol{E}}} \overline{\boldsymbol{\sigma}}\}^T$, and $\overline{\boldsymbol{\epsilon}} = \partial_{\overline{\boldsymbol{E}}} \overline{\boldsymbol{D}}$. In order to derive these moduli, we must compute the partial derivatives of the volume integrals given in (2), so (1) appears as

$$\begin{bmatrix} \Delta\overline{\boldsymbol{\sigma}} \\ -\Delta\overline{\boldsymbol{D}} \end{bmatrix} = \frac{1}{V} \begin{bmatrix} \partial_{\overline{\boldsymbol{\varepsilon}}} \left\{ \int\limits_{\mathrm{RVE}} \boldsymbol{\sigma} \, dv \right\} & \partial_{\overline{\boldsymbol{E}}} \left\{ \int\limits_{\mathrm{RVE}} \boldsymbol{\sigma} \, dv \right\} \\ -\partial_{\overline{\boldsymbol{\varepsilon}}} \left\{ \int\limits_{\mathrm{RVE}} \boldsymbol{D} \, dv \right\} & -\partial_{\overline{\boldsymbol{E}}} \left\{ \int\limits_{\mathrm{RVE}} \boldsymbol{D} \, dv \right\} \end{bmatrix} \begin{bmatrix} \Delta\overline{\boldsymbol{\varepsilon}} \\ \Delta\overline{\boldsymbol{E}} \end{bmatrix}.$$

Additively splitting the microscopic strains and electric field into a constant part and a fluctuating part $\boldsymbol{\varepsilon} = \mathrm{sym}[\nabla \boldsymbol{u}(\boldsymbol{x})] = \overline{\boldsymbol{\varepsilon}} + \widetilde{\boldsymbol{\varepsilon}}$ and $\boldsymbol{E} = -\nabla\phi = \overline{\boldsymbol{E}} + \widetilde{\boldsymbol{E}}$ (with $\int_{\mathrm{RVE}} \widetilde{\boldsymbol{\varepsilon}} \, dv = \boldsymbol{0}$ and $\int_{\mathrm{RVE}} \widetilde{\boldsymbol{E}} \, dv = \boldsymbol{0}$) leads, using the chain rule, to

$$\begin{bmatrix} \Delta\overline{\boldsymbol{\sigma}} \\ -\Delta\overline{\boldsymbol{D}} \end{bmatrix} = \frac{1}{V} \left(\int\limits_{\mathrm{RVE}} \begin{bmatrix} \mathbb{C} & -\boldsymbol{e}^T \\ -\boldsymbol{e} & -\boldsymbol{\epsilon} \end{bmatrix} + \begin{bmatrix} \mathbb{C} : \partial_{\overline{\boldsymbol{\varepsilon}}} \widetilde{\boldsymbol{\varepsilon}} & -\boldsymbol{e}^T \cdot \partial_{\overline{\boldsymbol{E}}} \widetilde{\boldsymbol{E}} \\ -\boldsymbol{e} : \partial_{\overline{\boldsymbol{\varepsilon}}} \widetilde{\boldsymbol{\varepsilon}} & -\boldsymbol{\epsilon} \cdot \partial_{\overline{\boldsymbol{E}}} \widetilde{\boldsymbol{E}} \end{bmatrix} dv \right) \begin{bmatrix} \Delta\overline{\boldsymbol{\varepsilon}} \\ \Delta\overline{\boldsymbol{E}} \end{bmatrix},$$

In order to compute the appearing partial derivatives we analyze the microscopic weak forms in an equilibrium state

$$\begin{aligned} \int\limits_{\mathrm{RVE}} \delta\widetilde{\boldsymbol{\varepsilon}} : \mathbb{C} : (\Delta\overline{\boldsymbol{\varepsilon}} + \Delta\widetilde{\boldsymbol{\varepsilon}}) \; dv - \int\limits_{\mathrm{RVE}} \delta\widetilde{\boldsymbol{\varepsilon}} : \boldsymbol{e}^T \cdot \left(\Delta\overline{\boldsymbol{E}} + \Delta\widetilde{\boldsymbol{E}} \right) \; dv = 0, \\ \int\limits_{\mathrm{RVE}} \delta\widetilde{\boldsymbol{E}} \cdot \boldsymbol{e} : (\Delta\overline{\boldsymbol{\varepsilon}} + \Delta\widetilde{\boldsymbol{\varepsilon}}) \; dv + \int\limits_{\mathrm{RVE}} \delta\widetilde{\boldsymbol{E}} \cdot \boldsymbol{\epsilon} \cdot \left(\Delta\overline{\boldsymbol{E}} + \Delta\widetilde{\boldsymbol{E}} \right) \; dv = 0. \end{aligned}$$

Using the finite element discretization of the microscopic RVE gives after some algebraic manipulations the consistent tangent

$$\begin{aligned} \begin{bmatrix} \overline{\mathbb{C}} & -\overline{\boldsymbol{e}}^T \\ -\overline{\boldsymbol{e}} & -\overline{\boldsymbol{\epsilon}} \end{bmatrix} = \frac{1}{V} \int\limits_{\mathrm{RVE}} \begin{bmatrix} \mathbb{C} & -\boldsymbol{e}^T \\ -\boldsymbol{e} & -\boldsymbol{\epsilon} \end{bmatrix} dv \\ - \frac{1}{V} \begin{bmatrix} \boldsymbol{L}_{uu}^T & \boldsymbol{L}_{\phi u}^T \\ \boldsymbol{L}_{u\phi}^T & \boldsymbol{L}_{\phi\phi}^T \end{bmatrix} \begin{bmatrix} \boldsymbol{K}_{uu} & \boldsymbol{K}_{u\phi} \\ \boldsymbol{K}_{\phi u} & \boldsymbol{K}_{\phi\phi} \end{bmatrix}^{-1} \begin{bmatrix} \boldsymbol{L}_{uu} & \boldsymbol{L}_{u\phi} \\ \boldsymbol{L}_{\phi u} & \boldsymbol{L}_{\phi\phi} \end{bmatrix} \end{aligned}$$

with the FE matrices $\boldsymbol{L}$ and the inverse global (microscopic) stiffness matrix $\boldsymbol{K}$. For a detailed derivation see [1] – [4].

References

[1] J. Schröder, M.-A. Keip, *Multiscale modeling of electro-mechanically coupled materials: homogenization procedure and computation of overall moduli*, M. Kuna, A. Ricoeur (Eds.): IUTAM Symposium on Multiscale Modelling of Fatigue, Damage and Fracture in Smart Materials, IUTAM Bookseries **24**, 265–276, Springer, Netherlands, 2011.

[2] M.-A. Keip, J. Schröder, *Effective electromechanical properties of heterogeneous piezoelectrics*, B. Markert (Ed.): Advances in Extended and Multifield Theories for Continua, Lecture Notes in Applied and Computational Mechanics **59**, 109–128, Springer, Berlin, 2011.

[3] M.-A. Keip, *Modeling of electro-mechanically coupled materials on multiple scales*, Institute of Mechanics, Faculty of Engineering Science, Department of Civil Engineering, University of Duisburg-Essen, 2012.

[4] J. Schröder, M.-A. Keip, *Two-scale homogenization of electromechanically coupled problems: consistent linearization and applications*, submitted to Computational Mechanics.

Bifurcation phenomena in hole expansion testing

Christian Krempaszky

Several methods have been developed to characterize the formablility of sheet materials. Besides standard tensile testing, providing ductility measures sufficient to describe the deep drawability, tests characterizing the stretch flangeability are becoming increasingly important, especially in case of advanced high strength steels. One of the well-established methods quantifying stretch flangeability is hole expansion testing. The forming limits are in this case determined by stretching a machined hole by a conical punch until the first through-thickness crack can be observed, usually appearing at the hole edge. The so-called hole expansion ratio serves as a measure of the stretch flangeability and is defined as the technical strain of the edge fiber in circumferential direction at failure. Due to the mechanical boundary conditions the stress state in the edge fiber of the stretched hole in circumferential direction is uniaxial, similar to a tensile test. However, compared to a uniaxial tensile test specimen exhibiting a homogeneous strain distribution until uniform elongation, the strain distribution in a deformed hole expansion specimen is always highly inhomogeneous. Due to the stabilizing effect of the lesser strained material around the edge fiber, the plastic instability in form of local necking is shifted to much higher plastic strains. Therefore, in hole expansion generally much higher strains can be achieved than in tensile testing. Hole expansion tests of high strength dual-phase steels show, that in most cases no plastic instability can be observed, but the forming limit is reached due to local damage of the dual-phase microstructure [1]. In contrast, the microstructure complex-phase steels is "mechanically" more homogenous, the local stresses in the vicinity of phase boundaries are much lower than in the dual-phase microstructure of similar macroscopic strength at the same macroscopic deformation. Therefore complex-phase steels can be deformed to higher strains than dual-phase steels of similar strength level. However, complex-phase steels may show a plastic instability in hole expansion testing in form of a pronounced periodical necking of the edge-fiber [2]. Within the scope of this contribution a stability analysis is presented on the basis of the membrane shell theory to estimate and to discuss the

occurrence of plastic instabilities in dependence of the strain-hardening behavior, the stress state and the significant geometrical test parameters. The diffuse bifurcation modes of the elastic-plastic membrane shell are investigated in the sense of Shanley [3] as if it were an elastic solid with given tangent moduli as material coefficients. In contrast to classical analyses taking into account homogeneous distributions of the pre-stress state (e.g. [4]) here the emphasis is placed on the analysis of inhomogeneous (axisymmetric) distributions of pre-stress and tangent stiffness. It is shown that the model captures the stabilizing effect of the lesser strained material around the edge fiber and predicts the experimentally observed periodical localization patterns.

References

[1] A. Karelova, C. Krempaszky, E. Werner, P. Tsipouridis, T. Hebesberger, A. Pichler, *Hole expansion of dual-phase and complex-phase AHS steels; effect of the edge conditions*, Steel Research **80** (2009), 71-77.

[2] A. Karelova, C. Krempaszky, M. Dünckelmeyer, E. Werner, T. Hebesberger, A. Pichler, *Formability of advanced high strength steels determined by instrumented hole expansion testing*, Proc. MS&T 2009 Iron & Steel Society and TMS (2009), 1358-1368.

[3] Shanley, F. R., *Inelastic column theory*, J. Aero. Sci. **14** (1947), 261-268.

[4] R. Hill, J. W. Hutchinson, *Bifurcation phenomena in the plane tension test*, J. Mech. Phys. Solids **23** (1975), 239-264.

Continuum dislocation theory and formation of microstructure in ductile single crystals

Khanh Chau Le

(joint work with D. Kochmann, B.D. Nguyen)

The characteristics of plastic deformation of engineering materials depend to a high degree on the material microstructure comprising all structural characteristics on the microscale. Along with the properties of the periodic crystal lattice, the microstructural defects are integral components to determine the macroscopic mechanical response of the material. The most important mechanism for plastic yielding is the nucleation and motion of dislocations in crystals. Dislocation sliding and climbing accomodate plastic deformation, cross-slip or pile-up of dislocations are only two examples of mechanisms responsible for work hardening. Furthermore, dislocations are not only a key microstructural defect for plastic slip but also the core ingredient for forming microstructural patterns and substructures. The formation of microstructure like deformation twinning, polygonization, recrystalization, grain growth, texturing etc. exhibits various rearrangements of dislocation patterns. The aim of this talk is to show that the continuum dislocation theory can be used to describe such formation of microstructure, where we focus just on two continuum models of deformation twinning and of polygonization.

Slip and twinning are the major deformation modes which accomodate a change of shape under the action of applied tractions or displacements. Experimental evidence for deformation twinning was found long time ago and has been reported

to occur especially in bcc, hcp and lower symmetry metals and alloys but also in many fcc metals and alloys with low stacking-fault energy, or other intermetallic compounds as well as in geological materials such as calcite or quartz. Twinning becomes particularly important in metals with only a limited number of slip systems, as it can operate to provide the five slip systems required to satisfy the criterion for a general slip deformation. Deformation twinning basically divides the originally uniform single crystal into two volumetric parts – a parent phase (with unaltered crystal lattice) and a twin phase (with a different crystal lattice orientation). Both phases normally occur in the form of lamellar structures, where a bicrystal consisting of neighboring parent and twin phase is commonly referred to as a *twin*. The twin lattice can be generated either by a rotation of the original crystal lattice by 180° about some axis (mode I) or by reflection in some plane (mode II) so that in both cases – when joint with the undistorted parent phase – an unfaulted single crystal is formed, which exhibits a twin boundary with coincident lattice positions at the interface.

A new ingredient of our theory (see [1]) is the so-called twinning shear produced by the existing dislocations in the already active slip system, which plays a similar role as Bain's strain in the theory of martensitic phase transformations, see e.g. [2]. This twinning shear followed by a rotation enables the initially homogeneous crystal to form the twin phase from the parent phase. The underlying mechanism of twin formation is closely related to that of [3], where a decomposition of the deformation into shear and rotation was employed. The introduction of the twinning shear into the energy of the twin renders the energy multi-welled and non-convex. Besides, there is a dependence of the energy on the gradient of the plastic distortion due the dislocation density. It can be shown by standard variational calculus that, in a certain range of straining, a mixing of parent and twin phase is energetically more preferable and the volume fraction of the twin phase has a finite value at the onset of deformation twinning. This finite jump provides space (or mean free path) for the subsequent dislocation pile-up within the twin phase. In spite of the dislocation pile-up in the twin phase and the elastic behavior of the parent phase, the formation of the twin phase does not lead to hardening of the material but rather to a load drop in the stress-strain curve, until the transition from parent to twin phase is completed and the material hardens again. The load-drop can be explained by the spontaneous formation and subsequent increase of the volume fraction of the twin phase near the second minimum of the energy which considerably lowers the total energy of the material.

The second part of this talk is devoted to the continuum model of polygonization of the single crystal beam. The experimental observations of polygonization have been reported in the late forties of the last century; see for example [4, 5]. The first attempt of taking into account the dislocations in the plastically bent beam was made by Nye [6] who expressed the curvature of a beam caused by dislocations in terms of the dislocation density tensor bearing now his name. However, the qualitative modelling of polygonization based on the continuum dislocation theory was proposed only recently by Le and Nguyen in [7]. In that paper the simplest

case of polygonization of the single crystal beam with one active slip system parallel to the beam axis was considered. The obtained results confirmed the LEDS (low energy dislocation structures) hypothesis. We extend this continuum model to the case of single crystal having one active slip system inclined at some angle to the beam axis (see [8]) and compare the results with the experiments reported in [5]. To match Gilman's experimental setup, we specify the displacements of one face of the beam rather than applying the bending moment to the ends of the beam. We then consider the exact two-dimensional variational problem of minimizing energy of the bent beam within the continuum dislocation theory. Applying the variational asymptotic procedure, we simplify this energy functional and then find the smooth minimizer in closed analytical form. Based on this smooth solution we then construct a sequence of piecewise smooth displacements and piecewise constant plastic distortions having the same bending moment as that of the smooth minimizer. By including also energy contributions at jumps of the plastic distortion, proposed in accordance with the Read-Shockley formula for the low angle tilt boundaries, we show that these discontinuous functions do reduce the total energy of the bent beam. We give also the estimation of the number of polygons depending on the radius of curvature of the bent beam.

References

[1] D. Kochmann, K.C. Le, *A continuum model for initiation and evolution of deformation twinning*, Journal of Physics and Mechanics of Solids **57** (2009), 987–1002.

[2] K. Bhattacharya, *Microstructure of Martensite*, Oxford University Press, Oxford (2003).

[3] R. Bullough, *Deformation twinning in the diamond structure*, Proc. Roy. Soc. Lond. **A 241** (1957), 568–577.

[4] R.W. Cahn, *Recrystallization of single crystals after plastic bending*, Journal of the Institute of Metals **76** (1949), 121–143.

[5] J.J. Gilman, *Structure and polygonization of bent zinc monocrystals*, Acta Metall. **3** (1955), 277–288.

[6] J.F. Nye, *Some geometrical relations in dislocated crystals*, Acta Metall. **1** (1953), 153–162.

[7] K.C. Le, Q.S. Nguyen, *Polygonization as low energy dislocation structure*, Continuum Mech. Thermodyn. **22** (2011), 291–298.

[8] K.C. Le, B.D. Nguyen, *Polygonization: theory and comparison with experiments*, Int. Journal of Engineering Science (to appear).

Second gradient homogenization framework

Darby J. Luscher

(joint work with David L. McDowell, Curt A. Bronkhorst)

The second gradient homogenization framework is part of a hierarchical multiscale approach for modeling microstructure evolution developed by Luscher et al. [1, 2] that places special focus on scale invariance principles needed to assure physical consistency across scales. Within this multiscale framework, the second gradient is used as a nonlocal kinematic link between the deformation of a material point at the coarse scale and the response of a neighborhood of material points at the fine scale contained with the volume Ω. In particular, the deformed position, $\mathbf{y}$,

of points within the fine scale volume element are given by the truncated Taylor series

$$\mathbf{y} = \mathbf{F}\left(\mathbf{x}_o\right) \cdot \mathbf{y}_o + \tfrac{1}{2}\mathbf{G}\left(\mathbf{x}_o\right) : \ \mathbf{y}_o \otimes \mathbf{y}_o + \mathbf{h}\left(\mathbf{y}_o\right) , \tag{1}$$

where $\mathbf{F}$ is the coarse scale deformation gradient, $\mathbf{G}$ is the second gradient of the coarse scale displacement field, $\mathbf{h}$ is a fine scale fluctuation field defined over the referential fine scale coordinates, $\mathbf{y}_o$. Kinematic consistency between two scales demands that the fluctuation field have zero net projection onto coarse scale variables. Additionally, independence of coarse scale variables results in requirements for constraints on the fluctuation field leading to the definition of specific sets of generalized fine scale boundary conditions, (cf. [3]), based upon the orthogonality condition

$$\int_{\Omega} \mathbf{f}^T \cdot \mathbf{f} d\Omega = \mathbf{0} , \tag{2}$$

where $\mathbf{f}$ is the fine scale deformation gradient. A distinct feature of boundary conditions satisfying this requirement is a constraint on the volume average of the fine scale fluctuation field for non-zero second gradient modes of deformation. This aspect of higher-ordered boundary conditions, absent from previous literature, gives rise to an internal body force field, $\mathbf{b}$. The principle of virtual velocities (PVV) is applied to the fine scale volume element to weaken the fine scale linear momentum balance, accordingly

$$\int_{\Gamma} \mathbf{t} \cdot \delta\mathbf{v} d\Gamma + \int_{\Omega} \rho_o \mathbf{b} \cdot \delta\mathbf{v} d\Omega = \int_{\Omega} \mathbf{p} : \delta\dot{\mathbf{f}}^T d\Omega + \int_{\Omega} \rho_o \dot{\mathbf{v}} \cdot \delta\mathbf{v} d\Omega , \tag{3}$$

where $\mathbf{t}$ are tractions on the volume element boundary, Γ, $\mathbf{v}$ is the fine scale velocity field, δ reflects virtual quantities, ρ_o is fine scale mass density, and $\mathbf{p}$ is the fine scale nominal stress. Substitution of the multiscale kinematic decomposition and fluctuation field constraints into this PVV leads to definition of coarse scale nominal stress, $\mathbf{P}$, coarse scale second order stress $\mathbf{Q}$, an extended dynamic second order Hill-Mandel condition, and the variational power used for developing the coarse scale global momentum balance solution. The results from this step differ from previous approaches in the accounting of distributed body forces (important considering internal fluctuation constraints) and microinertial fields (important considering dynamic cases). For example, contrast with Kouznetsova et al. [4, 5]. A multiscale internal state variable (ISV) constitutive theory is developed that is couched in the coarse scale intermediate configuration and from which an important new concept in scale transitions emerges, namely scale invariance of dissipation. The coarse scale Helmholtz free energy is postulated as a state function of elastic strain, $\mathbf{E}_e$, elastic second order strain, $\mathbf{\Gamma}_e$, temperature, T, and a set of k internal state variables $\boldsymbol{\xi}_1, \boldsymbol{\xi}_2, ..., \boldsymbol{\xi}_k$, i.e.,

$$\bar{\psi} = \bar{\psi}\left(\mathbf{E}_e, \mathbf{\Gamma}_e, T, \bar{\boldsymbol{\xi}}_1, \bar{\boldsymbol{\xi}}_2, ..., \bar{\boldsymbol{\xi}}_k\right) . \tag{4}$$

The separate quantities of elastically recoverable and stored free energy and dissipated energy are required to be equal at the fine and coarse scales. These conditions lead to constraints on potential constitutive equations, for example,

$$\dot{\bar{\psi}}_s = \langle \psi_s \rangle + \mathbf{P} : \dot{\mathbf{F}}_{in}^T + \mathbf{Q} \dot{:} \dot{\mathbf{\Gamma}}_{in} - \langle \mathbf{p} : \dot{\mathbf{f}}_{in}^T \rangle \,, \tag{5}$$

where the subscripts s and in denote stored and inelastic quantities, respectively; thus the rate at which energy is stored at the coarse scale consist of a term reflecting volume averages (denoted by $\langle \cdot \rangle$) of sub-fine scale dissipation, e.g. energy stored in lattice strain around dislocations, and a term reflecting the inelastic incompatibility of the fine scale intermediate configuration. Currently, the fine scale material is treated as a classical coaxial Cauchy continuum, for example, modeled using a finite element solution of fine scale momentum balance. The coarse scale problem is solved using a mixed-field finite element implementation of the second-gradient continuum and constitutive equations.

Future work on this framework should include the identification of length scale parameters from carefully integrated modeling and experimental work, the extension of the fine scale material description to include higher-ordered generalized continuum descriptions, e.g. micromorphic crystal plasticity, and extension of strategies for developing meaningful kinematic ISVs, free energy functions, and the associated evolution kinetics.

References

[1] D.J. Luscher, D.L. McDowell, *An Extended Multiscale Principle of Virtual Velocities Approach for Evolving Microstructure*, Procedia Engineering (Mesomechanics 2009, Oxford) **1**(1) (2009), 117–121.

[2] D.J. Luscher, D.L. McDowell, C.A. Bronkhorst, *A Second Gradient Theoretical Framework for Hierarchical Multiscale Modeling of Materials*, Int. J. Plasticity **26**(8) (2010), 1248–1275.

[3] D.J. Luscher, D.L. McDowell, C.A. Bronkhorst, *Essential Features of Fine Scale Boundary Conditions for Second Gradient Multiscale Homogenization of Statistical Volume Elements*, Int. J. Multiscale Computational Engineering **10**(4) (2012), to appear.

[4] V. Kouznetsova, M.G.D. Geers, W.A.M Brekelmans, *Multi-scale constitutive modelling of heterogeneous materials with a gradient-enhanced computational homogenization scheme*, Int. J. Numer. Methods Eng. **54**(8) (2002), 1235–1260.

[5] V. Kouznetsova, M.G.D. Geers, W.A.M Brekelmans, *Multi-scale second-order computational homogenization of multi-phase materials: A nested finite element solution strategy*, Comput. Methods Appl. Mech. Eng., **193**(48-51) (2004), 5525–5550.

Goal oriented adaptivity for phase-field simulation

Rolf Mahnken

For the simulation of arbitrary microstructures phase-field models have become a flexible tool. They allow the incorporation of different energy types, such as free energy, interfacial energy, elastic-strain energy, magnetic energy and electrostatic energy. Different microstructural processes such as phase transformations, elastic and inelastic deformations and long range diffussion within an diffuse-interface can be considered. As a main advantage of phase-field models, the interfaces are free

boundaries with high gradients. Then, with the help of order parameters they can vary smoothly in space during a microstructure evolution. From this viewpoint phase field models are also referred as diffuse-interface models, [1], and are in contrast to a sharp interface description.

In general the theory of phase-field models renders a set of parabolic differential equations, which in most applications are solved with the finite-difference-method for equally refined grids, both in space and in time. Typically its solutions are highly nonhomogenous, and therefore, non-equally refined grids with dense meshes at interfaces between different phases and coarse meshes in homogenous regions would be more advantageous. Consequently, in this paper we concentrate on a general framework for adaptive simulations based on goal-oriented error estimates, as proposed in [2].

Adaptive simulations in general are based on computable a posteriori error estimates, where the energy norm is a common choice. In [4] an important ingredient for derivation of an a posteriori estimate is the Galerkin-orthogonality, which means that the error $\underline{e}_u = \underline{u} - \underline{u}_h$ between the exact solution $\underline{u}$ and the discrete solution $\underline{u}_h$ is orthogonal on the discrete test space with respect to the related bilinear form. For phase field simulations control of an error quantity $Q(.)$ of physical significance, such as a phase field variable or a temperature at specific points can be of interest. Furthermore, for an arbitrary goal functional $Q(.)$ a dual problem is defined, which, by use of the Galerkin-orthogonality, is evaluated for an error representation $Q(\underline{e}_u)$. In order to account for nonlinearity of the variational equations we introduce a secant form for the dual problem, see [3], which for practical purposes is approximated by a tangent form. We also point out the analogous procedure for spatial and temporal goal oriented adaptive refinement.

References

[1] Emmerich, H.: *The Diffuse Interface Approach in Materials Science: Thermodynamic Concepts and Applications of Phase-field Models.* Springer Verlag, Heidelberg, 2003

[2] Eriksson, K.; Johnson, C.; Logg, A., *Adaptive computational methods for parabolic problems*, In: Encycl. of Comp. Mechs., Eds. E. Stein, R. de Borst, J.R. Hughes, John Wiley & Sons, Ltd., 2004

[3] Rüter, M., *Error-controlled Adaptive Finite Element Methods in Large Strain Hyperelasticity and Fracture Mechanics*, Dissertation, University of Hannover, ISBN 3-935732-08-2, 2004

[4] Mahnken, R., *Goal oriented adaptive refinement for phase field modeling with finite elements*, submitted, 2012

Topics in multiscale modeling

S. Dj. Mesarovic

Two fundamental problems of multiscale modeling are:

- the theoretical problem: Mathematically consistent definition of the coarse-scale model, on the basis of the fine-scale model, and,

- the computational problem: Boundary/Interface conditions between domains.

In this talk, two examples of addressing the theoretical problem are considered.

1) Particles to continuum

We use numerical simulations to uncover the (1) micromechanism of dilatancy and critical state, (2) the intrinsic length scale that characterizes shear bands in granular materials.

Dense granular materials exhibit a peculiar behaviour termed *dilatancy*, i.e. a volume increase when sheared under constant pressure. More precisely, when sheared under constant pressure, their volume either dilates or decreases, depending on the combination of pressure and porosity. The *critical state* is the boundary between dilating and compacting states when material shears at constant volume. The set of critical state points in the pressure-porosity space forms the critical state line. The phenomenological Critical State Theory, based on such observations, and its modifications, are at the core of modern geomechanics. Yet, current understanding of dilatancy and critical state is purely empirical. The fundamental question: what are the micromechanisms that produce dilatancy and compaction? This has not been answered, except in a vague manner. The classic simplistic answer that nearly rigid particles must climb over each other to accommodate the imposed shear, only brings about other questions: Why do other materials not dilate as the rigid sphere model of atoms would predict? Why does the critical state depend on pressure?

We show that the key to this distinct granular behaviour is the presence of *intrinsic stress*, the existence of which has been postulated earlier, but its physical nature has remained conjectural. We use the graph theory representation of particles assemblies, first to provide the micromechanical definition of the intrinsic stress, then to quantify its effect on the change of volume under shear.

Persistent shear bands in granular materials occur at later stages of deformation. Typically, widths of shear bands are about 10-20 particle diameters. What determines this length? Strain localization in the form of shear bands is accompanied by accompanied by massive rolling of particle. On a single contact level, rolling is favored over frictional sliding, as a mechanism for rearrangement of particles. Yet, on a level of an assembly, rolling is constrained by neighbors. The result is a characteristic rolling correlation length. Our numerical simulations, specifically designed for this problem, indicate that the transmission of rotations depends on direction. Specifically, it depends on the strength of the force chain branch in that direction. The maximum propagation distance is comparable to observed widths of shear bands.

2.) Dislocations to continuum crystal plasticity

Plasticity in heterogeneous materials with small domains (e.g., polycrystals) is governed by the interactions/reactions of dislocations at interfaces. These include reactions of existing dislocations, as well as the nucleation of dislocations at an

interface. The rational for interface dominated plasticity is simple: dislocations glide through the single crystal domain with relative ease, but pile up at interfaces, so that interface reactions become a critical step in continuing plastic deformation.

While the details of dislocation reactions at interfaces take place at the atomic scale, and the behavior of dislocations in bulk is most accurately modeled by discrete dislocation dynamics, both of these models are much too expensive and impractical for analyzing the resulting bulk behavior. The need for a continuum framework for describing the plasticity across crystal interfaces, including the ubiquitous size effects, is acute.

Recently developed size-dependent crystal plasticity theory employs the representation of the singular part of dislocation pile-up boundary layers as superdislocation boundary layers, or equivalently, as jumps in slip at the boundary, but internal to the crystal. These boundary superdislocations exist on two sides of an interface and react or combine to lower the total energy under certain conditions.

In this paper, we develop the continuum framework for interactions of dislocations at interfaces. The framework includes continuum kinematic description of dislocation reactions across an interface, geometrical and thermodynamic conditions for reactions, energy dissipation in interface reactions, as well as the kinetic barriers thresholds for the reactions.

We analyze the problem of single and double-slip shear of a thin film, and compare the results of continuum model with dislocation dynamics simulations.

Explicit forms of the entropy production and the degree of irreversibility for Navier-Stokes and Bingham fluids

Wolfgang H. Müller
(joint work with B. Emek Abali)

1) The entropy inequality, normally known as the 2nd Law of Thermodynamics, is able to provide a measure of irreversibility. In here we consider an irreversible process, namely the flow of a non-linear viscous fluid in a two-dimensional channel, and use it in order to calculate the corresponding production of entropy as a function of classical material parameters, such as viscosity and heat conduction.
2) Thermodynamics of Irreversible Processes (T.I.P.) can be used to define a balance of entropy [1] with a strictly positive production term $\Sigma \geq 0$ by starting from the balance of internal energy (1st Law of Thermodynamics):

$$\rho \frac{\mathrm{d}u}{\mathrm{d}t} = -\frac{\partial q_i}{\partial x_i} + \sigma_{ij} \frac{\partial v_i}{\partial x_j}\,, \tag{1}$$

employing the stress tensor in decomposed form $\sigma_{ij} = \frac{1}{3}\sigma_{kk}\delta_{ij} + \sigma_{\langle ij\rangle}$ and by assuming that the specific internal energy (per mass) $u = u(p, v)$ solely depends on the thermodynamical pressure p and the specific volume v, such that Eqn. (1) can be recast with the Gibbs' equation:

$$\frac{\mathrm{d}s}{\mathrm{d}t} = \frac{1}{T}\Big(\frac{\mathrm{d}u}{\mathrm{d}t} + p\frac{\mathrm{d}v}{\mathrm{d}t}\Big)\,, \tag{2}$$

into the balance of entropy:

$$\frac{\mathrm{d}}{\mathrm{d}t}\int_{V(t)} \rho s \,\mathrm{d}V = -\oint_{\partial V(t)} \frac{q_i}{T}\,\mathrm{d}a_i + \int_{V(t)} \Sigma \,\mathrm{d}V\,,$$

$$\Sigma = q_i \frac{\partial 1/T}{\partial x_i} + \sigma_{\langle ij\rangle}\frac{\partial v_{\langle i}}{\partial x_{j\rangle}} + \frac{1}{T}\Big(\frac{1}{3}\sigma_{kk} + p\Big)\frac{\partial v_i}{\partial x_i}\,, \tag{3}$$

where absolute temperature $T > 0$ and mass density ρ are the primary variables and the heat flux q_i as well as the stress tensor σ_{ij} need to be specified in terms of those by constitutive relations. The first term on the right hand side may be interpreted as the flux of entropy across the boundaries of the thermodynamical system. Moreover the second term represents a production term, where the integrand Σ is always positive and reflects the 2$^{\text{nd}}$ Law.

3) The constitutive relations must be in agreement with the latter condition. In order to see this more clearly, we rewrite the production term slightly:

$$\Sigma = -\frac{q_i}{T^2}\frac{\partial T}{\partial x_i} + \sigma_{\langle ij\rangle}\frac{\partial v_{\langle i}}{\partial x_{j\rangle}} + \frac{1}{T}\Big(\frac{1}{3}\sigma_{kk} + p\Big)\frac{\partial v_i}{\partial x_i}\,. \tag{4}$$

It is now obvious that linear relations as proposed in [2], namely Fourier's law $q_i = -\kappa\frac{\partial T}{\partial x_i}$ and $\sigma_{\langle ij\rangle} = \mu\frac{\partial v_{\langle i}}{\partial x_{j\rangle}}$ by putting $\kappa > 0, \mu > 0$ guarantee a non-negative production in case of an incompressible flow $\frac{\partial v_i}{\partial x_i}$. In particular we use for stress tensor a velocity dependent variable viscosity as in [3]:

$$\sigma_{ij} = -p\delta_{ij} + 2\mu(d_{(2)})d_{ij}\,,\ d_{ij} = \frac{\partial v_{(i}}{\partial x_{j)}}\,,\ d_{(2)} = \frac{1}{2}d_{ij}d_{ij}\,,$$

$$\mu = \mu_0 + \frac{1}{\pi}\frac{k}{\sqrt{d_{(2)}}}\arctan\Big(\frac{\sqrt{d_{(2)}}}{b}\Big)\,. \tag{5}$$

The three parameters μ_0, k, b are positive material constants. The first parameter μ_0 is the usual viscosity. If k vanishes the well-known Navier-Stokes relation for fluid matter results. Another limit case is obtained for vanishing b, so that the stress relation assumes a Bingham-type form. Then d_{ij}'s different from zero lead to an additional stress k, which can be interpreted in terms of a yield stress, known from solid matter. For this case it is even possible to find an analytical solution, which is briefly shown below.

4) Consider a two-dimensional finite channel filled with a viscous fluid, expressed in Cartesian coordinates with the horizontal x_1 and vertical x_2 axes. If the left and right ends of the channel experience a pressure gradient fluid motion will result. Also, if the top and bottom walls of the channel move at different speeds a velocity field in the fluid is created. We assume that both cases happen simultaneously and the flow process reaches a stationary state. If the fluid is pumped with a pressure gradient and sheared with moving walls, we assume that the motion occurs only in the horizontal direction depending on the height between the walls. This is generally the case for viscous fluids and can be represented by the semi-inverse ansatz $v_i = (v_1(x_2), 0)$. By using the aforementioned stress, heat flux relations for

the stationary case, the balance of momentum, introducing normalized quantities:

$$\bar{x} = \frac{x_2}{R}\,,\ \bar{v} = \frac{v_1}{v_0}\,,\ v_0 = \frac{|p'|R^2}{\mu_0}\,,\ \bar{\sigma} = \bar{v}' \mp \bar{k}\,,\ \bar{k} = \frac{k}{|p'|R}\,,\ \bar{\sigma}_{ij} = \frac{\sigma_{21}}{|p'|R}\,, \tag{6}$$

the velocity field reads:

$$\bar{v}(\bar{x}) = \begin{cases} \frac{1}{2}\left(1-\bar{x}^2\right) - \xi\,(1+\eta)\,(1-\bar{x}) + v_{\text{top}} & , \quad \forall \bar{x} : \xi + \eta\xi \le \bar{x} \le 1 \\ \text{const.} & , \quad \forall \bar{x} : -\xi + \eta\xi \le \bar{x} \le \xi + \eta\xi \\ \frac{1}{2}\left(1-\bar{x}^2\right) - \xi\,(1-\eta)\,(1+\bar{x}) + v_{\text{bottom}} & , \quad \forall \bar{x} : -1 \le \bar{x} \le -\xi + \eta\xi. \end{cases} \tag{7}$$

From the balance of internal energy:

$$-\kappa \frac{\mathrm{d}^2 T}{\mathrm{d}x_2^2} = \sigma_{21} \frac{\mathrm{d}v_1}{\mathrm{d}x_2}\,,\ \bar{T} = \frac{T}{T_0}\,,\ \bar{p} = \frac{|p'|R}{k}\,,\ \bar{\kappa} = \frac{\kappa T_0}{k v_0 R}\,,$$

$$\bar{T} = \frac{\bar{p}}{12\bar{\kappa}}\left(1 - \bar{x}^4 - 2(\bar{x}^3 \pm 1)\alpha + 6(\bar{x}^2+1)\beta\right) + c(\bar{x} \mp 1) + 1\,, \tag{8}$$

$$\alpha = 2\eta\xi \pm 2\xi \mp \bar{k}\,,\ \beta = \xi^2(1+\eta^2) \pm 2\eta\xi^2 - \bar{k}\xi(1 \pm \eta)\,, \tag{9}$$

we obtain a temperature distribution for the case of identical temperatures at the boundaries $T|_{\pm 1} = T_0$, identical heat fluxes in the transition points $\bar{\kappa}\frac{\mathrm{d}\bar{T}}{\mathrm{d}\bar{x}}|_{\xi\eta+\xi} = \bar{\kappa}\frac{\mathrm{d}\bar{T}}{\mathrm{d}\bar{x}}|_{\xi\eta-\xi} = \bar{\kappa}c$, and the same thermal conductivities in both regimes. Finally we obtain for the entropy production or rather for the dissipation function Φ mentioned in [3]:

$$\Sigma = \frac{\kappa}{T^2}\left(\frac{\mathrm{d}T}{\mathrm{d}x_2}\right)^2 + \frac{1}{T}\sigma_{21}\frac{\mathrm{d}v_1}{\mathrm{d}x_2}\,,\ \bar{\Sigma} = \frac{T_0 R}{k v_0}\Sigma \tag{10}$$

$$\Phi = \bar{T}\bar{\Sigma} = \frac{\bar{\kappa}}{\bar{T}}\left(\frac{\mathrm{d}\bar{T}}{\mathrm{d}\bar{x}}\right)^2 + \frac{1}{\bar{k}}\left(\frac{\mathrm{d}\bar{v}}{\mathrm{d}\bar{x}}\right)^2 \mp \frac{\mathrm{d}\bar{v}}{\mathrm{d}\bar{x}}\,. \tag{11}$$

This function can be considered as a measure of irreversibility. It consists of two coupled parts, a mechanical and a thermal one. Although we start with a mechanically driven system, the calculation shows that the induced temperature field adds an important amount to the dissipation function. Hence, as the dissipation function with its mechanical and thermal parts for a flow with velocity field can be seen in Fig. 1, even in a purely mechanically driven viscous flow, one shall not neglect the thermal dissipation out of the system.

References

[1] C. Eckart, *The thermodynamics of irreversible processes*, Phys. Rev. **73**(4) (1948), 373–382.

[2] L. Onsager, *Reciprocal relations in irreversible processes*, Phys. Rev. **37**(4) (1931), 405.

[3] H. Ziegler, C. Wehrli, *The derivation of constitutive relations from the free energy and the dissipation function*, Adv. Appl. Mech. **25** (1987), 183–238.

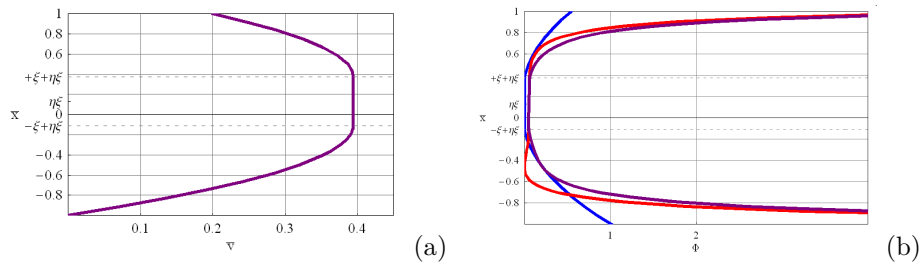

FIGURE 1. (a) Velocity profile, (b) Dissipation function (purple) with its mechanical (red) and thermal (blue) parts.

Material instability: Implications for extracting material response from specimen measurements

ALAN NEEDLEMAN

(joint work with Shelby B. Hutchens, Nisha Mohan, Julia R.Greer)

Vertically aligned carbon nanotubes (VACNTs) have shown promising mechanical properties for use in a variety of applications, for example, energy absorption, compliant thermal interfaces and biomimetic dry adhesives. In some cases VACNTs have displayed high recoverability after significant strain while other in other cases permanent deformations have been observed. In particular, Hutchens et al. [1] have observed large permanent deformations in compression of micron scale pillars that deform by progressive buckling. The relative density of the pillars (pillar density/fully dense material) is about 13% so these materials are highly compressible. The overall response that is obtained from such a test is a "structural" response in that the response depends on the pillar geometry and the loading (and support) conditions. One would like to be able to extract a material property from this response where by a material property is meant a parameter value or a function that can be used to predict the response of the material under other loading conditions. Of course, what constitutes a property depends on the constitutive theory used to describe the material response.

Calculations in [2] showed that a simple rate dependent elastic-viscoplastic constitutive relation with a hardening-softening-hardening form of the flow strength as a function of plastic strain that also accounted for plastic compressibility could at qualitatively, and in some aspects quantitatively, represent the main observed features. A microstructurally motivation for this constitutive description is given in [3].

The analyses in [2] raise the question of how to extract material properties from tests on materials exhibiting this type of constitutive response. To explore this we consider the response of a compressible elastic-viscoplastic solid with the four flow strength relations shown in Fig. 1 subject to: (i) uniaxial tension, (ii) uniaxial compression and (iii) indentation with a sharp indenter. Material A, which exhibits softening, is representative of the flow strength description used in [2].

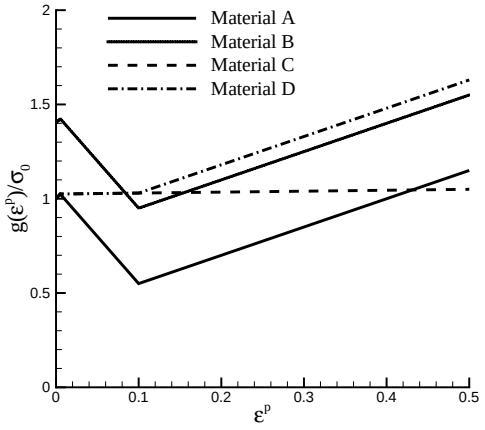

FIGURE 1. Plot of the various hardening functions considered.

One question addressed is which loadings, if any, exhibit a qualitative difference between a hardening (or ideally plastic) relation and a softening relation. The numerical results show that compressibility has a large effect on the relation between indentation hardness and material flow strength but that there is no qualitative difference between the indentation response of softening and non-softening materials. A more complete desciption of the modeling formulation and the numerical results is given in [4].

REFERENCES

[1] S.B. Hutchens, L.J. Hall, J.R. Greer, *In situ mechanical testing reveals periodic buckle nucleation and propagation in carbon nanotube bundles*, Advanced Functional Materials **20** (2010) 2338–2346.

[2] S. B. Hutchens, A. Needleman, and J. R. Greer, *Analysis of uniaxial compression of vertically aligned carbon nanotubes*, Journal of the Mechanics and Physics of Solids **59** (2011) 2227–2237.

[3] S.B. Hutchens, A. Needleman, J. R. Greer, *A microstructurally motivated description of the deformation of vertically aligned carbon nanotube structures*, Applied Physics Letters, to be published.

[4] A. Needleman, S.B. Hutchens, N. Mohan,J.R.Greer, *Deformation of plastically compressible softening-hardening solids*, in preparation.

A statistical physics approach describing martensitic phase transformations

Eduard Roman Oberaigner
(joint work with Mario Leindl)

The martensitic phase transformation is a structural or displacive phase transformation, where single crystals jump within a very short time from the austenitic into the martensitic phase or backwards. The nonlinear geometric theory can describe in the stress-free case many features very well. The situation, however, becomes in the case of applied stress and/or internal eigenstress especially in the polycrystalline case very complicated.
One main research interest of the author of this research report is the behaviour of polycrystalline shape memory alloys (SMAs) by using concepts of statistical physics.
So far there exist different approaches to attack the problem of understanding the thermomechanical behaviour of polycrystalline SMAs. One approach is, to make assumptions on the internal variables like martensitic volume fraction or transformation strain, another approach is to start with assumptions on driving forces and thresholds, again others are based upon the Landau or Landau-Devonshire model to describe ferromagnets, the Ginzburg-Landau model to describe superconductivity, or the phase-field method, which was adapted in material science first to describe dendritic growth.
Within each approach there exist several models of many authors (for an overview see, e.g., [1, 2, 3, 4]). The approach of the author is different from the models presented so far in literature. Starting point is the idea, that in the phase-transformation regime and its vicinity, a physical system (magnet, fluid, ferroelectric material, crystalline solid, etc.) exhibits a self-similar behaviour over many orders of magnitudes in the length scale, and the so-called correlation length becomes very large, in case of crossing a critical point theoretically even infinitely large. Therefore, one can in the mathematical description of a phase-transforming material start, e.g., in a ferromagnetic spin system, with blocks of spins and attribute to such a block so-called block-spin properties (Hamiltonians), which can be derived via a renormalisation procedure from a single-spin system. In such a way one derives also effective interaction Hamiltonians. From these, one can derive the partition function of the physical system and, from there the Helmholtz or the Gibbs free energy, resp., and finally from, there, within the concepts of irreversible thermodynamics, other physical quantities. The author of this report started to adapt this procedure, together with colleagues, to the polycrystalline SMAs. This idea was first formulated in [5] and with computational results in [6].
One starts with a representative volume element (RVE), which is large enough, that an averaging or homogenisation makes sense, but still small enough compared to a specimen (the scaling problem is discussed in [7]). Due to the small size of such a RVE, one can assume, that in such a small region within a short time there exists thermodynamic equilibrium. Of course, a neighbouring RVE is

in general in a different thermodynamic equilibrium state, and this leads to fluxes between such RVEs. In irreversible thermodynamics, this approach is called "local thermodynamic equilibrium concept". This way allows to use within an RVE the mathematical apparatus of equilibrium statistical mechanics, which is much easier to handle then that of non-equilibrium statistical mechanics.
The RVE is divided in this approach into (not necessarily equisized) cells, which contain single crystals, which are either in the austenitic or martensitic phase. Such cells correspond to crystallites. If a RVE contains n cells, which can be in m different phases (here, one austenitic phase and a certain number of martensitic variants, depending on the point group of the material), then there are m^n different thermodynamic states for the RVE possible, each with a (mostly different) probability.
If one has, e.g., one austenitic phase and three martensitic variants, then there exist in case of plane RVE with four 4×4 cells 4^{16} possible thermodynamic states, effectively one can show that one needs only up to 8 cells leading maximal to 4^8 thermodynamic states. Each state ν is described by an analytical function H_ν, the Hamiltonian of the state. Let H_i denote the Hamiltonian of a cell, which can be in this example either H_A or H_{M_j} ($j \in \{1,2,3\}$), M_j denotes the j-th martensitic variant, H_{M_j} the Hamiltonian of the j-th martensitic variant, H_A the Hamiltonian for an austenite, each one of these depending on the actual stress and temperature). Within this notation, H_ν is given by $H_\nu = \sum_{i=1}^{n}(H_{\nu\, i} + H_{\nu\, Ii,i+1})$. $H_{\nu\, i}$ denotes for the ν-th state the Hamiltonian of the i-th cell, $H_{\nu\, Ii,i+1}$ denotes for the ν-th state the interaction Hamiltonian between the i-th and the $(i+1)$-th cell. The neighbour of the n-th cell is the first cell (cyclic boundary condition). This makes sense, since all RVEs are of the same structure, and the actual neighbour of the n-th cell in RVE is the first cell in the neighbouring RVE in a linear chain. In two and three dimensions this can be organised accordingly. Besides, cyclic boundary conditions have an essential computational advantage. With given H_ν, the partition function reads

$$Z = \sum_{\nu} e^{-\beta H_\nu} \qquad \text{with} \qquad \beta := \frac{1}{kT},$$

k denotes the (renormalised) Boltzmann constant, T the absolute temperature.
In case of applied stress one gets for the polycrystalline RVE under constant stress and temperature the Gibbs free energy

$$G(\sigma^{ij}, T) = -kT \ln Z$$

σ^{ij} denotes the effective Cauchy stress within the considered RVE (sum of applied stress and eigenstress). Since G is a thermodynamic state function, it contains the whole information of the considered thermodynamic system. Once gets, e.g., the total strain via

$$\varepsilon_{ij} = \frac{\partial g}{\partial \sigma^{ij}} \,,$$

if g denotes the Gibbs free energy per mole. Most thermodynamical quantities can be gained via an ensemble average to

$$< A >= \frac{1}{Z} \sum_{\nu} A_\nu \exp(-\beta H_\nu) \ .$$

Applied to the total volume V_T of the RVE this reads

$$< V_T >= \frac{1}{Z} \sum_{\nu} V_\nu \exp(-\beta H_\nu) \ .$$

The total average mole density is then

$$< \eta_T >= \frac{N_T}{< V_T >} \ ,$$

where N_T is the total mole number of the system. Since the mole number of the RVE remains constant and mostly not the total volume, the block-spin approach from statistical physics can be considered as a finite mole method (FMM). With $< \eta_T >$, one gets the martensitic volume fraction ξ_M according to [6] via

$$< \xi_M >= \frac{\eta_A - < \eta_T >}{\eta_A - \eta_M} \ ,$$

where η_A and η_M denote mole densities of the austenitic and martensitic single crystal phase, resp. The elastic strain is derived accordingly via

$$< \varepsilon_{ij}^{\mathrm{el}} >= \frac{1}{Z} \sum_{\nu} \varepsilon_{ij\,\nu}^{\mathrm{el}} \exp(-\beta H_\nu),$$

analogously the thermal strain $< \varepsilon_{ij}^{\mathrm{th}} >$. The transformation strain $\varepsilon_{ij}^{\mathrm{tr}}$ is then

$$\varepsilon_{ij}^{\mathrm{tr}} = \varepsilon_{ij} - < \varepsilon_{ij}^{\mathrm{el}} > - < \varepsilon_{ij}^{\mathrm{th}} > \ .$$

The rates are gained via, e.g.,

$$\dot{\xi}_M = \frac{\partial \xi_M}{\partial \sigma^{ij}} \frac{\partial \sigma^{ij}}{\partial t} + \frac{\partial \xi_M}{\partial T} \frac{\partial T}{\partial t} \ .$$

In most experiments one uses one or two components and leaves the temperature and the other components constant resp., and vice verse. In case one changes a component of σ^{ij} or T, one does this mostly with a constant rate. Then in the above formula most derivatives with respect to time are zero and one (or two) is (are) constant, and thus there remains just a factor besides the temperature and stress derivatives of ξ_M. Those aspects are discussed in more detail in [8]. In the just mentioned and in a series of further publications of the author and colleagues, e.g., [9, 10, 11] a series of further results are discussed and presented also graphically. Further on, the block-spin approach has been shown to be applicable in practical computations such as stress-wave propagation and damping with the help of induced phase transformations.

Ongoing work shows, that this approach is also applicable to understand phase transformations in other materials such as polymers and ceramics better, or even the phenomenon of crystal plasticity.

References

[1] D.C. Lagoudas *Shape Memory Alloys: Modeling and Engineering Applications*, Springer, Berlin Heidelberg New York, 2008.

[2] D.C. Lagoudas, P.B. Entchev, P. Popov, E. Patoor, L.C. Brinson, X. Gao, *Shape memory alloys, Part 2: Modeling of polycrystals*, Mechanics of Materials **38** (2006), 430–462.

[3] E. Patoor, D.C. Lagoudas, P.B. Entchev, L.C. Brinson, X. Gao *Shape memory alloys, Part 1: General properties and modeling of single crystals*, Mechanics of Materials **38** (2006), 391–429.

[4] F.D. Fischer, M. Berveiller, K. Tanaka, E.R. Oberaigner *Continuum Mechanical Aspects of Phase Transformation in Solids*, Archive of Applied Mechanics **64** (1994), 54–85.

[5] E.R. Oberaigner *Festkörperumwandlungen aus der Sicht der Thermomechanik–Analytische Modelle und numerische Studien*, Montanuniversität Leoben, Habilitationsschrift, 1993.

[6] E.R. Oberaigner, M. Fischlschweiger *A statistical mechanics approach describing martensitic phase transformation*, Mechanics of Materials **43** (2011), 467–475.

[7] E.R. Oberaigner, M. Fischlschweiger, T. Antretter *A space-time concept for martensitic phase transformation based on statistical physics*, AIP Conference Proceedings, (2011), 97–102.

[8] M. Fischlschweiger, E.R. Oberaigner *Kinetics and rates of martensitic phase transformation based on statistical physics*, Computational Materials Science **52** (2012), 189–192.

[9] M. Leindl, M. Fischlschweiger, E.R. Oberaigner *Modeling stress dependent hysteretic SMA behavior based on a block-spin-approach from statistical mechanics*, Proceedings 3rd International Conference on Heterogeneous Materials Mechanics, (2011), 564–567.

[10] M. Leindl, M. Fischlschweiger, E.R. Oberaigner *Damping Behaviour of Vibrating Shape Memory Alloy Rods Investigated by a Novel Constitutive Model*, PAMM **11** (2011), 403–404.

[11] M. Mataln, M. Fischlschweiger, M. Leindl, E.R. Oberaigner *Sensitivity study of a statistical physics based method describing martensitic phase transformation*, 82nd Annual Scientific Conference on the International Association of Applied Mathematics and Mechancis (GAMM), (2011), 206.

Boundary migration during low temperature plastic deformation

Reinhard Pippan

(joint work with Anton Hohenwarter, Andrea Bachmaier, Georg Rathmayr, Martin Rester, Christian Motz, Daniel Kiener)

The main goal of this presentation is to show that in two very different subjects in the area of plastic deformation – severe plastic deformation and indentation – boundary migration plays a dominant role. Heavy plastic deformation at relatively low homologous temperatures, usually called Severe Plastic Deformation (SPD), is an efficient method in producing ultrafine grained or nanocrystalline structure in materials. Plastic deformation in coarse grained materials leads to the formation of dislocation structures, at first to dislocation cells and then to cell block with larger misorientation between the cell blocks. The cell block and dislocation cell structure, which are characteristic features at "small and medium" SPD, are transformed to a uniform ultrafine or nanocrystalline granular structure. These phenomena are very general for materials which deform predominately by dislocation glide [1], however even in materials where twinning or phase transformation

are the most important deformation mechanism the processes controlling the development of the steady state are similar [2]. The most important facts observed in many different metals and alloys can be summarized as follows

- SPD leads to a refinement of a coarse grained into a submicron- and nanocrystalline microstructure.
- At large strains saturation in the refinement is observed, grain size, fraction of low and high angle grain boundary and texture do not change with further deformation.
- Boundary migration is an essential mechanism to explain the saturation in the structural evolution. The following points support this assumption.
- Temperature, impurities and alloying are the most important parameters controlling the limitation in refinement.
- Strain rate dependence of the saturation grain size is stronger in the medium temperature regime than at low temperatures.
- The initial microstructure of a single phase material does not affect the saturation grain size. A coarse grained single phase material refines and a finer nanocrystalline material coarsens.

In the past few years, the deformation of miniaturized single-crystal samples was frequently investigated to examine the processes governing deformation on the micrometer and nanometer length scale. Indentation experiment, bending, tension and compression experiments have been developed for analyzing the plastic response from nanometer regime to the macro regime. Keeping the aforementioned facts during standard plastic deformation and SPD in mind, it becomes evident that the size of the investigated sample size covers a wide range of the different scales of the dislocation structural evolution which occur during the deformation of single or polycrystalline metals. Special attention is devoted to indentation, where it is easy to cover all length scales from nm to mm [3]. Detailed analyses of the deformed volume below the indent indicate that:

- During indentation in single crystals we are far away from self similarity. In the indentation experiments in single crystals the size of the deformed volume does not scale with the size of imprint.
- The response in hardness depends on the characteristic length scales of the generated dislocation structures, which varies significantly with the contact size.
- The development of deformation induced boundaries requires a certain deformed volume, the movement of these boundaries is essential for the size dependence of the hardness on the micro scale.

References

[1] R. Pippan, S. Scheriau, A. Taylor, M. Hafok, A. Hohenwarter, A. Bachmaier, *Saturation of fragmentation during severe plastic deformation*, Ann. Rev. Mater. Res. **40** (2010), 319–343.

[2] S. Scheriau, Z. Zhang, S. Kleber, R. Pippan, *Deformation mechanisms of a modified 316L austenitic steel subjected to high pressure torsion*, Mater. Sci. Engng A **528** (2011), 2776–2786.

[3] M. Rester, C. Motz, R. Pippan, *Microstructural investigation of the volume beneath nanoindentations in copper*, Acta Materialia **55** (2007) 6427–6435.

A coupled electro-chemo-mechanical framework for diffusion and deformation in solids

Jianmin Qu

Solid materials used in energy conversion and storage devices are often subjected to multiple driving forces (electrical, chemical, radiological, thermal, mechanical, etc.). The interactions among these different driving forces often impact the efficiency, reliability and durability of the devices. Understanding of how the different driving forces interact requires theories and models that are capable of accounting for the coupling of multi-physics processes.

In this talk, a framework is presented that couples the mechanical and chemical (or electrochemical) fields in solids via the use of stress-dependent chemical potentials. To illustrate the development and applications of this coupled electro-chemo-mechanical theory, two examples of practical interest will be discussed, namely, solid oxide fuel cells and lithium ion batteries. Our interest is to understand how solid diffusion generates mechanical stresses, and how such mechanical stresses affect the diffusion. The first example is concerned with the interactions between mechanical stresses and ionic transport in the electrolyte of a solid oxide fuel cell. It is found that the non-uniform oxygen vacancy concentration in the electrolyte can generate significant stresses whose amplitude is comparable to the thermal mismatch induced stress in the cell stack. More importantly, significant stress concentration near processing defects (voids and microcracks) occurs due to the presence of ionic fluxes. The second example is on the insertion of lithium into silicon in silicon anodes in lithium batteries. Using input from *ab initio* and molecular dynamic simulations, we investigated the mechanisms of lithium insertion and how the process is affected by mechanical stresses.

Removal of unphysical arbitrariness in constitutive equations for elastically anisotropic nonlinear elastic-viscoplastic solids

M. B. Rubin

Constitutive equations for elastically anisotropic nonlinear elastic-viscoplastic solids are often formulated assuming that the strain energy function Σ per unit mass depends on an elastic deformation gradient $\mathbf{F}_{\rm e}$ and a triad of linear independent vectors $\mathbf{M}_i$ $(i = 1, 2, 3)$, which characterize crystallographic orientations in an intermediate configuration (see 1).

$$\Sigma = \Sigma(\mathbf{F}_{\rm e}, \mathbf{M}_i)\,. \tag{1}$$

Moreover, $\mathbf{F}_{\rm e}$ can be determined by integration an evolution equation of the form

$$\dot{\mathbf{F}}_{\mathrm{e}} = (\mathbf{L} - \overline{\mathbf{L}}_{\mathrm{p}})\,\mathbf{F}_{\mathrm{p}}\,, \tag{2}$$

where a superposed $(\cdot)$ denotes material time differentiation, $\mathbf{L}$ is the velocity gradient and $\overline{\mathbf{L}}_{\mathrm{p}}$ is a second order tensor that characterizes the rate of relaxation due to plasticity and viscoplasticity and requires a constitutive equation.

More commonly, the total deformation gradient $\mathbf{F}$ and the plastic deformation gradient $\mathbf{F}_{\mathrm{p}}$ are determined by integrating evolution equations of the forms

$$\dot{\mathbf{F}} = \mathbf{L}\mathbf{F}\,, \quad \dot{\mathbf{F}}_{\mathrm{p}} = \mathbf{\Lambda}_{\mathrm{p}}\mathbf{F}_{\mathrm{p}}\,, \quad \mathbf{\Lambda}_{\mathrm{p}} = \mathbf{F}_{\mathrm{p}}^{-1}\overline{\mathbf{L}}_{\mathrm{p}}\mathbf{F}_{\mathrm{e}}\,, \tag{3}$$

which are consistent with the multiplicative relationship

$$\mathbf{F}_{\mathrm{e}} = \mathbf{F}\mathbf{F}_{\mathrm{p}}^{-1}\,. \tag{4}$$

In [1] constitutive equations for elastic-viscoplastic response were formulated in terms of a triad of three linearly independent vectors $\mathbf{m}_i$, which satisfy the evolution equations

$$\mathbf{m}_i = (\mathbf{L} - \mathbf{L}_{\mathrm{p}})\mathbf{m}_i\,, \tag{5}$$

where $\mathbf{L}_{\mathrm{p}}$ is another second order tensor that characterizes the rate of relaxation due to plasticity and viscoplasticity and requires a constitutive equation. Within this context, the strain energy function and the Cauchy stress $\mathbf{T}$ takes the forms

$$\Sigma = \Sigma(\mathrm{m}_{ij})\,, \quad \mathrm{m}_{ij} = \mathbf{m}_i\mathbf{m}_j\,, \quad \mathbf{T} = 2\rho\frac{\partial\Sigma}{\partial \mathrm{m}_{ij}}\mathbf{m}_i \otimes \mathbf{m}_j\,, \tag{6}$$

where m_{ij} is a metric of elastic deformation, ρ is the mass density in the present configuration, $\otimes$ denotes the tensor product operator and the usual summation convention is used for repeated indices.

The objective of this paper is to demonstrate that the elastic $\mathbf{F}_{\mathrm{e}}$, total $\mathbf{F}$ and plastic $\mathbf{F}_{\mathrm{p}}$ deformation measures and the vectors $\mathbf{M}_i$ used to characterize directions of material anisotropy contain unphysical arbitrariness which prevents them from being measured [2].

References

[1] M.B. Rubin, *Plasticity theory formulated in terms of physically based microstructural variables – Part I: Theory*, Int. J. Solids Structures **31** (1994), 2615–2634.

[2] M.B. Rubin, *Removal of unphysical arbitrariness in constitutive equations for elastically anisotropic nonlinear elastic-viscoplastic solids*, Int. J. Engng. Sci. **53** (2012), 38–45.

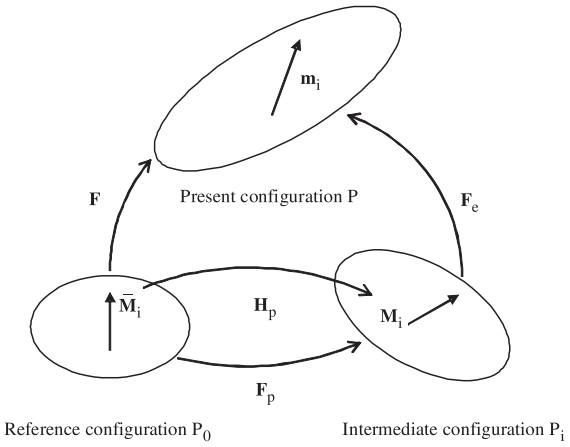

FIGURE 1. Sketch of the mappings between the reference configuration P_0, the intermediate configuration P_i and the present configuration P.

Upscaling defects in steel via Γ-convergence

LUCIA SCARDIA
(joint work with Marc Geers, Ron Peerlings, Mark Peletier)

One of the hard open problems in engineering is the upscaling of large numbers of *dislocations* and describing their collective behaviour in terms of a continuum quantity: the dislocation density. This transition has been done mainly phenomenologically and has produced a number of competing dislocation density models models. These models describe the time-evolution of the density via conservation laws equipped with constitutive laws both for the velocity of the dislocations and for their interaction (internal or back-stress) and they differer in the expression of the internal stress that they propose.

Here comes the essential difference of our approach: We derive a continuum model for the dislocation density by starting from a more fundamental discrete dislocation model via a rigorous mathematical approach (Γ-convergence). Our starting point is the discrete model of an idealised pile-up considered in [2] and shown in Figure 1. This model describes the equilibrium positions of n dislocation walls under the influence of an applied stress σ that pushes the walls towards an impenetrable barrier. The barrier is modelled as a wall of pinned dislocations at $x_0 = 0$.

The equilibrium equations for the positions of the n walls can be written as

$$\sigma^i_{\text{int}} - \sigma = 0, \quad i = 1, \dots, n, \tag{1}$$

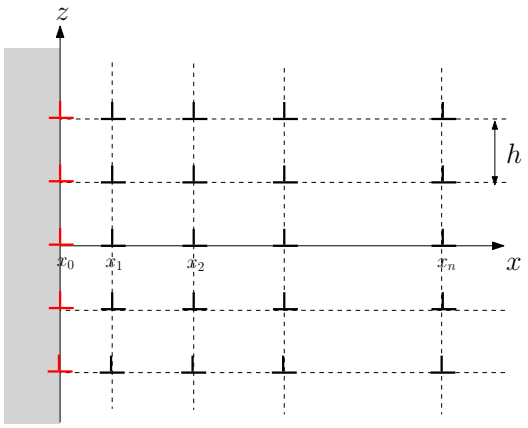

FIGURE 1. The dislocation configuration

where the discrete internal stress for the i-th wall accounts for the interactions with all the other walls. One can intuitively imagine that passing to the (continuum) limit in (1) should give an expression for a continuum version of the internal stress. Which is exactly the object we want to characterise.

The mesoscopic internal stresses we obtain do not depend on the dislocation density only, but contain also some more *local* information about the discrete arrangement of the dislocations, that the density alone fails to capture. This additional information can be expressed in terms of an aspect ratio a, defined as the ratio between the in-plane distance Δx between two consecutive dislocations and the in-wall distance h.

The upscaling procedure we adopt focusses on the discrete energy of the system of dislocations. The discrete-to-continuum upscaling is done by letting the number of dislocations n become infinitely large. According to the different asymptotic behaviour of the aspect ratio a (i.e., according to the *local* distribution of the dislocations), five different expressions for the continuum energy can be derived; and, accordingly, five different expressions for the upscaled internal stress (see [1] and [3]). The results we obtain show that the simplified discrete model taken as a starting point is not *too simple*. In fact the internal stresses resulting from our derivation are more general than many well-known models proposed in the engineering literature.

The great advantage of our rigorous approach to the upscaling compared to the phenomenological derivation of the internal stress is that it is exact. This means that once a discrete model is chosen (with its simplifications and limitations) the corresponding upscaled continuum model obtained by following our method is univoquely determined.

References

[1] M.G.D. Geers, R.H.J. Peerlings, M.A. Peletier, L. Scardia, *Asymptotic behaviour of a pile-up of infinite walls of edge dislocations*, submitted paper.
[2] A. Roy, R.H.J. Peerlings, M.G.D. Geers and Y. Kasyanyuk, *Continnum modeling of dislocation interactions: Why discreteness matters?*, Mater. Sci. Engng. A **486** (2008), 653–661.
[3] L. Scardia, R.H.J. Peerlings, M.A. Peletier, M.G.D. Geers, *Mechanics of dislocation pile-ups: A unification of scaling regimes*, in preparation.

A discrete-to-continuum analysis for crystal cleavage in a 2d model problem

Bernd Schmidt
(joint work with Manuel Friedrich)

The behavior of brittle materials is of great interest in applications as well as from a theoretical point of view. Major challenges in the experimental sciences and theoretical studies are to identify critical loads at which such a body fails and to determine the geometry of crack paths that occur in the fractured regime.

In crystals under tensile boundary loads fracture typically occurs in the form of cleavage along crystallographic hyperplanes of the atomic lattice. On the continuum side such behavior can be modelled by anisotropic surface terms which are locally minimized for these crack geometries. A discrete model has been investiged by Braides, Lew and Ortiz [2], who assume that fracture can only occur in these directions and then calculate a limiting continuum energy: a cleavage law. This assumption leads to an effective one-dimenional problem which is much easier to analyze. However, all 1d ansatzes discussed in the current literature necessarily fall short of rigorous arguments that indeed in more than one dimension, if fracture occurs at all, then it is energetically favorable to cleave the specimen along particular crystallographic hyperplanes. The main goal of this talk is to provide a rigorous and rather complete study of a two dimensional model problem.

Our model, although a toy model from a physical point of view, retains the following key features: It is (1) at least two-dimensional with (2) vector-valued deformations, is (3) fully frame indifferent with (4) with non-degenerate elastic contributions in the bulk, leading (5) to surface contributions sensitive to the crack geometry with competing crystallographic hyperplanes: We consider a 2d strip with atoms on a (generically) rotated triangular lattice interacting via a NN Lennard-Jones type interactions under uniaxial stretch.

Our main results are sharp energy estimates on minimizers and a complete analysis on the geometry of limiting configurations, when the number of atoms becomes large and interatomic distances small: There is a critical boundary displacement up to which minimizers are homogeneous elastic deformations and beyond which the body completely cracks along a specific crystallographic line and is asymptotically rigid on two separated bulk parts.

All quantitites describing the limiting optimal configurations, such as the subcritical homogeneous strain, crack geometry and critical load are given explicitly

in terms of (1) derivatives of the pair interaction potential at equilibrium, (2) the behavior of this potential at infinity, (3) the aspect ratio of the body and (4) the lattice orientation.

More precisely, assume that in the reference configuration the atoms occupy positions $\varepsilon\mathcal{L} \cap \big((0,l)\times(0,1)\big)$, $l > 1/\sqrt{3}$, where

$$\mathcal{L} = \begin{pmatrix} \cos\phi & -\sin\phi \\ \sin\phi & \cos\phi \end{pmatrix} \begin{pmatrix} 1 & \frac{1}{2} \\ 0 & \frac{\sqrt{3}}{2} \end{pmatrix} \mathbb{Z}^2, \qquad \phi \in \Big[0, \frac{\pi}{3}\Big)$$

(a rotated triangular lattice). We consider lattice deformations $y : \varepsilon\mathcal{L} \cap \big((0,l)\times(0,1)\big) \to \mathbb{R}^2$ satisfying the boundary conditions (tacitly assumed in the sequel)

$$y_1(\cdot, x_2) = \begin{cases} 0 & \text{near } x_1 = 0, \\ (1+\sqrt{\varepsilon}a)l & \text{near } x_1 = l \end{cases}$$

with $a \geq 0$. (The scaling with $\sqrt{\varepsilon}$ is the critical scaling when elastic deformations and cracked configurations are energetically of the same order.) The atomic energy of a lattice deformation y is given by

$$E_\varepsilon(y) = \frac{\varepsilon}{2} \sum_{\substack{x,x' \in \mathcal{L}_\varepsilon \\ |x-x'|=\varepsilon}} W\left(\frac{|y(x') - y(x)|}{\varepsilon}\right),$$

where

(i) $W \geq 0$ and $W(r) = 0 \iff r = 1$,
(ii) W is C^4 near 1 with, say, $W''(1) = \alpha$, $W'''(1) = \alpha'$,
(iii) $W(r) = \beta + O(r^{-2})$, $\beta > 0$, for $r \to \infty$.

Set $\gamma = \frac{\sqrt{3}\cos\phi}{2} + \frac{\sin\phi}{2} \in [\frac{\sqrt{3}}{2}, 1]$ and denote the lattice direction with maximal $\mathbf{e}_2$-projection by $\mathbf{v}_\gamma$. For the sake of simpliciy we exclude here the one lattice orientation leading to non-unique $\mathbf{v}_\gamma$, although our methods are also applicable to that case.

Theorem 1 (Cleavage law with sharp energy estimates)**.**

$$\liminf_{\varepsilon\to 0} E_\varepsilon = \min\left\{ \frac{al}{\sqrt{3}}a^2 + \frac{6\alpha + 7\alpha' - 2(3\alpha - \alpha')\cos(6\phi)}{27\sqrt{3}} l\sqrt{\varepsilon}a^3, \frac{2\beta}{\gamma} \right\} + O(\varepsilon).$$

(Note that surface contributions are of order $O(\varepsilon)$.)

Theorem 2 (Strong convergence of minimizers)**.** *If $E_\varepsilon(\mathrm{id} + \sqrt{\varepsilon}u_\varepsilon) = \inf E_\varepsilon + O(\varepsilon)$ and $\tilde{u}_\varepsilon$ denotes the piecewise affine interpolation of u_ε, then there exist $\bar{u}_\varepsilon : (0,l)\times(0,1) \to \mathbb{R}^2$ with $|\{x : \bar{u}_\varepsilon(x) \neq \tilde{u}_\varepsilon(x)\}| = O(\varepsilon)$ such that:*

(i) *If $a < a_{\mathrm{crit}}$, then there is a sequence $s_\varepsilon \in \mathbb{R}$ such that*

$$\|\bar{u}_\varepsilon - (0, s_\varepsilon) - F^a \cdot\|_{H^1(\Omega)} \to 0,$$

where $F^a = \begin{pmatrix} a & 0 \\ 0 & -\frac{a}{3} \end{pmatrix}$.

(ii) *If* $a > a_{\mathrm{crit}}$*, then there exist sequences* $p_\varepsilon \in (0,l)$*,* $s_\varepsilon, t_\varepsilon \in \mathbb{R}$ *such that* $(p_\varepsilon, 0) + \mathbb{R}\mathbf{v}_\gamma$ *intersects both the segments* $(0,l)\times\{0\}$ *and* $(0,l)\times\{1\}$ *and, for the parts to the left and right of* $(p_\varepsilon,0)+\mathbb{R}\mathbf{v}_\gamma$

$$\Omega^{(1)} := \{x : 0 < x_1 < p_\varepsilon + (\mathbf{v}_\gamma \cdot e_1)x_2\} \text{ and}$$
$$\Omega^{(2)} := \{x : p_\varepsilon + (\mathbf{v}_\gamma \cdot e_1)x_2 < x_1 < l\},$$

respectively, we have – possibly after rotating $\mathrm{id} + \sqrt{\varepsilon}u_\varepsilon$ *by* π *on* $\Omega^{(1)}$ *or* $\Omega^{(2)}$ *–*

$$\|\bar{u}_\varepsilon - (0, s_\varepsilon)\|_{H^1(\Omega^{(1)})} + \|\bar{u}_\varepsilon - (al, t_\varepsilon)\|_{H^1(\Omega^{(2)})} \to 0.$$

For the proofs of these results we refer the reader to [1].

References

[1] M. Friedrich, B. Schmidt, *From atomistic to continuum theory for brittle materials: A two-dimensional model problem*, preprint available at http://arxiv.org/abs/1108.3696.

[2] A. Braides, A. Lew, M. Ortiz, *Effective cohesive behavior of layers of interatomic planes*, Arch. Ration. Mech. Anal. **180** (2006), 151–182.

Consistent anisotropic plate theories and the uniform-approximation technique

Patrick Schneider

(joint work with Reinhold Kienzler)

In the talk, the uniform-approximation technique is proposed, which is a general framework for the derivation of theories (partial differential equations with corresponding boundary conditions) describing the linear elastic deformation of thin structures under a given load. The approach does not make use of any (classical) a priori assumptions and produces hierarchical sets of approximating theories with increasing accuracy. It is based upon the paradigm to approximate all governing equations with the same accuracy. In the remainder of the talk, the first- and second-order theories for homogeneous monoclinic plates with constant thickness are derived and compared to classical theories.

Under *thin* structures we understand structures which characteristic length is in one or two directions small compared to the other directions, like, e.g., beams, plates or shells. While there is only one theory of three-dimensional linear elasticity, there are plenty of theories for thin structures. Lots of them are, furthermore, motivated by disputable a priori assumptions. Therefore, we derive theories for thin structures from the three-dimensional theory by the use of series expansions.

We start from the weak Navier-Lamé formulation of three-dimensional elasticity. It is made dimensionless by the introduction of dimensionless coordinates and characteristic parameters indicating the relative "thinness" of the structure. The unknown displacement field and the test function are developed into series-expansions in the "thin" directions with respect to a basis of scaled Legendre polynomials with fast decreasing L_2-Norm. By the use of the variational lemma,

the equations are separated into an infinite, linear, second-order PDE-system with an infinite number of unknown displacement variables. Each PDE is a power-series in the characteristic parameters. This formulation is shown to be an exact one- or two-dimensional representation of the three-dimensional problem. However, it is not tractable in practice. By the uniform truncation of the system with respect to the power of characteristic parameters, finite PDE systems in a finite number of unknown displacement coefficients are derived. The greatest power of characteristic parameters that is not neglected defines the approximation-order of the resulting theory. The systems are pseudo-reduced to easier tractable systems by a pseudo-reduction approach. The key idea of the pseudo reduction is to treat the PDE system like linear equation systems and apply the methods of linear algebra to reduce the number of PDEs that have to be solved and the number of variables in this equations by successive elimination. Partial differentiation behaves like multiplication by a factor, since the PDEs are linear with constant coefficients. To avoid a loss of accuracy, different powers of characteristic parameters with the same displacement variables are formally treated as independent variables during the pseudo reduction. We overcome the underdetermination of the resulting system by generating new, linear independent equations by multiplication of original equations with powers of characteristic parameters and the retruncation to the approximation order.

For the example of a monoclinic plate the characteristic parameter is chosen as $c := \frac{h}{\sqrt{12}a} << 1$ and the n-th basis polynomial $b^n : \mathbb{R} \longrightarrow \mathbb{R}$ is selected as

$$b^n(\xi) := \sqrt{(2n+1)}c^n p^n(\frac{1}{\sqrt{3}c}\xi),$$

where p^n is the n-th Legendre polynomial. The resulting field equations after pseudo-reduction are formulated in the two variables $w := u_3^0$, the mid-plane displacement, and $\psi := \frac{\partial u_2^1}{\partial \xi_1} - \frac{\partial u_1^1}{\partial \xi_2}$, a shear measure, where u_i^l is the coefficient of the displacement field u_i with respect to the basis polynomial b^l ($u_i = \sum_{l=0}^{\infty} u_i^l b^l$) and turn out to be

$$\begin{aligned}
&5c^2 E_{3333}\left(E_{2323}E_{1313} - E_{2313}^2\right)\left(E_{\alpha\beta\gamma\delta}E_{3333} - E_{\alpha\beta33}E_{\gamma\delta33}\right) w_{,\alpha\beta\gamma\delta} \\
&+ 6c^4 \varepsilon_{3\alpha\beta}\varepsilon_{3\gamma\delta}E_{\alpha3\gamma3}\left(E_{\beta\eta\iota\kappa}E_{3333} - E_{\beta\eta33}E_{\iota\kappa33}\right)\left(E_{\delta\mu\nu\vartheta}E_{3333} - E_{\delta\mu33}E_{\nu\vartheta33}\right) w_{,\eta\iota\kappa\mu\nu\vartheta} \\
&- 6c^4 E_{1212}E_{3333}\varepsilon_{3\alpha\beta}E_{\alpha3\gamma3}\left(E_{\delta\eta\iota\beta}E_{3333} - E_{\delta\eta33}E_{\iota\beta33}\right)\psi_{,\delta\eta\iota\gamma} \\
&= 5E_{3333}\left(E_{2323}E_{1313} - E_{2313}^2\right)\frac{a}{h}\left(E_{3333}P_3^0 + c^2 E_{\alpha\beta33}\left(\frac{1}{\sqrt{5}}P_3^2 + \frac{2}{5}P_3^0\right)_{,\alpha\beta}\right) + O(c^6),
\end{aligned}$$

$$\begin{aligned}
&5c^2 E_{3333}\left(E_{2323}E_{1313} - E_{2313}^2\right)\psi \\
&+ 6c^4 \varepsilon_{3\alpha\beta}E_{\alpha3\gamma3}\left(E_{\delta\eta\iota\beta}E_{3333} - E_{\delta\eta33}E_{\iota\beta33}\right) w_{,\delta\eta\iota\gamma} \\
&- 6c^4 E_{1212}E_{3333}E_{\alpha3\beta3}\psi_{,\alpha\beta} \\
&= 0 + O(c^6).
\end{aligned}$$

Up to now the presented theory is the only consistent second-order theory available for actual monoclinic materials. By neglecting terms of order $O(c^4)$ it is equivalent to the classical theory for anisotropic plates, mainly developed by M.T. Huber. For isotropic material it is equivalent to E. Reissner's plate theory and by neglecting terms of order $O(c^4)$ for isotropic material it is equivalent to Kirchhoff's plate theory. A detailed article has been submitted [1].

References

[1] P. Schneider, R. Kienzler, M. Böhm, *Modelling of consistent second-order plate theories for monoclin material*, submitted to ZAMM.

Examples for the importance of being curved

Cornelia Schwarz
(joint work with Radan Sedláček, Ewald Werner)

Some highly relevant problems in the field of mechanics of materials on small length scales can be meaningfully addressed by means of a continuum theory of dislocations, presumed that a more complete description of the dislocation population than possible by the classical Kröner dislocation density tensor is provided. One typical application field is the modeling of size-effects that can be observed during plastic deformation of specimens on the micro-scale.
The approach to a feasible continuum theory taken in our research is based on the scalar dislocation density $\rho(x)$ (= line length per volume) and the notion of single valued dislocation fields [1, 2]. Thereby it is assumed that the dislocation population (in a slip system) is such that in every spatial point all dislocations passing through that point have the same unit line tangent $\boldsymbol{\xi}$ and orientation ϑ (= angle enclosed by $\boldsymbol{\xi}$ and the x-axis). This is for example a reasonable assumption for a dislocation population emanated from only one dislocation source. Within one such single valued field no loss of information due to averaging takes place. Considering several such single valued fields allows for a description of more complex dislocation populations then.

$$\frac{\partial b\rho}{\partial t} = -\partial_{\boldsymbol{\nu}}(b\rho V)\,, \quad b\rho\frac{\partial \vartheta}{\partial t} = \partial_{\boldsymbol{\xi}}(b\rho V) \tag{1}$$

Evolution equations for the dislocation density and the orientation of the individual single-valued fields, see Eq. (1), an up-link to a continuum mechanics framework via the plastic shear rate and a down-link via a yield-function like equation of motion for the dislocations of the field complete the model. The latter part, defining the glide velocity V of dislocations in direction $\boldsymbol{\nu}$ normal to the dislocation line, introduces a major ingredient for the model to account for size-effects. Including the self-force, it is taken into account that the dislocation curvature $\kappa = -\mathrm{div}\,\boldsymbol{\nu}$, which is higher in 'small-scaled', confined regions of the material, impedes the motion of the dislocations, thus strengthening the material. The approach was sharpened

by a refined consideration of short-range interactions among the dislocations by including the contribution of a back stress [3].
The continuum dislocation-based model on the basis of single-valued dislocation fields was applied to several benchmark problems in micro-scale plasticity. Some interesting problems could be treated in a spatially one-dimensional framework, e.g. the constrained shearing of a thin film [4], the bending of a free-standing strip [5], and internal stresses in dislocation cell structures [6]. For the application of the model to spatially two-dimensional problems, e.g. the response of a simple composite structure to a shear load [7], some computational challenges had to be overcome.
Problems to be addressed in the future include the application to the problem of mechanical annealing observed in compression tests on micro-pillars [8] and the incorporation of dislocation sources as well as dislocation - grain boundary interactions, which are required for the application of the model to a multi-crystal.

References

[1] R. Sedláček, J. Kratochvíl, E. Werner, *The importance of being curved: bowing dislocations in a continuum description*, Philosophical Magazine **83** (2003), 3735–3752.
[2] R. Sedláček, C. Schwarz, J. Kratochvíl, E. Werner, *Continuum theory of evolving dislocation fields*, Philosophical Magazine **87** (2007), 1225–1260.
[3] C. Schwarz, R. Sedláček, E. Werner, *Refined short-range interactions in the continuum dislocation-based model of plasticity at the microscale*, Acta Materialia **56** (2008), 341–350.
[4] R. Sedláček, E. Werner, *Constrained shearing of a thin crystalline strip: Application of a continuum dislocation-based model*, Phys. Rev. B **69** (2004), 134114.
[5] R. Sedláček, *Orowan-type size effect in plastic bending of free-standing thin crystalline strips*, Materials Science and Engineering A **393** (2005), 387–395.
[6] R. Sedláček, C. Schwarz, J. Kratochvíl, E. Werner, *Modeling of size-dependent internal stresses in dislocation cell structures*, Materials Science and Engineering A **474** (2008), 323–327.
[7] C. Schwarz, R. Sedláček, E. Werner, *Plastic deformation of a composite and the source-shortening effect simulated by the continuum dislocation-based model*, Modelling and Simulation in Materials Science and Engineering **15** (2007), S37- S49.
[8] Z.W. Shan, R.K. Mishra, S.A. Syed Asif, O.L. Warren, A.M. Minor, *Mechanical annealing and source-limited deformation in submicrometre-diameter Ni crystals*, Nature Materials **7** (2007), 115–119.

Materials design by assembly and topological interlocking

Thomas Siegmund

The motivation for such an investigation arises from observations on natural structures. I have found inspiration for this investigation in the armor of the armadillo, and the tesserae of sharks. These structures are hard yet highly deformable, a characteristic not available in common engineering materials, and both structures are assemblies of a multitude of identical (or at least similar) unit elements. Packing and tiling with polyhedra has been of interest to generations of researchers, and this interest continues until today [1, 2]. Recently, there has also been interest in obtaining the mechanical properties of polyhedral packing or tiling structures

[3]. The present work focuses on the mechanical properties of the densest planar packing of tetrahedra [1]. This packing is of interest as it leads to a structure that can carry transverse loads [4].

In one research direction, I have investigated the fundamental mechanical properties of monolayer assemblies of densely packed tetrahedral unit elements. Thereby, a rigid frame confines the assembly of unit polyhedral. Polyhedra are considered to no only be dense but also are considered as cellular units. Due to the discontinuous nature of the assembly load transfer occurs through the formation of distinct force chains in only few selected cross-section planes. These force chains are activated sequentially, and thus the overall deformation response emerges as the superposition of the contribution from individual force chains. Drawing from the thrust line analysis approach developed in structural mechanics, and recognizing the statically indeterminate nature of the problem, it is possible to obtain equations that describe the deformation behavior of the monolayers when subjected to transverse load. The model predictions are in good agreement with experiments for both dense and cellular structures.

To demonstrate the material design opportunities inherent to the assembled materials, we have conducted physical and computational experimentation on monolayer assemblies made from cellular unit elements. We expand our models to incorporate considerations on the failure characteristics of the monolayers and demonstrate the relationships between elastic stiffness, strength and toughness for this novel class of hybrid materials. Our experiments in agreement with the theory – demonstrate that – in contrast to conventional solid materials - in this hybrid material, strength and toughness as well as strength and stiffness are positively correlated. In addition, the cellular nature of the unit elements opens the door for the creation of multifunctional materials in which polyhedral unit elements are packed in dense form and create mechanical crystals.

References

[1] J.H. Conway, S. Torquato, *Packing, tiling, and covering with tetrahedra*, Proc. Natl. Acad. Sci. U S A. **103**(28) (2006), 10612–10617.

[2] A. Haji-Akbari, M. Engel, A.S. Keys, X. Zheng, R.G. Petschek, P. Palffy-Muhoray, S.C. Glotzer, *Disordered, quasicrystalline and crystalline phases of densely packed tetrahedra*, Nature **462** (2008), 773–777.

[3] Y. Estrin, A.V. Dyskin, E. Pasternak, *Topological interlocking as a material design concept*, Mater. Sci. Engng. C **31** (2011), 1189–1194.

[4] M. Glickman, *The G-Block system of vertically interlocking paving*, Proceedings Second International Conference on Concrete Block Paving, Delft, Netherlands (1984), 345–348.

Deformation and fracture of cortical bone

Vadim Silberschmidt

The mechanical behaviour of cortical bone is defined by its hierarchical structure as well as by the mechanical properties of its microstructural constituents. These features also control its fracture process including crack initiation and crack propagation as well as the crack path. Even limiting analysis to two out of known seven hierarchical levels - the entire cross section and the osteonal level - still presupposes availability of both mechanical data and microstructure characteristics for specific parts of the bone (cortex). A non-uniform distribution of osteons in a cortical bone tissue results in a localization of deformation processes and affects fracture initiation. Anisotropy (though with a small contrast of around two for longitudinal and transversal directions) and an elasto-visco-plastic behaviour as well as a difference of responses to tensile and compressive regimes needs significant experimental efforts to quantify the mentioned properties for different cortices. On the other hand, moving to the microscopic (i.e. osteonal) level, it is also necessary to study both morphology of cortical microstructure and mechanical properties of its constituents. Quantification of the properties of cortical bone's microstructural constituents can help to accurately model and interpret its fracture and deformation mechanisms. Hence, our experimental studies of macroscopic specimens with varying orientations (with regard to the bone's longitudinal axis) exposed to various loading regimes (quasi-static, cyclic and dynamic) [1, 2] were accompanied by nanoindentation analysis of post-yield behaviour of bone constituents. With these data, some cases of deformation and fracture of bone can be tackled numerically. It is well known, that on the one hand, bone can be exposed to impact loading in situations, such as traumatic falls or sports injuries. On the other hand, cutting of bone is a standard procedure in orthopaedic surgery. In both cases, the stresses imposed on a bone can be far higher than its strength and lead to fracture or material separation. For an impact loading regime, a number of finite-element models were developed in order to analyse its deformation and fracture using the extended finite-element (FE) method implemented into the software package Abaqus 6.11. Those models included: (1) two- and three-dimensional (3D) FE models to simulate fracture and deformation of cortical bone tissue at macro-scale level for the Izod impact test setup [2, 3]; (2) macroscopic 3D FE models for tensile-impact loading conditions; (3) 2D micro-scale model with direct introduction of bone's microstructure. To model cutting of cortical bone, a finite-element model was developed to simulate the initiation and propagation of damage during tool-bone interaction combining smooth particle hydrodynamics with a continuum domain. The developed models provided a deeper insight into deformation and fracture mechanisms and, most importantly, they adequately reflected the obtained experimental data.

References

[1] A.A. Abdel-Wahab, K. Alam, V.V. Silberschmidt, *Analysis of anisotropic viscoelastoplastic properties of cortical bone tissues*, Journal of the Mechanical Behavior of Biomedical Materials **4**(5) (2011), 807–820.

[2] A.A. Abdel-Wahab, K. Alam, V.V. Silberschmidt, *Dynamic properties of cortical bone tissue: Izod tests and numerical study*, Computers, Materials & Continua **19**(3) (2010), 217–238.

[3] A.A. Abdel-Wahab, K. Alam, V.V. Silberschmidt, *Numerical modelling of impact fracture of cortical bone tissue using X-FEM*, Journal of Theoretical and Applied Mechanics **49**(3) (2011), 599–619.

Fluid saturated porous media with non-classical damping

Holger Steeb

We present a three-phase multi-scale model describing wave propagation phenomena in residual saturated porous media like reservoir rocks. The residual saturated porous medium is characterized through a wetting pore liquid which rests in the pore space. These liquid blobs or liquid ensembles (clusters) are pinned at the pore walls by high capillary forces. In the residual saturation case, blobs and/or clusters of the wetting fluid are disconnected from each other and each blob or cluster occupies only a single or several pores. Depending on the pore geometry, the size of the individual fluid clusters can be widely distributed, for example in certain heterogeneous reservoir rocks. The acoustic properties (effective phase velocities and attenuation) strongly depend on the distribution of fluid cluster size. Propagating waves at low seismic frequencies ($f < 100$ Hz) are not affected by the discontinuous wetting fluid, because the wavelength is much larger than the characteristic cluster sizes. On the other hand, a wave propagating through the continuous solid skeleton or through the continuous non-wetting fluid at higher frequencies is able to excite the blobs of wetting fluid through an exchange of momentum. If the liquid clusters are excited, energy is trapped in the discontinuous phase and the propagating wave is attenuated. The frequency range of this hidden attenuation mode is related to the (lowest) eigenfrequency of the fluid blob/cluster and therefore to the microscopical geometry of the liquid phase.

We develop a continuum mixture theory-based model which is able to describe two continuous phases, i.e. the solid skeleton and the non-wetting pore fluid (gas), and, in addition, a discontinuous phase, i.e. the wetting fluid (liquid). Resonance effects of the single liquid bridges and/or liquid clusters are captured with miscellaneous eigenfrequencies taking into account a viscoelastic restoring force (pinned oscillations and/or sliding motion of the contact line).

The aim of the current work is to develop and discuss a basic multi-scale modelling framework which takes into account the dynamics of statistically-distributed phases in a macro-scale continuum approach. It will be shown, that such a three-phase model allows to study frequency-dependent attenuation due to fluid oscillations and attenuation with respect to wave-induced flow. Furthermore, the distinct model could be applied to waves in reservoir rocks in the seismic range (field scale)

and ultrasound range (lab scale). We will show that the results of the model are consistent with well-established limits, i.e. the low and high frequency limits of the biphasic poroelastic Biot model. In addition, we will show that for the quasi-static limit case the results of the model are identical with the phase velocity obtained by the Gassmann-Wood limit.

References

[1] H. Steeb, M. Frehner, S.M. Schmalholz, *Waves in residual saturated porous media*, in G.A. Maugin & A.V. Metrikine, Eds., Generalized Continuum Mechanics: One Hundred years after the Cosserats, Springer-Verlag, Berlin (2010), 179–190.

[2] B. Quintal, H. Steeb, M. Frehner, S.M. Schmalholz, *Quasi-static finite element modeling of seismic attenuation and dispersion due to wave-induced fluid flow in poroelastic media*, Journal of Geophysical Research **116** (2011), B01201.

[3] E.H. Saenger, F. Enzmann, Y. Keehm, H. Steeb, *Digital rock physics: Effect of fluid viscosity on effective elastic properties*, Journal of Applied Geophysics **74** (2011), 236–241.

[4] B. Quintal, H. Steeb, M. Frehner, S.M. Schmalholz, E.H. Saenger, *Pore fluid effects on S-wave attenuation caused by wave-induced fluid flow*, Geophysics **77** (2012), 10.1190/GEO2011-0233.1

[5] H. Steeb, P.S. Kurzeja, M. Frehner, S.M. Schmalholz, *Phase velocity dispersion and attenuation of seismic waves due to trapped fluids in residual saturated porous media*, Vadose Zone Journal (2012), under review.

Thermodynamic variational formulation of dislocation field theory at large deformation

Bob Svendsen

The purpose of this work is the formulation of field models for continua containing dislocations via the application of recently developed variational approaches to the formulation of boundary value problems for continuum thermodynamic models at large deformation. In the large-deformation context, both spatial and material representation of the variational formulation are examined. In particular, whereas the former is based on the Cauchy stress and variations of the intermediate local configuration, the latter is formulated with the help of the Eshelby stress and variations of the material local configuration. Assuming further that the local inelastic deformation is material isomorphic and/or uniform, further results ensue. For simplicity, attention is focused in this work on continua containing static distributions of dislocations; extension to the case of evolving dislocation microstructure as based on rate-variational methods represents work in progress. A number of examples will be given, and in particular the reduction of the formulation to small deformation in order to make connection with the recent work of Groma and colleagues on this subject.

Thermomechanical modeling via energy and entropy using GENERIC

Marita Thomas
(joint work with Alexander Mielke)

The traditional way of thermomechanical modeling of physical and chemical processes is based on the interplay of the universal balance laws and the particular constitutive laws for the system under consideration. Here we propose an alternative way of modeling that is more adapted to the underlying mathematical structures and tools. The general evolution of a system will be described as the sum of a reversible part, a Hamiltonian system driven by the energy, and an irreversible part, a gradient or Onsager system driven by the entropy. The proper coupling is done in the framework of **GENERIC**, the **G**eneral **E**quation of **N**on-**E**quilibrium **R**eversible **I**rreversible **C**oupling. This approach was developed by H.C. Öttinger and Grmela [1] for fluid dynamics. Comparably only recently, its applicability for the modeling in solid mechanics was realized, see e.g. [2] and it was stated in a more general context [3, 4].

The fundamental ingredients of GENERIC are Hamiltonian systems for reversible dynamics and Onsager systems for irreversible dynamics. Both are formulated on a state space $\mathcal{Q}$ via a driving potential $\Phi : \mathcal{Q} \to \mathbb{R}$ and a geometric structure. For simplicity, we assume that $\mathcal{Q}$ is a Banach space with dual pairing $\langle \cdot, \cdot \rangle$. The driving force is given by the functional derivative $\mathrm{D}\Phi(q) \in \mathcal{Q}^*$. Moreover, here we restrict the discussion to thermodynamically closed systems.

Hamiltonian systems $(\mathcal{Q}, \mathcal{E}, J)$: In the spirit of Hamiltonian mechanics, a general Hamiltonian system accounts for reversible dynamics, only. The equations of motion are given by $\dot{q} = J\mathrm{D}\mathcal{E}(q)$. The driving potential of reversible dynamics is the energy of the system $\mathcal{E} : \mathcal{Q} \to \mathbb{R}$, which may comprise kinetic, mechanical and thermal energy. Characteristic for a Hamiltonian system is that the associated geometric structure J, also called a Poisson structure, is symplectic. This means,

(1) J is antisymmetric, $J = -J^*$, and satisfies Jacobi's identity,

i.e. $\{\Phi_1, \{\Phi_2, \Phi_3\}\} + \{\Phi_3, \{\Phi_1, \Phi_2\}\} + \{\Phi_2, \{\Phi_3, \Phi_1\}\} = 0$ for all $\Phi_i : \mathcal{Q} \to \mathbb{R}$. Here, the Poisson bracket $\{\cdot, \cdot\}$ is defined via the dual pairing $\{\Phi_1, \Phi_2\} := \langle \mathrm{D}\Phi_1, J\mathrm{D}\Phi_2 \rangle$ for all $\Phi : \mathcal{Q} \to \mathbb{R}$. The antisymmetry of J ensures conservation of energy.

As an example we consider an elastodynamic system. The states $q = (\varphi, p)$ are given by the deformation $\varphi : \Omega \to \mathbb{R}^3$ and the momentum $p = \varrho\dot{\varphi}$ with ϱ as the mass density and $\Omega \subset \mathbb{R}^3$ as the reference domain. The energy of the system is composed of the kinetic energy, the stored elastic energy and the energy due to the external force f, i.e. $\mathcal{E}(q) := \int_\Omega E(\varphi, \nabla\varphi, p)\,\mathrm{d}x$, where the energy density takes the form $E(\varphi, \nabla\varphi, p) := |p|^2/(2\varrho) + W(\nabla\varphi) - f\varphi$. For $J = \begin{pmatrix} 0 & I \\ -I & 0 \end{pmatrix}$ the equations of motion $\dot{q} = J\mathrm{D}\mathcal{E}(q)$ read $\dot{\varphi} = \delta_p E = p/\varrho$ and $\dot{p} = -\delta_\varphi E = \operatorname{div} \partial_{\nabla\varphi} W + f$.

Onsager systems $(\mathcal{Q}, \mathcal{S}, K)$: An Onsager system is related to the dynamics of irreversible, dissipative effects. The evolution equations read $\dot{q} = K(q)\mathrm{D}\mathcal{S}(q)$. The driving functional is the total entropy $\mathcal{S}$, and the geometric structure is the

so-called Onsager operator:

(2) K is symmetric, $K = K^*$, and positive semidefinite, $\langle \xi, K\xi \rangle \geq 0$.

While the positive semidefiniteness is a manifestation of the second law of thermodynamcis, the symmetry of K is a generalization of Onsager's reciprocal relations.

As an example we consider heat conduction in a body Ω. The state is the temperature θ. We postulate the entropy $\mathcal{S}(\theta) = \int_\Omega \log\theta \, \mathrm{d}x$ and introduce the Onsager operator $K_H(\theta)$ via $K_H(\theta)\xi := -\frac{1}{c_V(\theta)} \operatorname{div}(\theta^2 \kappa(\theta) \nabla \xi)$, where $c_V(\theta)$ is the heat capacity and $\kappa(\theta)$ is the heat conduction coefficent. With this choice the Onsager system yields the well-known heat equation $\dot\theta = K_H \mathrm{D}\mathcal{S}(\theta) = \frac{1}{c_V(\theta)} \operatorname{div}(\kappa(\theta)\nabla\theta)$.

GENERIC systems $(\mathcal{Q}, \mathcal{E}, \mathcal{S}, J, K)$. A GENERIC system is a quintuple $(\mathcal{Q}, \mathcal{E}, \mathcal{S}, J, K)$ such that the triple $(\mathcal{Q}, \mathcal{E}, J)$ is a Hamiltonian system and $(\mathcal{Q}, \mathcal{S}, K)$ is an Onsager system. The associated evolution system has the form

$$\dot q = J(q)\mathrm{D}\mathcal{E}(q) + K(q)\mathrm{D}\mathcal{S}(q), \tag{3}$$

which clearly reveals the reversible and the irreversible part of the dynamics. However, there is a crucial coupling condition, which we call

(4) **noninteraction condition:** $K\mathrm{D}\mathcal{E} \equiv 0$ and $J\mathrm{D}\mathcal{S} \equiv 0$.

On the one hand, (4) ensures energy conservation and entropy production. On the other hand, (4) guarantees the validity of the maximum-entropy principle, i.e. if q_* maximizes $\mathcal{S}$ subject to $\mathcal{E}(q) = E_0$, then q_* is a steady state of (3).

As an example we consider a thermo-viscoelastic system. The states are given by the the deformation φ, the momentum p and the temperature θ. We postulate the energy density $E(\varphi, \nabla\varphi, p, \theta) := |p|^2/(2\varrho) + \frac{1}{2}\nabla\varphi : \mathbb{C} : \nabla\varphi - f\varphi + G(\theta)$, the entropy density $S(\nabla\varphi, \theta) := \nabla\varphi : \mathbb{C} : \mathbb{E} + g'(\theta)$ and the operators $K_{\mathrm{V}} A := \theta \mathbb{D} : A$, as well as $K_{\mathrm{H}} A := -\frac{1}{\partial_\theta E} \operatorname{div}(\theta^2 \mathbb{K}(\nabla\varphi, \theta)\nabla(A/\partial_\theta E))$ with $\partial_\theta E = G'(\theta) = c_V(\theta)$. Since we now couple reversible and irreverible processes we have to make sure that (4) holds. For this, we use the Gibbs relation $\partial_\theta E = \theta \partial_\theta S$. To preserve the antisymmetry of the Poisson operator we define $JA := M_{\mathcal{S}} J_0 M_{\mathcal{S}}^* A$ with

$$M_{\mathcal{S}} := \begin{pmatrix} I & 0 & 0 \\ 0 & I & 0 \\ -\frac{1}{\partial_\theta S}\Delta_\varphi S[\Box] & 0 & \frac{1}{\partial_\theta S} \end{pmatrix}, \; J_0 := \begin{pmatrix} 0 & I & 0 \\ -I & 0 & 0 \\ 0 & 0 & 0 \end{pmatrix}, \; M_{\mathcal{S}}^* := \begin{pmatrix} I & 0 & -\frac{\Box}{\partial_\theta S} * \delta_\varphi S \\ 0 & I & 0 \\ 0 & 0 & \frac{1}{\partial_\theta S} \end{pmatrix},$$

where $\alpha * \delta_a \Phi := \partial_a \Phi - \operatorname{div} \partial_{\nabla a} \Phi$ and $\Delta_a \Phi[v] := v \partial_a \Phi + \partial_{\nabla a} \Phi : \nabla v$. To preserve the symmetry of the Onsager operator we set it $K_{\mathrm{VH}} A := N_{\mathcal{E}} K_0 N_{\mathcal{E}}^* A$ with

$$N_{\mathcal{E}} := \begin{pmatrix} I & 0 & 0 \\ 0 & -\operatorname{div} & 0 \\ -\frac{1}{\partial_\theta E}\Delta_\varphi E[\Box] & -\frac{1}{\partial_\theta E}\nabla\partial_p E : \Box & 1 \end{pmatrix}, K_0 := \begin{pmatrix} 0 & 0 & 0 \\ 0 & K_{\mathrm{V}}\Box & 0 \\ 0 & 0 & K_{\mathrm{H}} \end{pmatrix},$$
$$N_{\mathcal{E}}^* := \begin{pmatrix} I & 0 & -\frac{\Box}{\partial_\theta E} * \delta_\varphi E \\ 0 & \nabla & -\frac{\Box}{\partial_\theta E} \dot F \\ 0 & 0 & 1 \end{pmatrix}.$$

One can easily check that $J_0 M_{\mathcal{S}}^* \mathrm{D}\mathcal{S} \equiv 0$ as well as $K_0 N_{\mathcal{E}}^* \mathrm{D}\mathcal{E} \equiv 0$, i.e. (4) holds, and hence we have energy conservation and entropy production. Moreover, using

that $\nabla\partial_p E = \nabla p = \dot{F} = \nabla\dot{\varphi}$ and $\Delta_\varphi S[\partial_\theta E] = \mathbb{E}:\mathbb{C}:\nabla\dot{\varphi}$ the system (3) reads

$$\begin{aligned}
\dot{\varphi} &= \partial_p E = p/\varrho,\\
\dot{p} &= -\partial_\varphi E + \operatorname{div}\partial_{\nabla\varphi} E + \theta\partial_\theta S - \operatorname{div}(\theta\partial_{\nabla\varphi} S) - \operatorname{div} K_{\mathrm{V}}(-\tfrac{1}{\theta}\dot{F})\\
&= \operatorname{div}(\mathbb{D}:\nabla\varphi + \mathbb{C}:(\nabla\varphi - \mathbb{E}\theta)) + f,\\
\dot{\theta} &= -\tfrac{1}{\partial_\theta S}\Delta_\varphi S[\partial_p E] - \tfrac{1}{\partial_\theta E}\nabla\partial_p E : K_{\mathrm{V}}(-\tfrac{1}{\theta}\dot{F}) + K_{\mathrm{H}}(\partial_\theta S)\\
&= \tfrac{1}{c_V(\theta)}\big(\nabla\dot{\varphi}:\mathbb{D}:\nabla\dot{\varphi} - \theta\mathbb{E}:\mathbb{C}:\nabla\dot{\varphi} + \operatorname{div}\mathbb{K}(\nabla\varphi,\theta):\nabla\theta\big).
\end{aligned}$$

For more examples on GENERIC systems in applications, such as Allen-Cahn, Cahn-Hilliard, Penrose-Fife systems, generalized standard materials, reaction-diffusion processes, mechanochemistry, bulk-interface interaction and applications to photovoltaics the reader is referred to [3, 4, 5].

References

[1] H.C. Öttinger, M. Grmela, *Dynamics and thermodynamics of complex fluids. I.Development of a general formalism + II.Illustrations of a general formalism*, Phys. Rev. E (3) **56** (1997), 6620–6632+6633–6655.

[2] M. Hütter, B. Svendsen, *On the formulation of continuum thermodynamic models as general equations for non-equilibrium reversible-irreversible coupling*, J. Elast. **104** (2011), 357-368.

[3] A. Mielke, *Formulation of thermoelastic dissipative material behavior using GENERIC*, Contin. Mech. Thermodyn. **23** (2011), pp. 233-256.

[4] A. Mielke, *A gradient structure for reaction diffusion systems and for energy-drift-diffusion systems*, Nonlinearity **24** (2011), pp. 1329–1346.

[5] A. Mielke, M. Thomas, *GENERIC: general theory and applications.* Lecture notes, autumn school, Pisa, in progress.

In-situ small scale coupled thermomechanical experiments combined with first principles calculations based on non-equilibrium Green's function

Vicas Tomar

Thermal and strain dependent mechanical properties of materials traditionally have been considered to be independent of each other. Thermal properties are attributed primarily to lattice vibrations in ceramics and semiconductors. In the case of metals electrons are considered as the major contributor to the thermal properties. On the other hand, the mechanical properties are attributed to larger scale acoustic loads that lead to lower frequency but larger wavelength deformation of a lattice. Owing to the larger wavelength and lower frequency of lattice vibrations in mechanical loading electrons are considered not to contribute mechanical properties of a material. Fundamentally, acoustic response of a material ranges from a time scale of microseconds in shock simulations to at a time scale of seconds in situations such as fatigue loading. The dominant phononic thermal vibrations have a maximum time scale of approximately picoseconds. Electronic vibrations occur at a timescale of femto-seconds. Recently, simultaneous thermal conductivity and stress measurements have been performed as a function of strain

in single crystalline Si [1]. It was observed that there is a direct coupling between measured thermal conductivity and mechanical stress in microscale single crystalline Si as a function of strain. The shape of the stress-strain curve and thermal conductivity-strain curve were the same for a range of samples. The authors of [2, 3, 4] observed similar stress-strain-thermal conduction correlation in Si-Ge superlattices and nanocomposites using classical molecular simulations. Such correlation, since it involves, multiple timescales is intriguing. Classical molecular simulations are limited in their capability to analyze fundamental solid state properties owing to the limitations regarding applicability to analyze electronic properties, phase transformation, atomic heterogeneity etc. The extent of contribution of the fundamental electron and phonon component to structural strength needs to be identified using *ab-initio* simulations in order to be able to present a complete picture regarding the effect of structural transformation and atomic heterogeneity on such behavior. This work presents such an understanding using a combination of small scale *in-situ* experiments and *ab-initio* models.

References

[1] M. Gan, V. Tomar, *Correlating microscale thermal conductivity of heavily-doped silicon with simultaneous measurements of stress*, J. Engng. Mater. Technol. (2011) in print.

[2] V. Samvedi, V. Tomar, *Analyses of interface thermal boundary resistance of Si-Ge superlattice system as a function of film thickness and periodicity*, Nanotechnology **20** (2009), 365701–365712.

[3] V. Samvedi, V. Tomar, *Role of heat flow direction, monolayer film thickness, and periodicity in controlling thermal conductivity of a Si-Ge superlattice system*, J. Appl. Phys. **105** (2009), 13541.

[4] V. Samvedi, V. Tomar, *Role of straining and morphology in thermal conductivity of a set of Si-Ge superlattices and biomimetic Si-Ge nanocomposites*, Journal of Physics D, Applied Physics **43** (2010), 135401–135412.

Computing the rates at which thermally activated deformation processes occur

D. H. Warner

The prediction of crack growth is one of the most technologically important and scientifically intriguing problems in mechanics of materials. Yet, despite decades of research, a comprehensive understanding of the process has remained elusive. As a quintessential multiscale phenomenon, crack growth is both a chemical and mechanical process, involving interatomic bond breakage driven by long range mechanical stress fields. While the advancement of concurrent multiscale modeling methodologies have opened the door for an atomic scale understanding of crack tip processes, a disparity in time scales between laboratory conditions and atomistic modeling remains.

In this talk, we will examine the use of transition state theory (TST) to overcome the challenge of time scale. Focusing here on dislocation nucleation in Al, we will examine the utility of five TST-based approaches. Using the finite temperature string method, we interpret the success/failure of each approach in terms of a

full energetic analysis of the nucleation processes. After showing that advanced TST approaches such as variational TST can accurately predict nucleation rates, we employ variational TST to study dislocation nucleation from a variety of free surfaces under ordinary laboratory conditions. The predictions (1) demonstrate that nucleation will only occur under very high stresses at room temperature, (2) provide an upper bound on the shear strength of Al in dislocation starved contexts, (3) provide a rate sensitivity signature of the nucleation process, and (4) provide insight into the role void growth via dislocation nucleation during ductile fracture.

A short note on elastic SH wave scattering in textile reinforced concrete

Bernd W. Zastrau
(joint work with Wolfgang Weber)

Textile reinforced concrete (TRC) is a composite material used in Civil Engineering gaining more and more interest in practical application [1, 2]. TRC consists of so-called fine grained concrete as matrix material and a textile reinforcement made of carbon or glass fabrics. As no concrete revetment is necessary, the creation of thin concrete structures is possible. Thus, TRC is very well suited for both the strengthening or rehabilitation of existing structures as well as the fabrication of new structural elements.

Whereas the static behaviour of TRC is understood quite well also concerning the long-term behaviour, there is still a lack of knowledge concerning its behaviour due to dynamic loads [3]. In this short note an analytical approach for investigating the reaction of a material clipping of TRC to time-harmonic waves is proposed. As a first model, the direction of reinforcement is assumed to be uni-directional. The focus is set on shear waves. The polarization of these shear waves is such that the direction of particle displacement is parallel to the axes of the reinforcement elements. Hence, SH waves are at hand [4]. The material behaviour of both the matrix and the reinforcement material is assumed to be linear elastic and isotropic. The same holds for the material behaviour of interface layers between reinforcement elements and the matrix. The problem is described by means of Navier's equation without body forces

$$\mu \Delta \mathbf{u} + (\lambda + \mu)\, \nabla \nabla \cdot \mathbf{u} = \varrho \ddot{\mathbf{u}} \tag{1}$$

with the Lamé constants μ, λ, Nabla operator ∇, the Laplace operator Δ, and the displacement field $\mathbf{u} = (u\, v\, w)^T$. For the axes of the reinforcement elements being parallel to the z-axis, the only non-trivial component of $\mathbf{u}$ is w. For time-harmonic loads this displacement has the form

$$w(x, y, t) = w_0 \cos(\omega t + \alpha) = Re\left\{\phi(x, y)\, e^{-\imath \omega t}\right\}, \tag{2}$$

where the complex amplitude ϕ with $|\phi| = w_0$, $Re\{\phi\} = w_0 \cos\alpha$ satisfies the HELMHOLTZ equation

$$\Delta\phi + \frac{\omega^2}{c_{\mathrm{T}}^2}\phi = 0 = \Delta\phi + k^2\phi\,, \tag{3}$$

which follows from introducing the ansatz (2) into NAVIER's equation (1). Herein the imaginary unit $\imath$, the circular frequency ω, the phase α, and the wave number k were introduced. Additionally, the wave speed c_{T} for the shear waves dealt with here can be calculated by $c_{\mathrm{T}} = \sqrt{\mu/\varrho}$. In the following the temporal factor $\exp\{-\imath\omega t\}$ will be omitted.

According to the shape of the reinforcement elements, the HELMHOLTZ equation (3) has to be solved within a proper coordinate system. For reinforcements of elliptical cross sections see e. g. [5]. In this contribution, circular cross sections are dealt with. With the LAPLACian in the polar coordinate system equation (3) yields

$$\frac{\partial^2\phi}{\partial r^2} + \frac{1}{r}\frac{\partial\phi}{\partial r} + \frac{1}{r^2}\frac{\partial^2\phi}{\partial\theta^2} + k^2\phi = 0\,, \tag{4}$$

cf. [6]. This equation may be solved for the respective materials of the matrix and the homogeneous elastic inclusion as done in e. g. [4]. For a layered built-up of the reinforcement, as it is the case for carbon- or glass-fibres dealt with here, see [7]. Hereto, equilibrium and compatibility across the interfaces have to be fulfilled under consideration of in- and outgoing waves within each layer.

Additional enhancements of the analytical model are beneath others the description of visco-elastic material behaviour, variable thicknesses of single layers in angular direction, the interaction of several reinforcement elements with each other, its application to P and SV waves, and the investigation of the influence of transient loads.

By means of the proposed analytical method deeper insight into the scattering of elastic waves in composite materials with inhomogeneous reinforcements are gained. These information may be used in numerical methods as i. e. the FEM, BEM, SFEM. The results obtained by the analytical approach also are necessary within a homogenization process in order to adequately model the dynamic properties of the respective structure. The proposed method is applicable to other composite materials as they occur in mechanical engineering, too.

REFERENCES

[1] M. Curbach; J. Hegger, *Textilbewehrter Beton*, Beton- und Stahlbetonbau **6** (2004).

[2] E. Lorenz; R. Ortlepp; J. Hausding; C. Cherif, *Effizienzsteigerung von Textilbeton durch Einsatz textiler Bewehrungen nach dem erweiterten Nähwirkverfahren*, Beton- und Stahlbetonbau **106** (2011), 21–30.

[3] A. Hummeltenberg; B. Beckmann; T. Weber; M. Curbach, *Betonplatten unter Stoßbelastung – Fallturmversuche*, Beton- und Stahlbetonbau **106** (2011), 160–168.

[4] K. F. Graff, *Wave motion in elastic solids*, Oxford University Press (1991).

[5] W. Weber; B. W. Zastrau, *On SH wave scattering in TRC – Part I: Concentric elliptical inclusion*, Machine Dynamics Problems **33** (2009), 105–118.

[6] P. M. Morse; H. Feshbach, *Methods of Theoretical Physics*, McGraw-Hill (1953).

[7] W. Weber, *Ein Beitrag zum Einfluss der Bewehrung auf die Körperwellenausbreitung in Verbundwerkstoffen*, Ph.D. thesis (2011).

Multiscale dislocation plasticity: Discrete to continuum

Hussein M. Zbib

The miniaturization of structural components to the sub-micrometer scale has created a significant challenge when attempting to engineer such structures using conventional models and simulation tools that are based solely on continuum approaches. Although there has been progress in strain-gradient continuum theories to model the mechanical behavior of metallic systems at small length scales, these theories fail to represent the variety of physical mechanisms involved in dislocation motion in small volumes where dislocations are scarce. The major difficulty in these theories lies in the notion that physical mechanisms which arise from dislocation motion that occur at the micrometer scale, and are intrinsically discrete events, can be represented in the form of continuum variables at the macro-meter length scale. This drastic jump between scales may be statistically meaningful for relatively large volumes but loses all sense when the volume is so small such that dislocations become in short supply. This situation, in turn, has brought about the need to develop novel multiscale material models and simulation tools that may enable engineers to design and analyze multiscale structures at such small scales. In parallel, this also necessitates the need to develop novel experimental techniques to determine and verify mechanical properties at the sub-micrometer scale for use in such models.

It is our point-of-view that accurate design of submicron systems can only be achieved by multiscale models that precisely combine microstructural and physical material properties together with structural dimensions; and that intrinsic mechanical properties and deformation/design maps for use in multiscale design and analysis of submicron structures can only be determined from test specimens that are subjected to homogenous deformation conditions with no (or minimum) strain gradients and stress concentrations effects as is the case with current testing methodologies. In our work, we capitalize on undergoing research efforts we have in the experimental area, higher order continuum theories, molecular dynamics as well as multiscale dislocation dynamics plasticity modeling of nanostructure materials. We investigate, using molecular dynamics and discrete dislocation dynamics analyses, how dislocation mechanisms and interactions contribute to strength, accumulation of damage and fatigue. Guided by these results, we develop a dislocation-based continuum crystal plasticity model, including dislocation densities, hardening laws based on dislocation-dislocation interaction, and a set of mechanisms-based evolution laws. The evolution laws consists of a set of terms each corresponding to a physical mechanisms that can be explicitly evaluated from the discrete dislocation analyses, including dislocation growth, annihilation, junction formation, junction breaking, dislocation-defect interaction and cross-slip. It

is shown that the discrete events of cross-slip of screw dislocations can be explicitly incorporated in the continuum theory based on a probability distribution function defined by activation energy and activation volume of cross-slip, and that is analogous to the one used for the discrete system. This enables the redistribution of dislocations and dislocation density patterning due to the effect of stacking fault energy. The formulation is employed for explaining the cross-slip phenomena during uniaxial tensile deformation of fcc and bcc single crystals.

Reporter: Ewald A. Werner

Participants

Prof. Dr. Holm Altenbach
Fakultät für Maschinenbau
Otto-von-Guericke-Universität
Universitätsplatz 12
39106 Magdeburg

Prof. Dr. Thomas Böhlke
Institut für Technische Mechanik
Fakultät für Maschinenbau
Universität Karlsruhe
Kaiserstraße 12
76131 Karlsruhe

Dr. Helmut J. Böhm
Institut für Leichtbau und
Struktur-Biomechanik
Technische Universität Wien
Gußhausstr. 25 - 29
A-1040 Wien

Prof. Dr. John D. Clayton
U.S.Army Research Laboratory
Aberdeen Proving Ground
Aberdeen Proving Ground , MD 21005-5066
USA

Prof. Dr. Alan Cocks
Dept. Engineering Science
University of Oxford
Parks Road
GB-Oxford OX1 3PJ

Prof. Dr. William A. Curtin
EPFL STI IGM-GE
ME A2 409 (Batiment ME)
Station 9
CH-1015 Lausanne

Prof. Dr. Samuel Forest
Centre des Materiaux
L'Ecole des Mines
Paristech
BP 87
F-91003 Evry Cedex

Prof. Dr. Gilles Francfort
LAGA UMR 7539
Institut Galilee
Universite Paris 13
Avenue Jean-Baptiste Clement
F-93430 Villetaneuse

Prof. Dr. Alexander B. Freidin
Institute for Problems in
Mechanical Engineering
of Russian Academy of Sciences
V.O., Bolshoy pr. 61
St. Petersburg 199178
RUSSIA

Dr. Rainer Glüge
Institut für Mechanik
Otto-von-Guericke-Universität
Magdeburg
Postfach 4120
39016 Magdeburg

Prof. Dr. Klaus Hackl
Lehrstuhl f. Mechanik / Materialtheorie
Ruhr-Universität Bochum
Fakultät f. Bau- u. Umweltingenieurwiss.
Universitätsstr. 150
44801 Bochum

Prof. Dr. Craig S. Hartley
Consultant,
El Arroyo Enterprises LLC
Sedona , AZ 86336-6341
USA

Prof. Dr. Stefan Hartmann
Institut für Technische Mechanik
TU Clausthal
Adolph-Roemer-Str. 2A
38678 Clausthal-Zellerfeld

Prof. Dr. Thomas Hochrainer
Universität Bremen
IW3
Postfach 330440
28334 Bremen

Prof. Dr. Hanchen Huang
School of Engineering
Department of Mechanical Engineering
University of Connecticut
191 Auditorium Road
Storrs , CT 06269-3139
USA

Prof. Dr. Harley T. Johnson
Dept. of Mechanical Science &
Engineering, University of Illinois
at Urbana-Champaign
1206 West Green Street
Urbana IL 61801
USA

Prof. Dr. Surya Kalidindi
Department of Materials Science and
Engineering
Drexel University
Philadelphia PA 19104
USA

Dr.-Ing. Marc-Andre Keip
Institut für Mechanik
Universität Duisburg-Essen
45117 Essen

Prof. Dr. Reinhold Kienzler
Universität Bremen
IW3
Postfach 330440
28334 Bremen

Dr.-Ing. Christian Krempaszky
Lehrstuhl für Werkstoffkunde und
Werkstoffmechanik
Technische Universität München
Boltzmannstr. 15
85747 Garching

Prof. Dr. Khanh Chau Le
Lehrstuhl für Allgemeine Mechanik
Ruhr-Universität Bochum
Fakultät für Bauingenieurwesen
Universitätsstr. 150
44801 Bochum

Dr. Darby J. Luscher
Los Alamos National Laboratory
Fluid Dynamics and Solid Mechanics (T-
3)
Theoretical Division
PO Box 1663 MS 216
Los Alamos , NM 87545
USA

Prof. Dr. Rolf Mahnken
Universität Paderborn
Lehrstuhl für Technische Mechanik
Warburger Str. 100
32309 Paderborn

Prof. Dr. David L. McDowell
School of Materials Science and
Engineering
Georgia Institute of Technology
Atlanta , GA 30332-0405
USA

Prof. Dr. Christof Melcher
Lehrstuhl I für Mathematik
RWTH Aachen
Wüllnerstr. 5b
52062 Aachen

Prof. Dr. Sinisa Mesarovic
School of Mechanical & Materials Engineering
Washington State University
Pullman WA 99164-2920
USA

Prof. Dr. Wolfgang Helmut Müller
Technische Universität Berlin
Institut für Mechanik Sekr. MS 2
FG Kontinuumsmechanik & Materialth.
Einsteinufer 5
10587 Berlin

Prof. Dr. Alan Needleman
Dept. of Materials Science & Engineering
University of North Texas
Discovery Park
1155 Union Circle
Denton , TX 76203-5017
USA

Prof. Dr. Eduard R. Oberaigner
Institut für Mechanik
Montanuniversität
Franz-Josef-Str. 18
A-8700 Leoben

Prof. Dr. Michael Ortiz
Division of Engineering and
Applied Sciences, MS 104-44
California Institute of Technology
Pasadena , CA 91125
USA

Prof. Dr. Reinhard Pippan
Erich Schmid Institute of the
Austrian Academy of Sciences
Jahnstraße 12
A-8700 Leoben

Prof. Dr. Jianmin Qu
Robert R. McCormick School of
Engineering & Applied Science
Northwestern University
2145 Sheridan Rd.
Evanston , Il 60208-3100
USA

Prof. Dr. Miles B. Rubin
Faculty of Mechanical Engineering
Technion-Israel Inst. of Technology
Technion City
32000 Haifa
ISRAEL

Dr. Lucia Scardia
Department of Mathematics
Eindhoven University of Technology
P.O.Box 513
NL-5600 MB Eindhoven

Prof. Dr. Bernd Schmidt
Institut für Mathematik
Universität Augsburg
86135 Augsburg

Patrick Schneider
Universität Bremen
IW3
Postfach 330440
28334 Bremen

Prof. Dr. Jörg Schröder
Institut für Mechanik
Universität Duisburg-Essen
45117 Essen

Dr.-Ing. Cornelia Schwarz
Lehrstuhl für Werkstoffkunde und
Werkstoffmechanik
Technische Universität München
Boltzmannstr. 15
85747 Garching

Prof. Dr. Thomas Siegmund
School of Mechanical Engineering
Purdue University
West Lafayette , IN 47907-1288
USA

Prof. Dr. Vadim V. Silberschmidt
The Wolfson School of Mechanical
and Manufacturing Engineering
Loughborough University
GB-Loughborough Leicestersh. LE11
3TU

Prof. Dr. Holger Steeb
Ruhr-Universität Bochum
Lehrstuhl für Kontinuumsmechanik
Universitätsstraße 150
44081 Bochum

Prof. Dr. Bob Svendsen
RWTH Aachen
Material Mechanics
Jülich Aachen Research Alliance
Schinkelstr. 2
52062 Aachen

Dipl.Math. Marita Thomas
Weierstraß-Institut für
Angewandte Analysis und Stochastik
Mohrenstr. 39
10117 Berlin

Dr. Vikas Tomar
School of Aeronautics & Astronautics
Purdue University
701 W Stadium Ave.
West Lafayette , IN 47907
USA

Prof. Dr. Derek H. Warner
College of Engineering
Cornell University
Carpenter Hall
Ithaca , NY 14853-2201
USA

Prof. Dr. Ewald A. Werner
Lehrstuhl für Werkstoffkunde und
Werkstoffmechanik
Technische Universität München
Boltzmannstr. 15
85747 Garching

Prof. Dr.-Ing. Bernd W. Zastrau
Technische Universität Dresden
Fakultät Bauingenieurwesen
Helmholtzstr. 10
01069 Dresden

Prof. Dr. Hussein M. Zbib
School of Mechanical & Materials
Engineering
Washington State University
Pullman WA 99164-2920
USA

Prof. Dr. Ting Zhu
Georgia Institute of Technology
The George W. Woodruff School of
Mechanical Engineering
U.S.Army Research Laboratory
Atlanta , GA 30332
USA